Physicochemical strengthening of nanoparticles for cancer hadron therapy and medical physics applications

Catalano Enrico, PhD

Scientia Fellows project –
Postdoctoral fellowship programme in Health Sciences

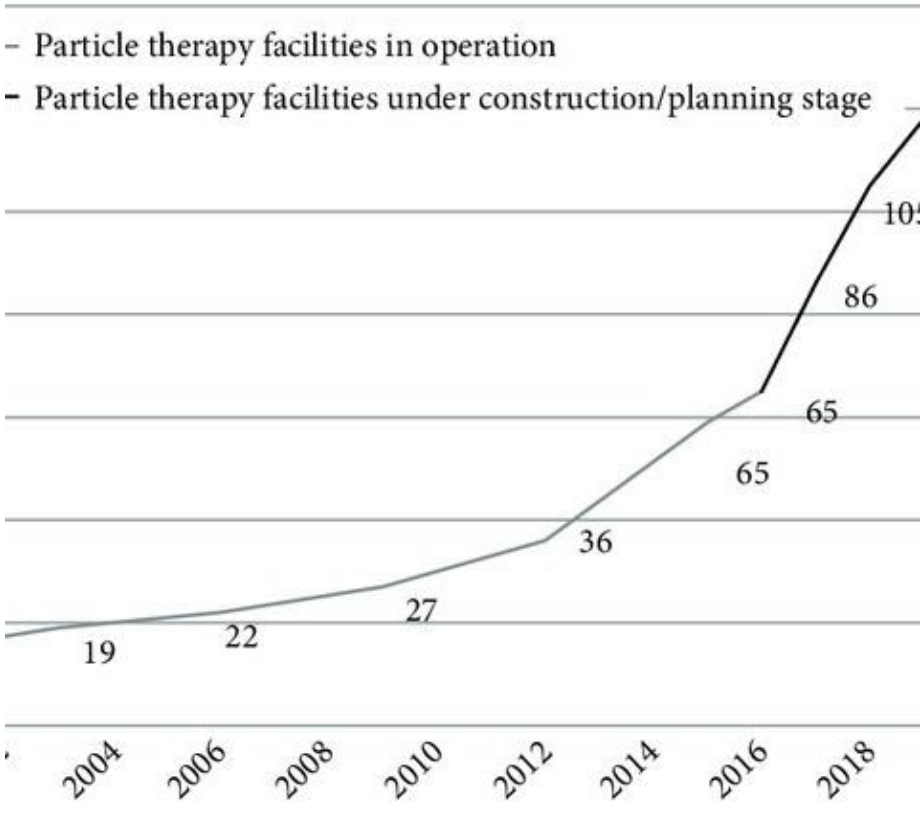
Particle therapy facilities in operation
Particle therapy facilities under construction/planning stage
19
22
27
36
65
65
86
2004
2006
2008
2010
2012
2014
2016
2018


Norm:Dose(60.000 Gy = 100%)
ref pnt X(cm): -1.27
Y(cm): -43.12
Z(cm): 6.45
dose(Gy): 59.987
local max(Gy):62.233
Isovalues(%)
DVH: 1000441,Proband^Dienst
100.00
80.00
60.00
40.00
20.00
0.00
0.00
20.00
40.00
60.00
80.00

Nanotechnology and its size range

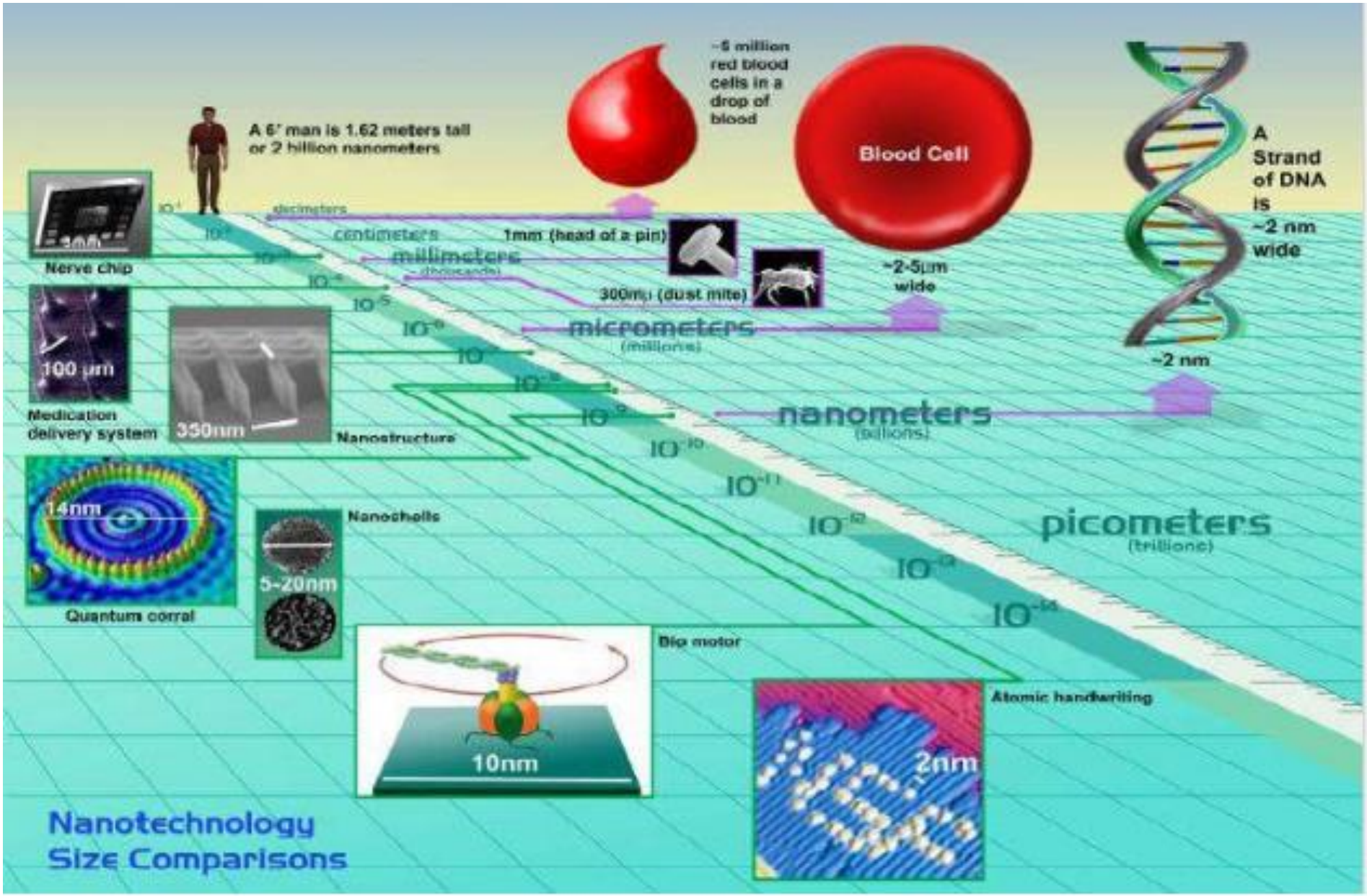

UNIVERSITÀ DEL PIEMONTE ORIENTALE

SUPSI
Scuola Universitaria Professionale
della Svizzera Italiana

UNIVERSITÀ DEGLI STUDI DI TORINO
ALMA UNIVERSITAS TAURINENSIS

Development of engineered magnetic nanoparticles for cancer therapy

Project supported by AIRC and Compagnia San Paolo

AIRC
ASSOCIAZIONE ITALIANA PER LA RICERCA SUL CANCRO

Compagnia di San Paolo

Integrative therapeutic anticancer approach

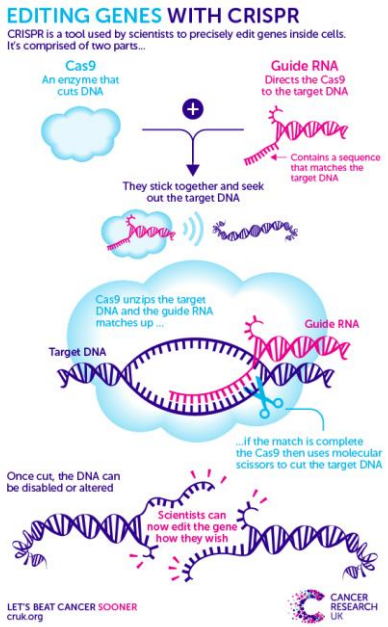

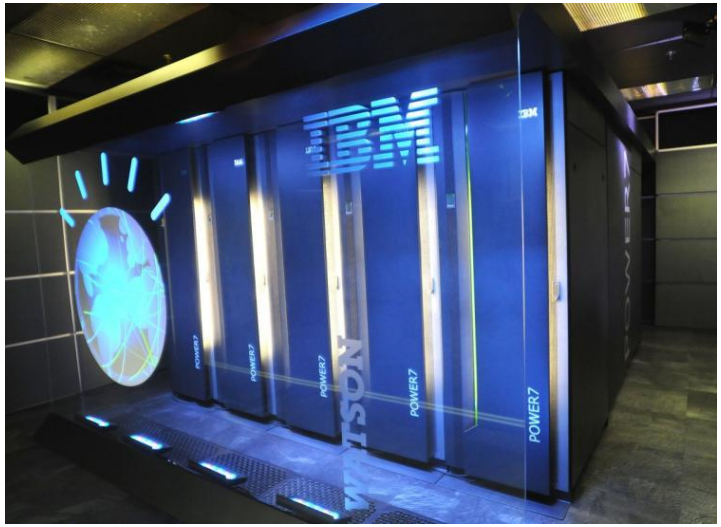

BIOMEDICINE

First trial of CRISPR in people

Chinese team approved to test gene-edited cells in people with lung cancer.

BY DAVID CYRANOSKI

Chinese scientists are on the verge of being first in the world to inject people with cells modified using the CRISPR–Cas9 gene-editing technique.

A team led by Lu You, an oncologist at Sichuan University's West China Hospital in Chengdu, received ethical approval to test the cells in people with lung cancer on 6 July, and plans to start the trial next month.

That timeline puts the proposal ahead of a planned US trial to test CRISPR–Cas9-modified cells, also for the treatment of cancer.

"It's an exciting step forward," says Carl June, a clinical researcher in immunotherapy at the University of Pennsylvania in Philadelphia.

Last month, the US trial was approved by an advisory panel of the US National Institutes of Health (NIH) but had yet to receive a green light from the US Food and Drug Administration (FDA) and a university review board. There have also been a number of human clinical trials using an alternative gene-editing technique, including one led by June, that have helped patients to combat HIV — but none so far has used CRISPR.

The Chinese trial will enrol patients who have metastatic non-small cell lung cancer and for whom chemotherapy, radiation therapy and other treatments have failed. "This technique is of great promise in bringing benefits to patients," says Lu.

CHROMOSOME SNIP

Lu's team will extract immune cells called T cells from the participants' blood, and use CRISPR–Cas9 technology — which pairs a molecular guide able to identify specific genetic sequences on a chromosome with an enzyme that can snip the chromosome at that spot — to knock out a specific gene in the

Nanomedicine and Cancer therapy

- Nanotechnology is at the forefront of both targeted drug delivery and intrinsic therapies.
- Nanoparticles can already be injected into the tumor and then be **activated to produce heat** and destroy cancer cells locally either by magnetic fields, X-Rays or light.
- The **encapsulation of existing chemotherapy drugs or genes** allows much more **localized delivery** both **reducing significantly the quantity of drugs absorbed by the patient for equal impact and the side effects on healthy tissues in the body**.

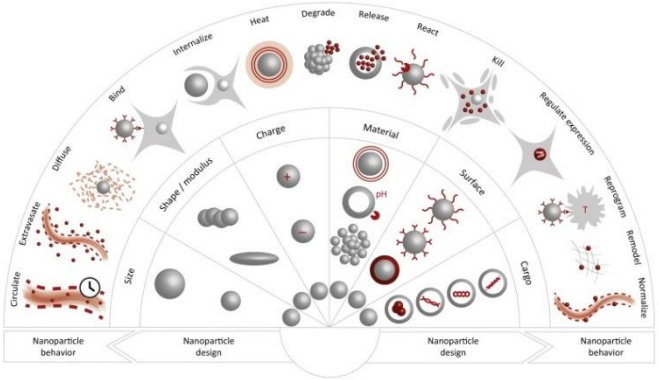

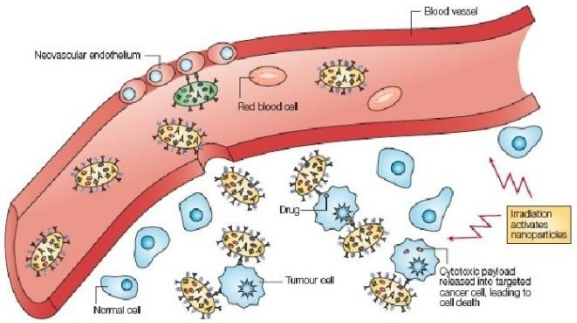

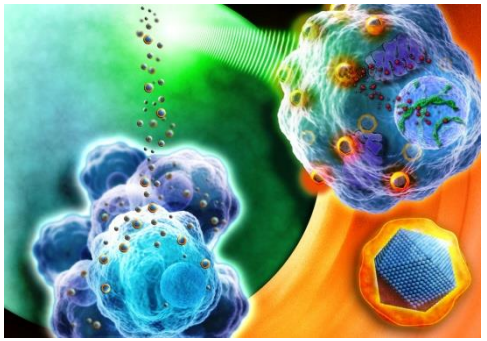

Beik J et al. J Control Release. 2016; 235:205-21.

Multifunctional theranostic nanoparticles

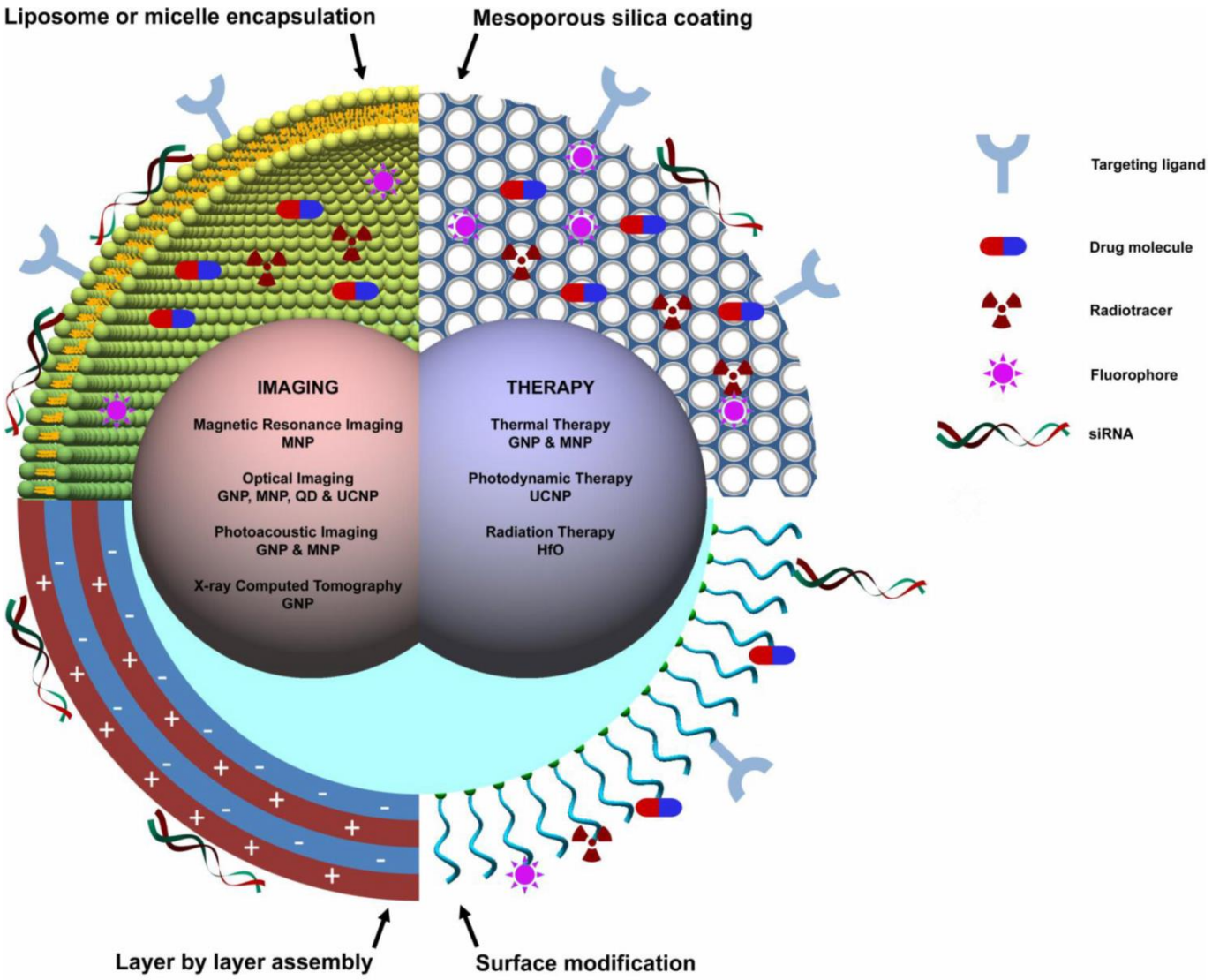

Sheng Tong et al. Ann Biomed Eng. 2014; 42(2): 243–259.

Targeted nano-drug delivery in tumor microenvironment

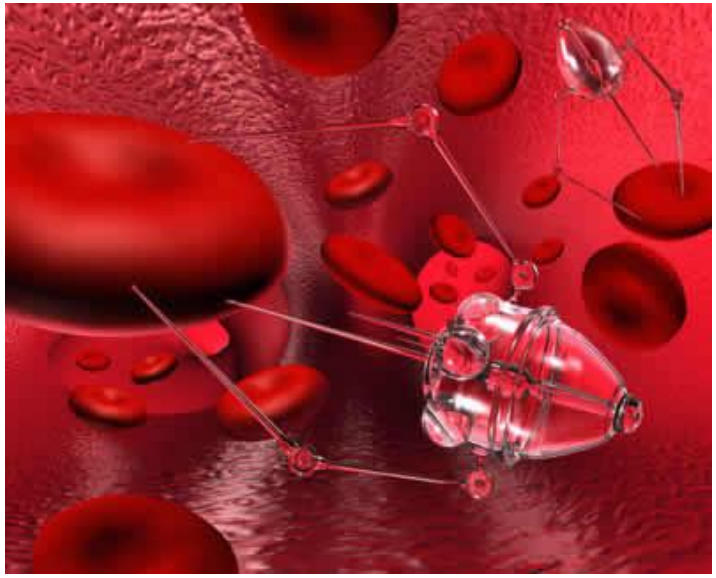

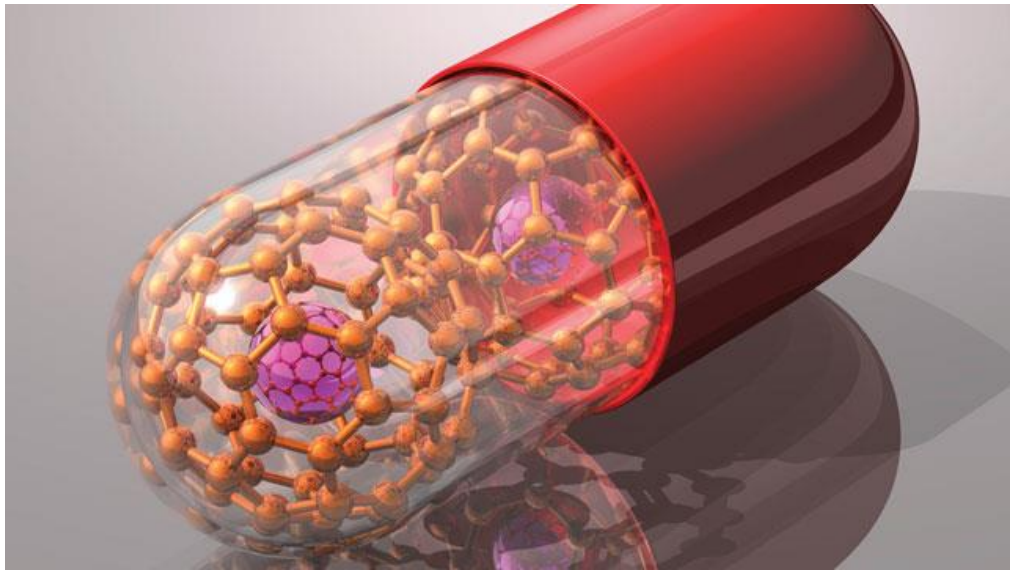

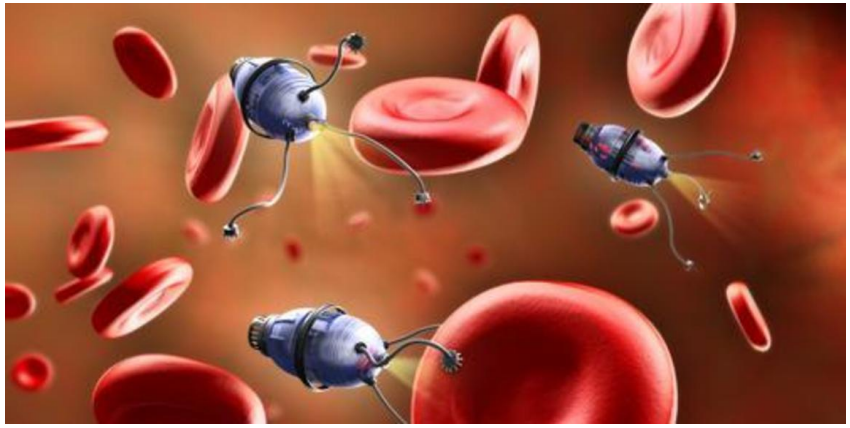

Drug targeting strategies and nanomedicine therapeutics in cancer care

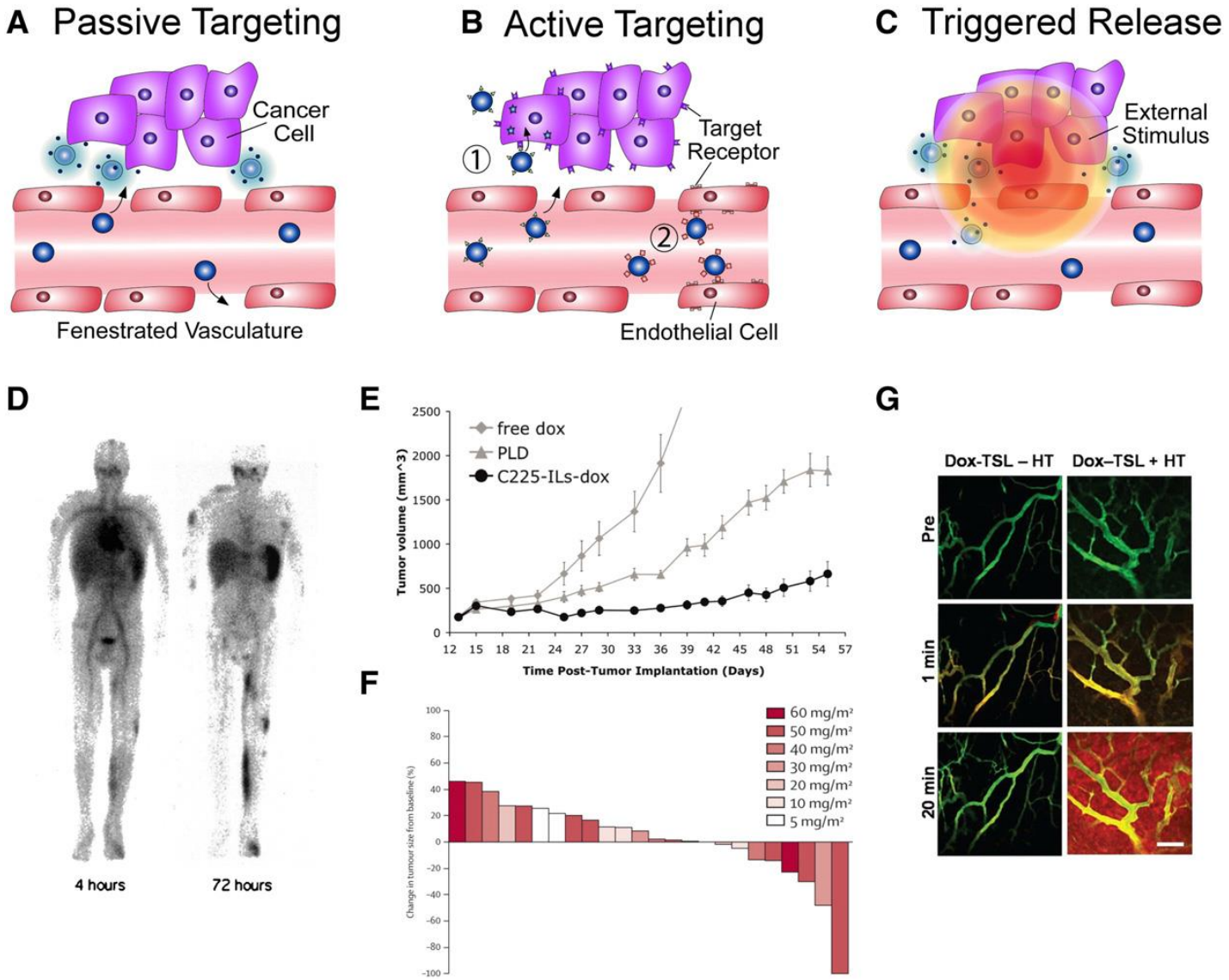

Wicki A et al., J Control Release. 2015; 200:138-57

Nanotherapeutic platforms

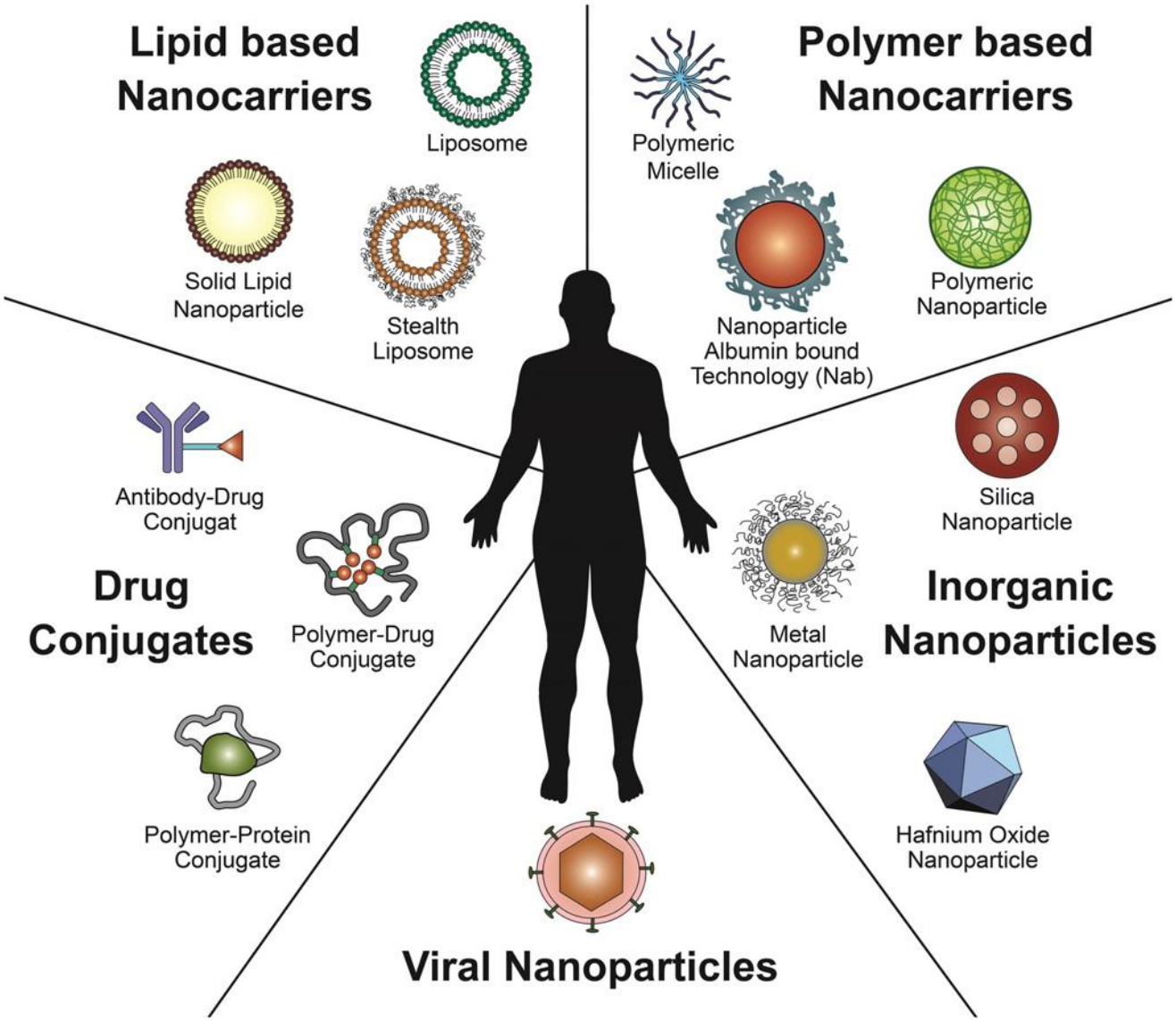

Wicki A et al., J Control Release. 2015; 200:138-57

Targeted drug delivery in cancer therapy

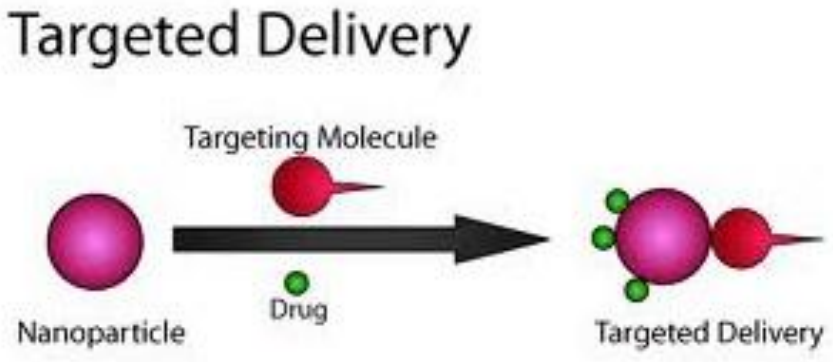

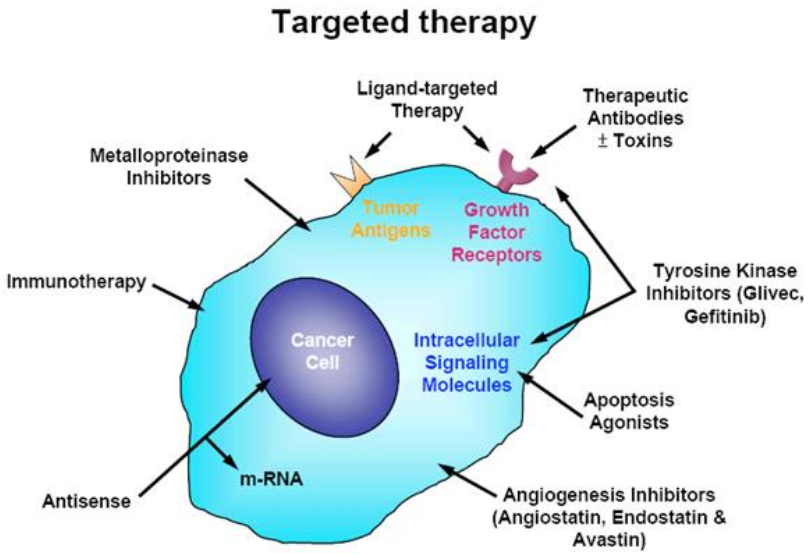

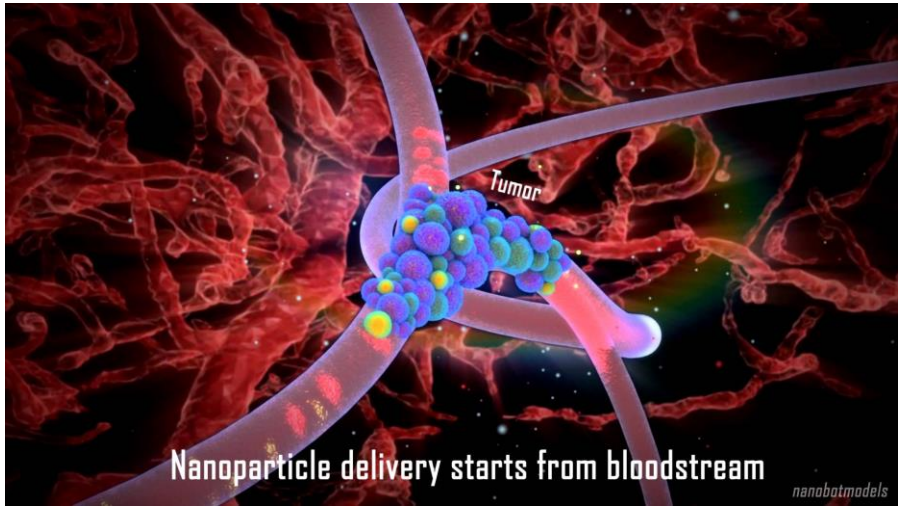

Applications of MNPs in biomedicine

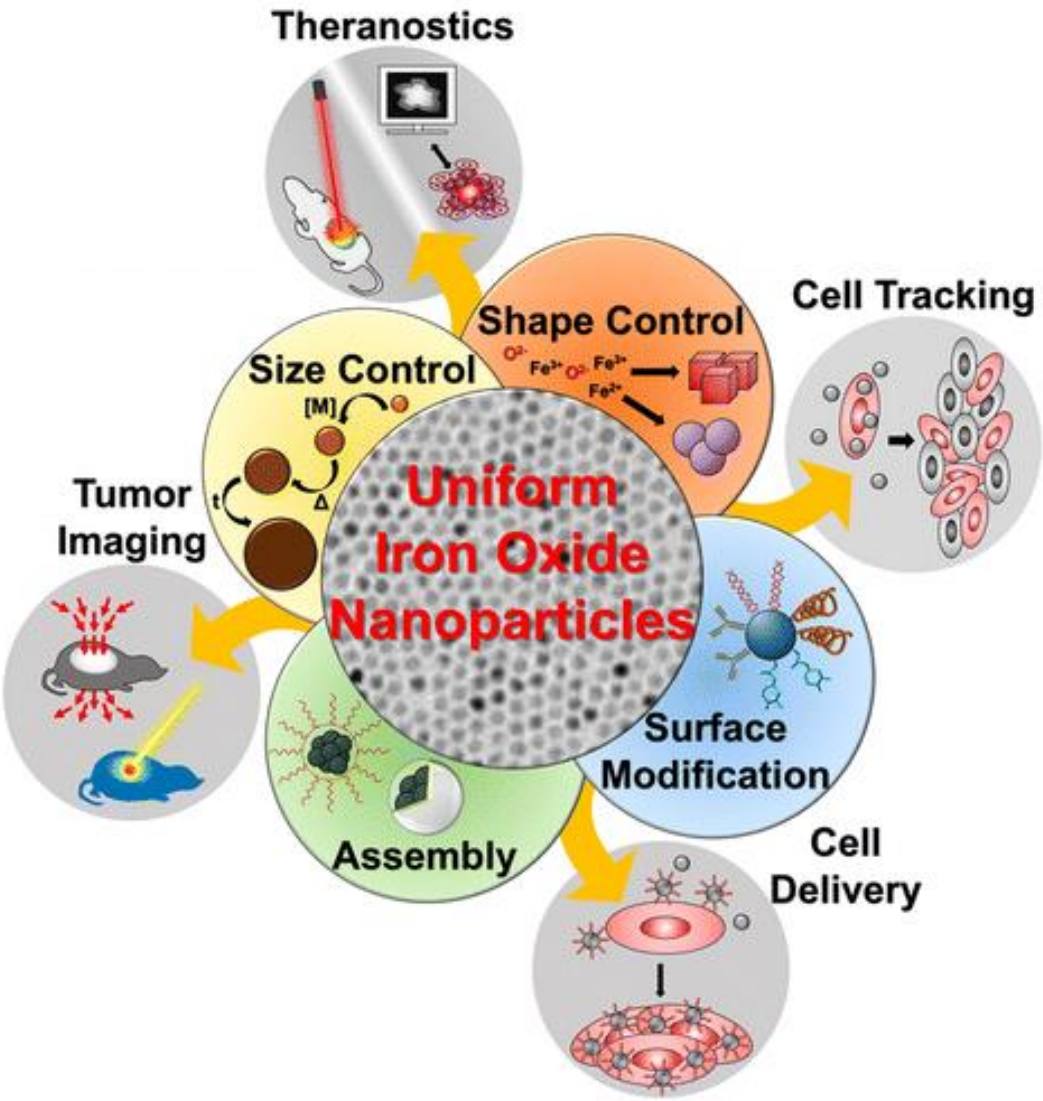

Daishun Ling et al. Acc. Chem. Res. 2015

Biomedical applications of iron-oxide nanoparticles

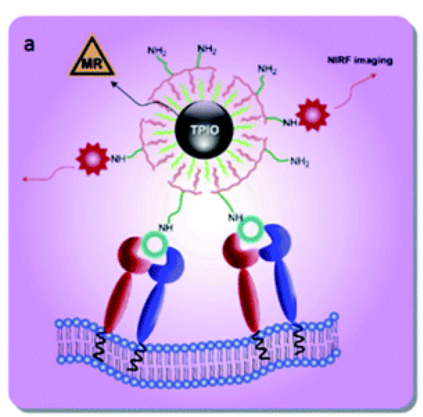

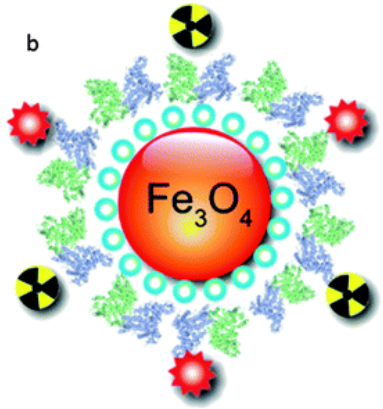

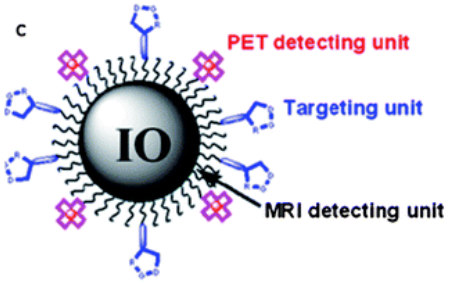

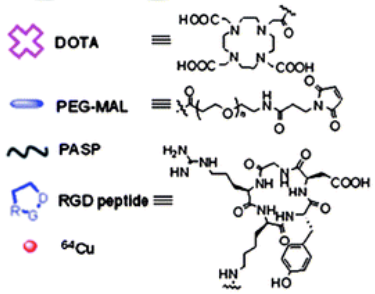

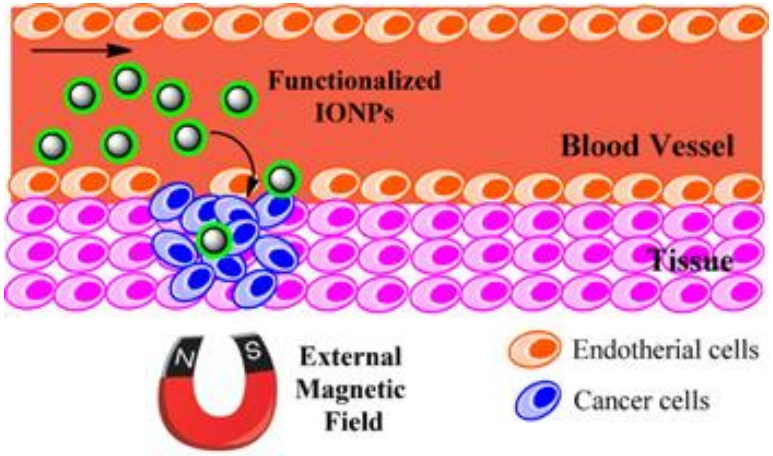

Hyperthermia to Treat Cancer by using magnetic nanoparticles

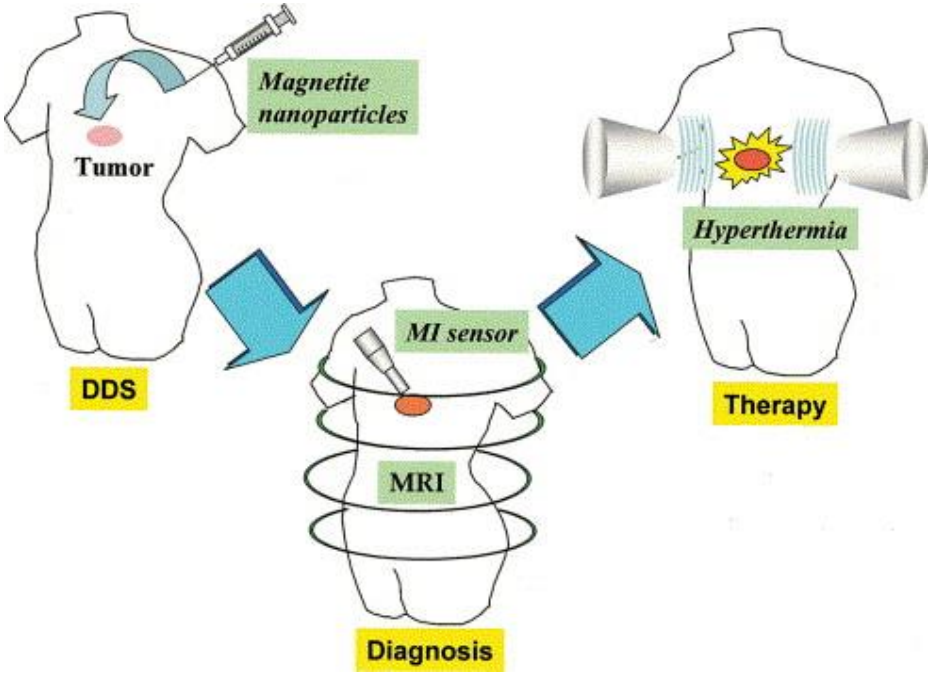

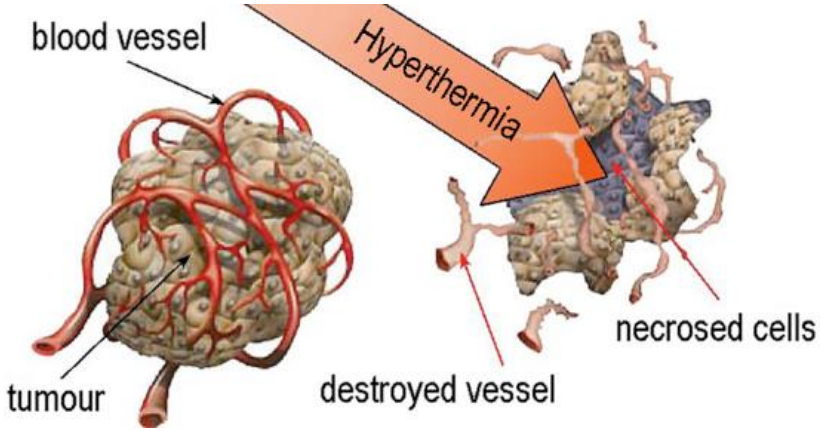

Magnetic nanoparticle heating in an AC magnetic field for magnetic hyperthermia

- When magnetic nanoparticles are subjected to an AC magnetic field they show heating effects due to losses during their magnetization reversal process. This remarkable heating effect shown by magnetic nanoparticles has opened up numerous applications within the natural sciences sector.

In the magnetic nanoparticles the heat generation is mainly through the following phenomenon

- **Hysteresis loss**
- **Néel relaxation loss**
- **Brown relaxation loss**
- **Losses due to friction in viscous suspensions**

Heat generation through Néel relaxation is due to rapid changes in the direction of magnetic moments, hindered by anisotropy energy that tends to turn the magnetic domain of the magnetic nanoparticle in a given direction according to their crystal lattice structure.

S. Laurent et al. / Advances in Colloid and Interface Science 166 (2011) 8–23

Advantages for the use of superparamagnetic iron-oxide nanoparticles (SPIONs) in cancer therapy

Iron-oxide nanoparticles offer distinct advantages over other drug delivery platforms used with anticancer medications:

a) **The pharmacokinetics of SPIONs are easily determined using non-invasive imaging techniques such as nuclear magnetic resonance (NMR);**
b) **SPIONs can easily be guided to cancer tissues using the electromagnetic field (EM);**
c) **SPIONs can selectively generate energy to destroy cancer cells;**
d) **and when functionalized with antibodies against cancer biomarkers, SPIONs can selectively deliver a "cocktail" of therapeutic pharmaceuticals.**

Radomska A et al. Adv Clin Exp Med. 2016; 25(1):151-62.

Biomedical applications of magnetic nanoparticles

- The possibility to convert dissipated magnetic energy into thermal energy in magnetic nanoparticles could led to an increase in research within the biomedical sciences sector and this technique has the following significant advantages

- 1) Cancer treatment by artificially inducing hyperthermia to kill cancer cells without affecting the nearby healthy tissue.
- 2) MNP's (Magnetic Nanoparticles) absorbed by cells through endocytosis, help to deliver therapeutic heat directly to the cells when subjected to AC magnetic field.
- 3) Cell specific binding made possible through surface functionalization of magnetic nanoparticles with biomolecules i.e. target specificity.
- 4) Controlled delivery of drugs using magnetic nanoparticles surface functionalized with thermo labile drugs or using thermo sensitive catheters/ stents set to release via magnetic nanoparticles when subjected to an AC magnetic field.

S. Laurent et al. / Advances in Colloid and Interface Science 166 (2011) 8–23

Physics of magnetism

$$B = \mu_0(H + M)$$

$$E(\theta) = (K_V V + K_S S)\, sin^2\theta$$

$$\tau = \tau_0 e^{\left(\frac{\Delta E}{k_B T}\right)}$$

$$SAR = 4.1868\frac{P}{m_e} = C_e\frac{dT}{dt}$$

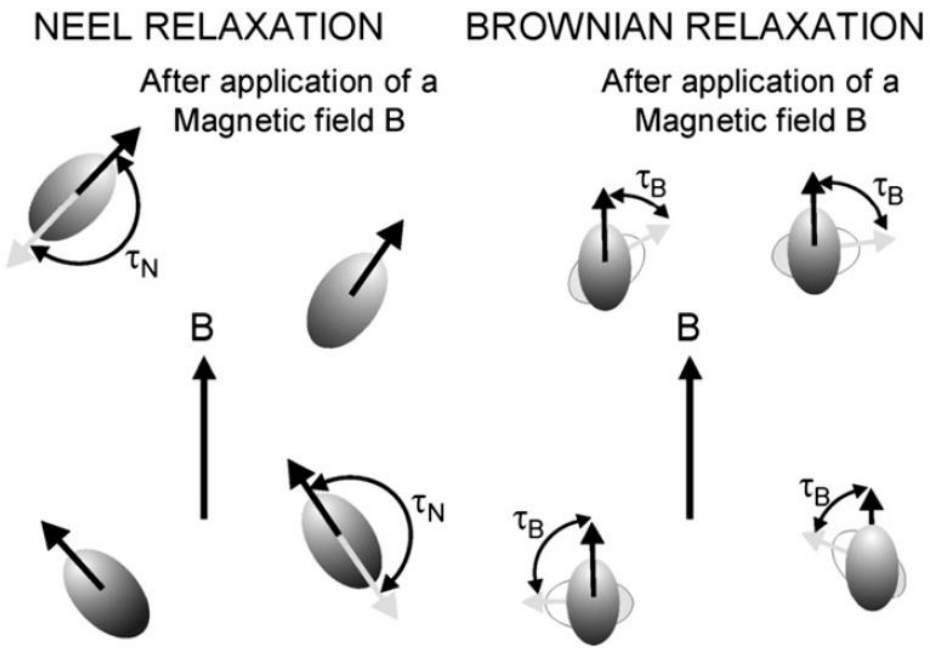

S. Laurent et al. / Advances in Colloid and Interface Science 166 (2011) 8–23

Article about applications of Iron oxide nanoparticles on tumor tissues on Nature Nanotechnology

nature nanotechnology

ARTICLES

PUBLISHED ONLINE: 26 SEPTEMBER 2016 | DOI: 10.1038/NNANO.2016.168

Iron oxide nanoparticles inhibit tumour growth by inducing pro-inflammatory macrophage polarization in tumour tissues

Saeid Zanganeh[1,2], Gregor Hutter[2,3], Ryan Spitler[1], Olga Lenkov[1,2], Morteza Mahmoudi[4], Aubie Shaw[5], Jukka Sakari Pajarinen[6], Hossein Nejadnik[1,2], Stuart Goodman[6], Michael Moseley[1], Lisa Marie Coussens[5] and Heike Elisabeth Daldrup-Link[1,2,7]*

Until now, the Food and Drug Administration (FDA)-approved iron supplement ferumoxytol and other iron oxide nanoparticles have been used for treating iron deficiency, as contrast agents for magnetic resonance imaging and as drug carriers. Here, we show an intrinsic therapeutic effect of ferumoxytol on the growth of early mammary cancers, and lung cancer metastases in liver and lungs. *In vitro*, adenocarcinoma cells co-incubated with ferumoxytol and macrophages showed increased caspase-3 activity. Macrophages exposed to ferumoxytol displayed increased mRNA associated with pro-inflammatory Th1-type responses. *In vivo*, ferumoxytol significantly inhibited growth of subcutaneous adenocarcinomas in mice. In addition, intravenous ferumoxytol treatment before intravenous tumour cell challenge prevented development of liver metastasis. Fluorescence-activated cell sorting (FACS) and histopathology studies showed that the observed tumour growth inhibition was accompanied by increased presence of pro-inflammatory M1 macrophages in the tumour tissues. Our results suggest that ferumoxytol could be applied 'off label' to protect the liver from metastatic seeds and

Multiple therapeutic approach of the project

Targeted chemotherapy

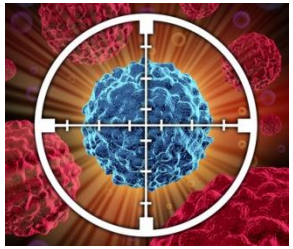

Cancer gene therapy

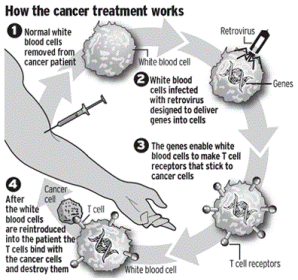

Hyperthermia in the cancer site

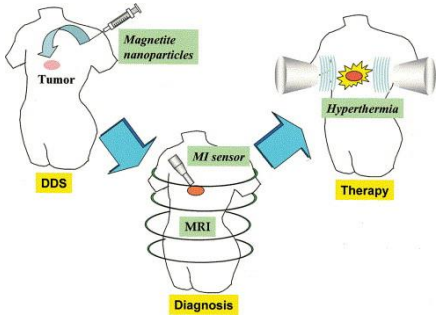

Objectives of the experimental work

- Physicochemical and biological characterization and validation of iron-oxide nanoparticles (MNPs or SPIONs) to be used in cancer therapy and biomedicine

Different applications of magnetic nanoparticles

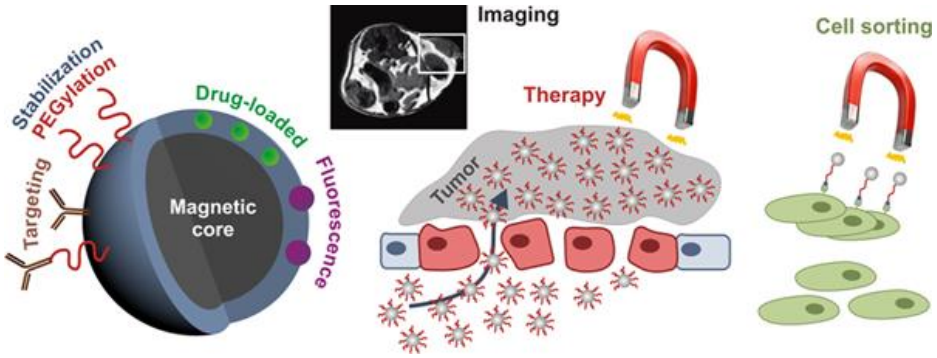

Industrial applications

Drug delivery

Hyperthermia

Tissue engineering and repair

Magnetic resonance imaging (MRI)

Biosensing and Bioanalysis

Biochemical separations

L. Harivardhan Reddy et al., Chem. Rev. 2012

Fe_3O_4

MNPs were prepared by coprecipitation…

*37.5ml 0.1M $FeCl_2 \cdot 4H_2O$

\+

50ml 0.1M $FeCl_3 \cdot 6H_2O$

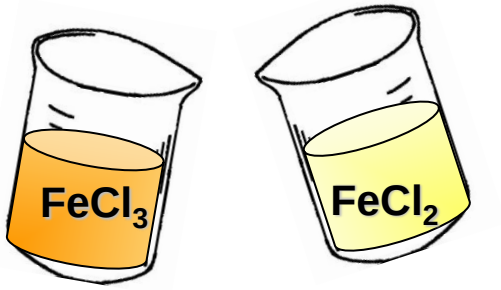

pH≅10

+ NH_4OH

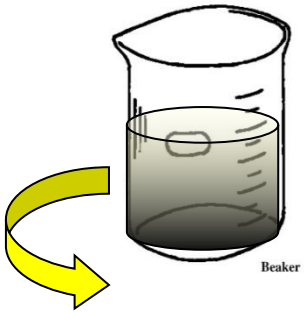

Mechanical stirring

Magnetite

$Fe^{2+} + 2Fe^{3+} + 8OH^- \rightarrow Fe_3O_4 + 4H_2O$

Maghemite

$2Fe_3O_4 + O_2 \rightarrow 3\gamma\text{-}Fe_2O_3$

…and dispersed in citric acid 0.05 M:

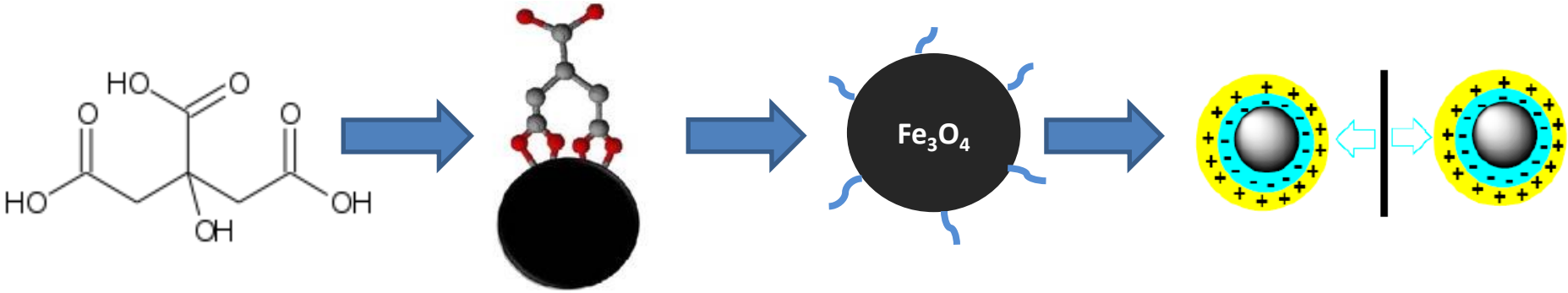

* Li Z., Kawashita M., Araki N., Mitsumori M., Hiraoka M., Doi M., 2010, Magnetite nanoparticles with high heating efficiencies for application in the hyperthermia of cancer. *Materials Science and Engineering C*, **30**, 990–996.

Silica shell coating (Mag-SiO_2 NPs): the silica shell was obtained by wet chemistry on the magnetic core stabilized with citric acid

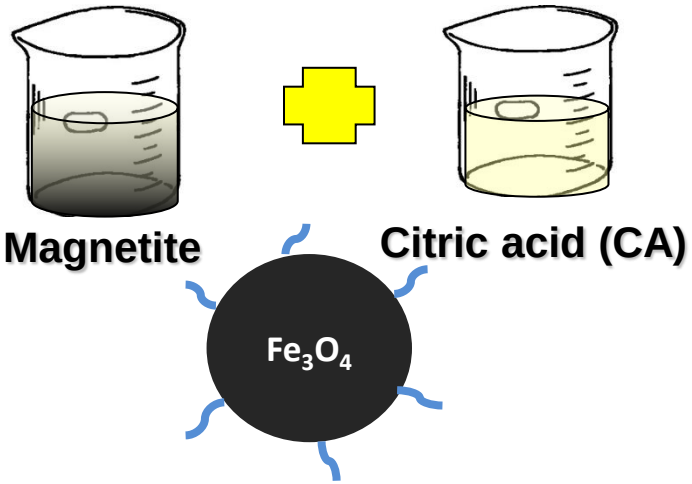

+

NH_4OH
(pH≈10)

water

ethanol

TEOS

(Stöber)

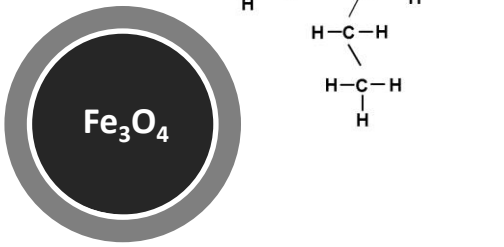

Mag-SiO_2

*[1] Singh R. K., Kim T. H., Patel K. D., 2012, *J Biomed Mater Res Part A*, published online in Wiley Online Library (wileyonlinelibrary.com)
*[2] Stöber W., Fink A., 1968, Controlled Growth of Monodisperse Silica Spheres in the Micron Size Range. *Journal of colloidal and interface science*, **26**, 62-69

Silica-Calcium shell coating (Mag-SiO_2-Ca(3) NPs) was obtained using two different precursors: calcium citrate and calcium hydroxide

Magnetite

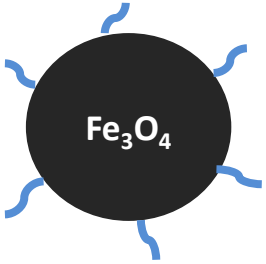

Citric Acid
0.05M

+

Ca citrate/
Ca hydroxide
water
ethanol
TEOS
(Stöber)

Si:Ca ratio 99:1

Mag-SiO_2-Ca(3)

NH_4OH
(pH≈10)

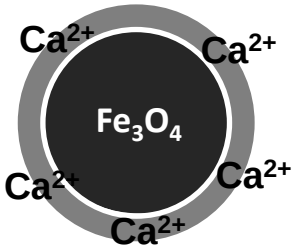

Mag-SiO_2-Ca(3)

*1 Singh R. K., Kim T. H., Patel K. D., 2012, *J Biomed Mater Res Part A*, published online in Wiley Online Library (wileyonlinelibrary.com)
*2 Stöber W., Fink A., 1968, Controlled Growth of Monodisperse Silica Spheres in the Micron Size Range. *Journal of colloidal and interface science*, **26**, 62-69

General characteristics of iron-oxide nanoparticles

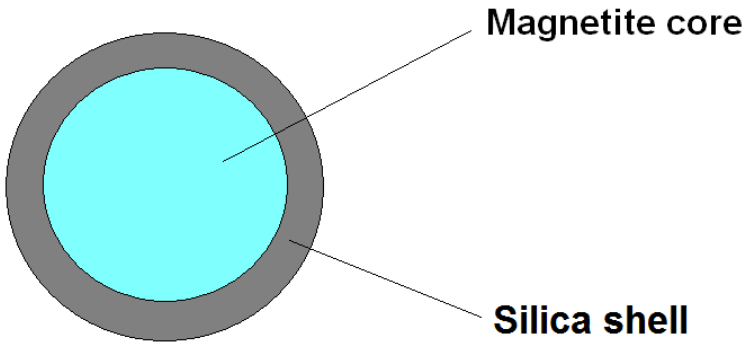

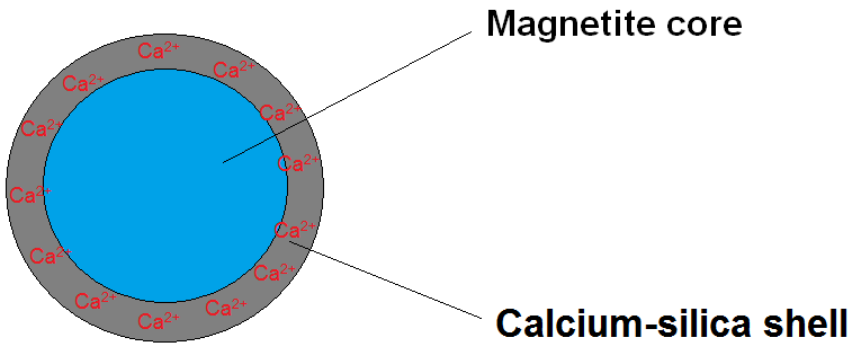

Type of nanoparticle	Medium	pH approx	Concentration
Magnetite (Fe_3O_4)	Water	9.6	1,8 mg/ml
Magnetite – silica (Fe_3O_4-SiO_2)	Water	7.9	3,4 mg/ml
Magnetite – silica – calcium (99:1) – Fe_3O_4-SiO_2-Ca(3) CITR	Water	9.2	4,4 mg/ml
Magnetite – silica – calcium (99:1) – Fe_3O_4-SiO_2-Ca(3) IDR	Water	8.3	4,5 mg/ml

Physicochemical characterization of MNPs

- The magnetic nanoparticles were characterized for:

→ Morphology and size (FESEM, TEM)

→ Surface chemical properties (EDS probe)

→ Superparamagnetic behavior of MNPs (Magnetic hysteresis)

→ Heating ability of MNPs in a magnetic field

→ Colloidal stability (Zeta potential)

TEM images of MNPs

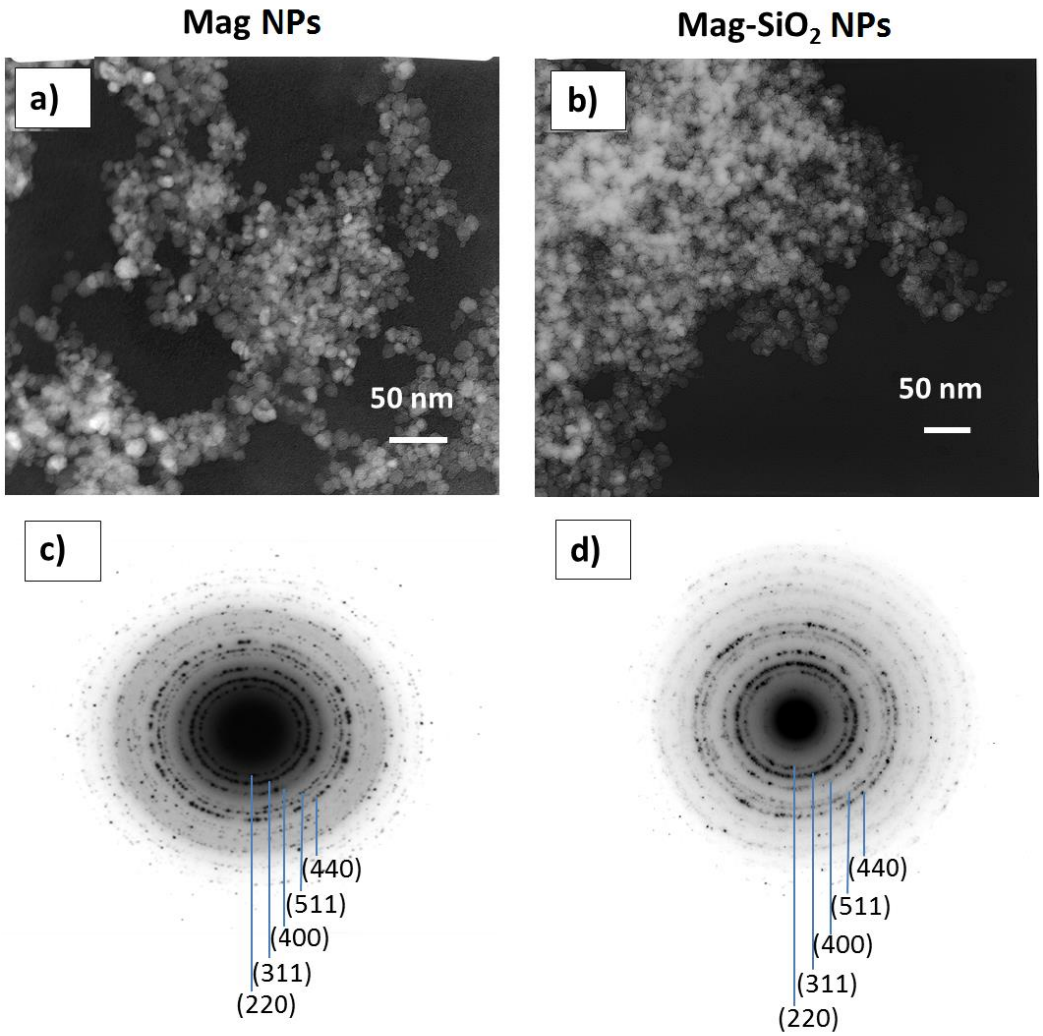

TEM Images and SAED patterns of Fe_3O_4 and Fe_3O_4 -SiO_2 samples. a) TEM image of Fe_3O_4, b) SAED pattern of Fe_3O_4, c) TEM image of Fe_3O_4-SiO_2, d) SAED pattern of Fe_3O_4-SiO_2.

FESEM images of MNPs

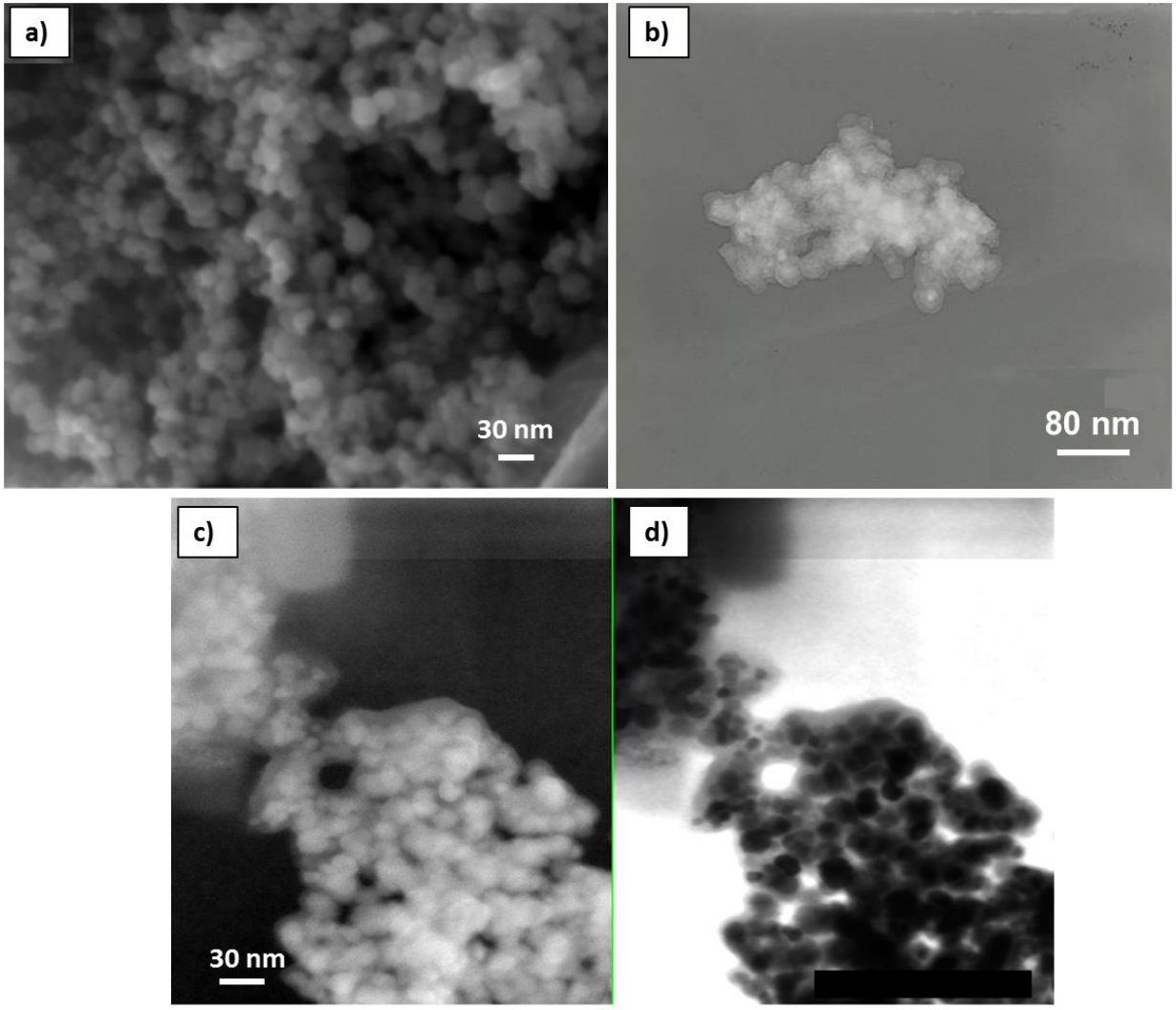

FESEM (a), **TEM** (b) and **STEM** (c - dark field mode, d - bright field mode) images of Fe_3O_4-SiO_2 NPs.

STEM images of iron-oxide nanoparticles

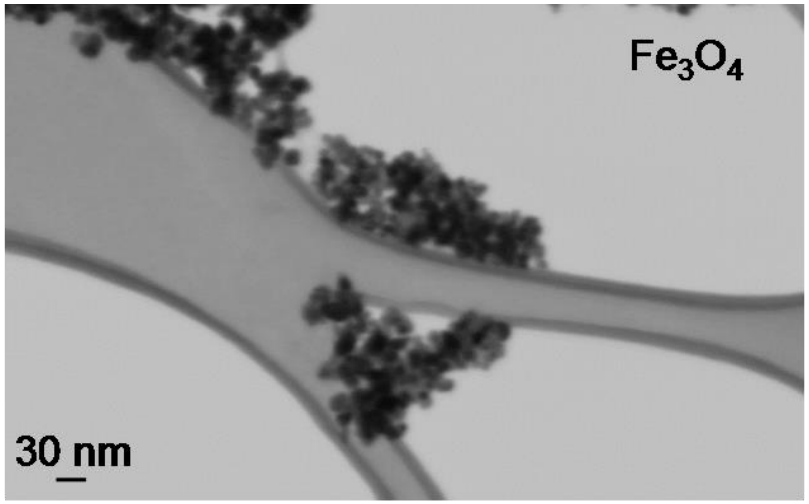

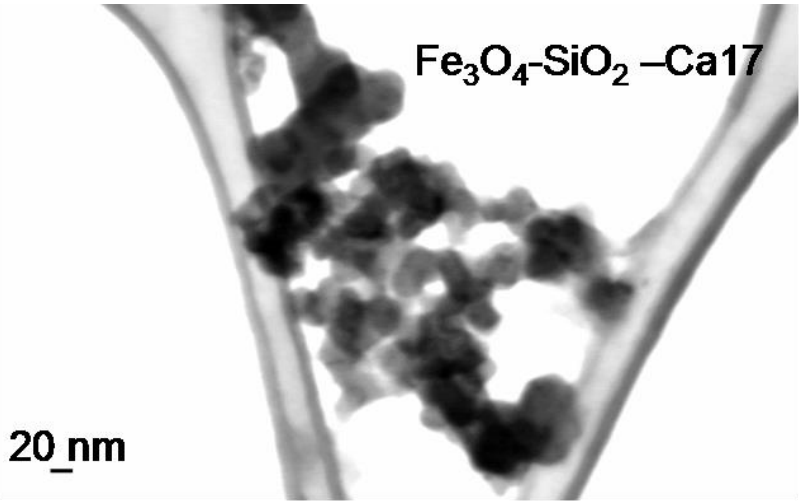

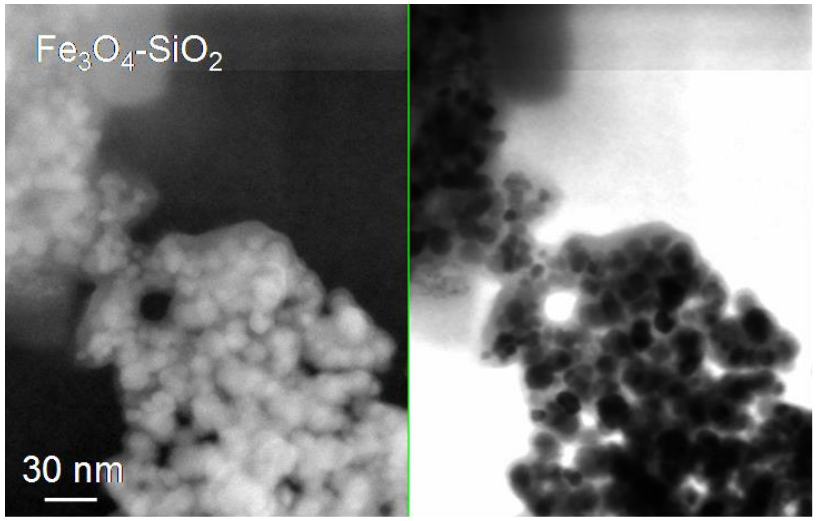

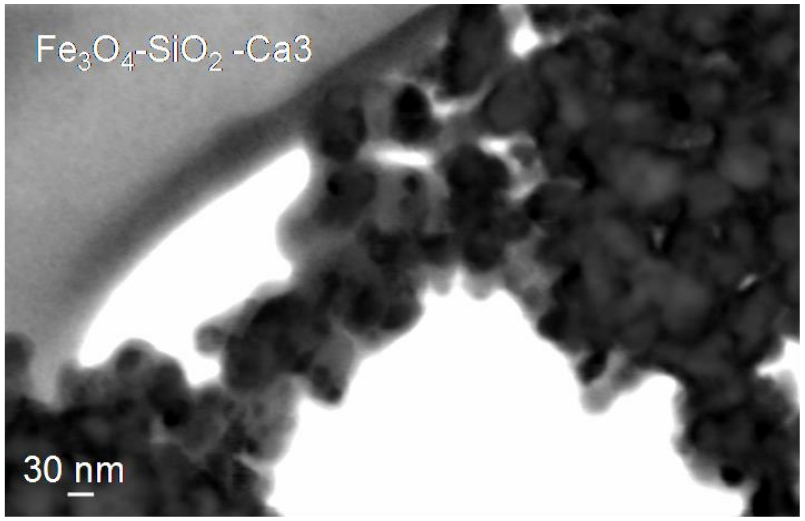

EDS analyses of iron-oxide nanoparticles

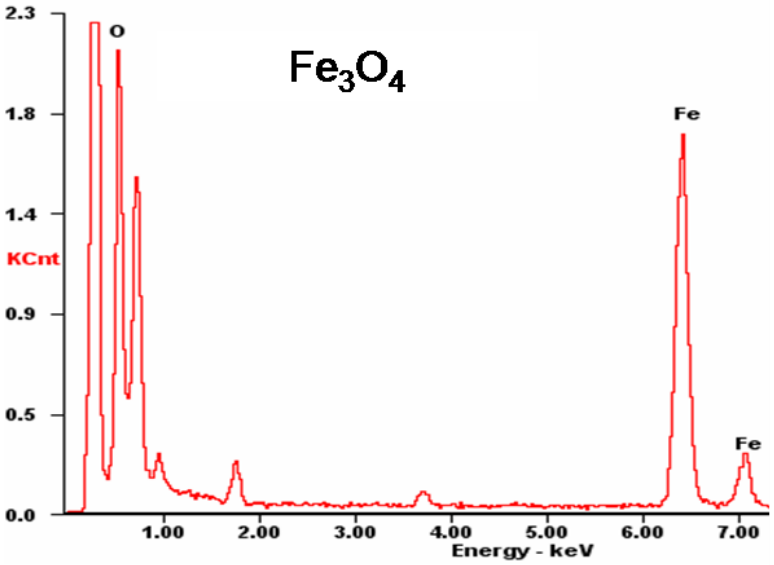

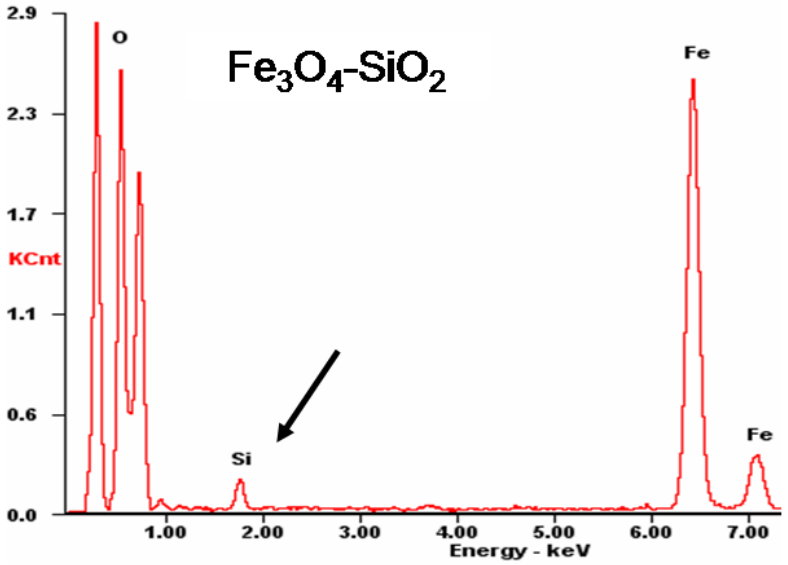

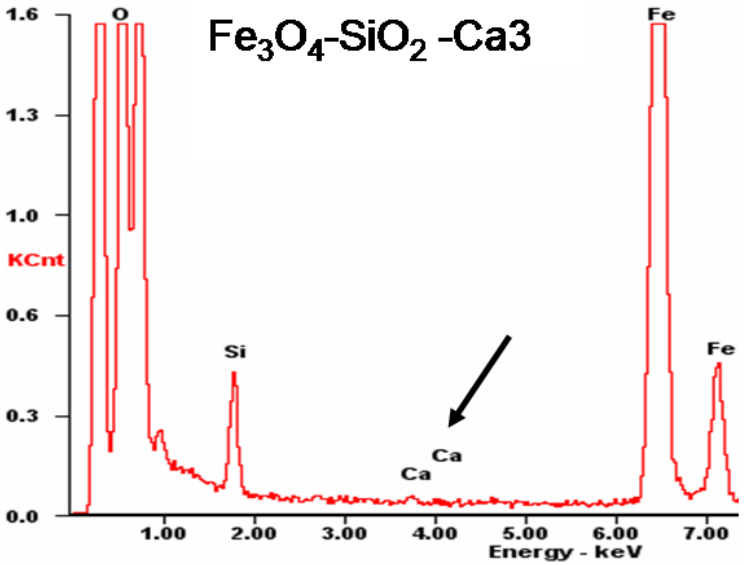

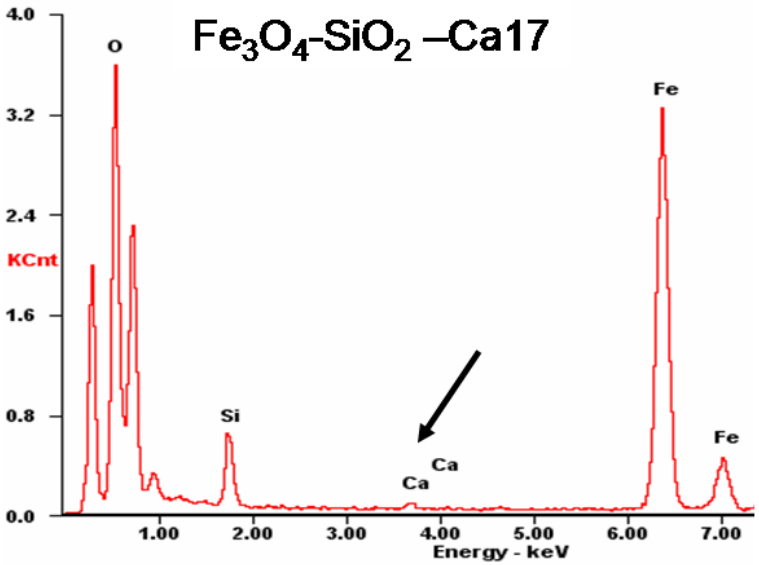

TEM images of iron-oxide nanoparticles

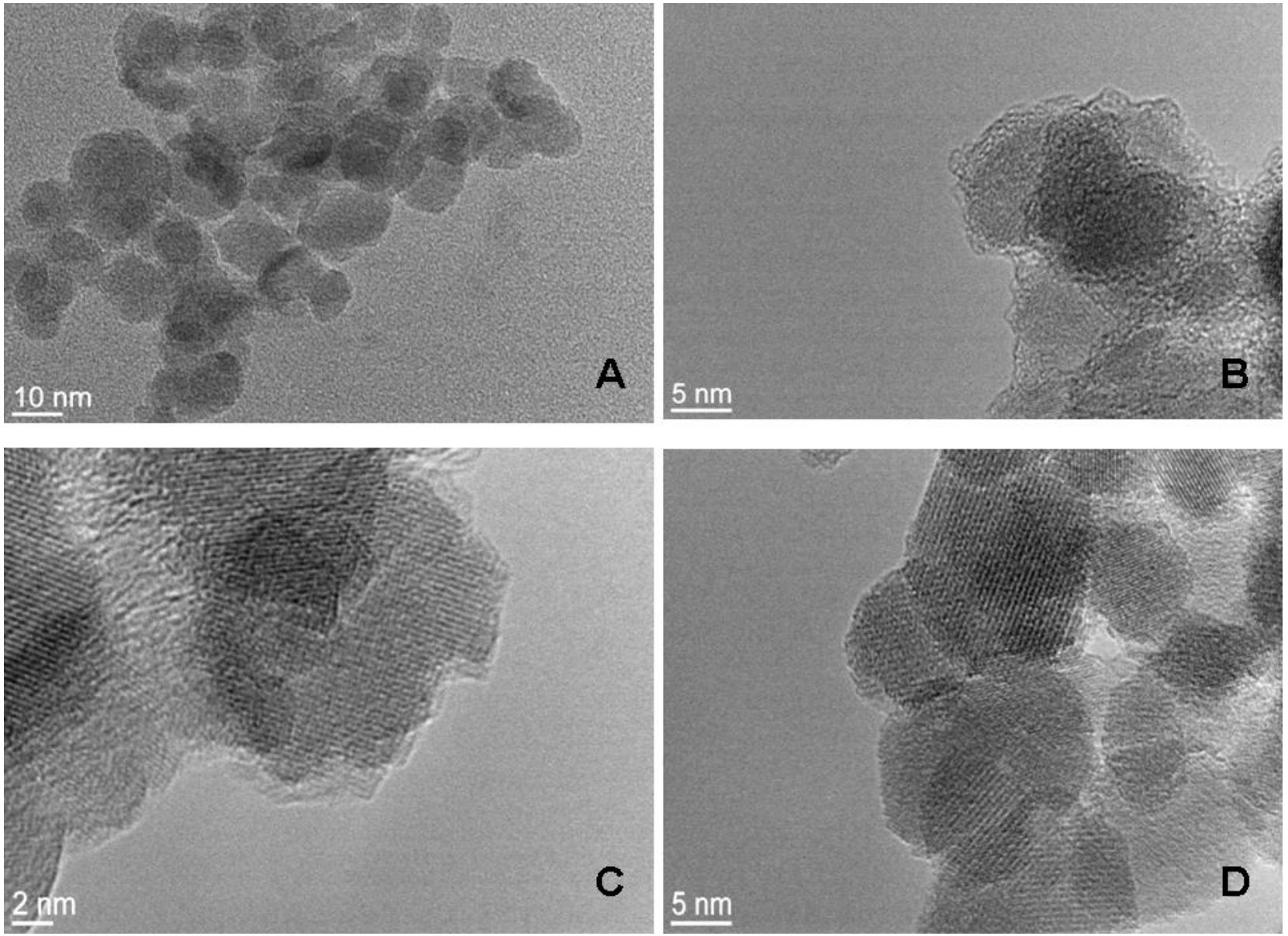

TEM images: Fe_3O_4 (A), Fe_3O_4-SiO_2 (B), Fe_3O_4-SiO_2-Ca3 (C), Fe_3O_4-SiO_2-Ca17 (D) nanoparticles.

Characterization of Fe_3O_4 NPs: TEM - FESEM - EDS

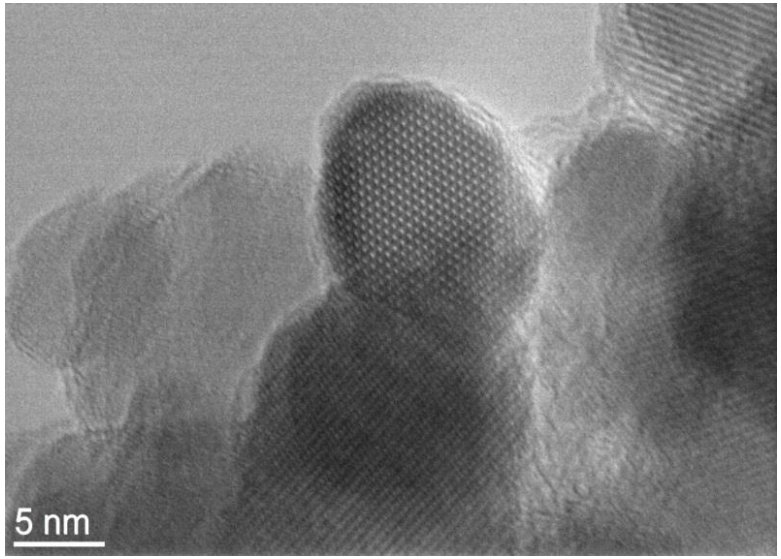

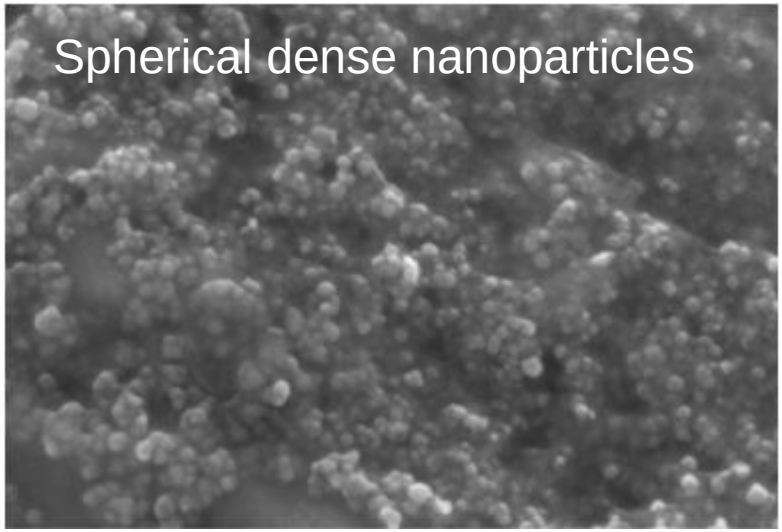

Diffraction signals of magnetite

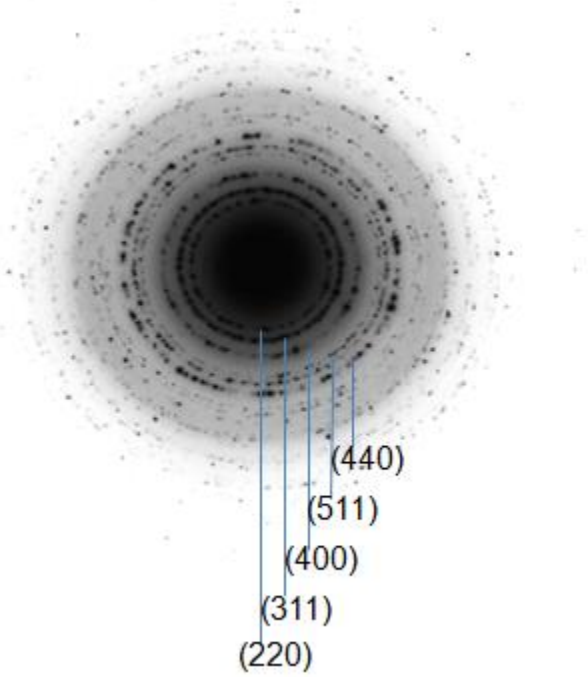

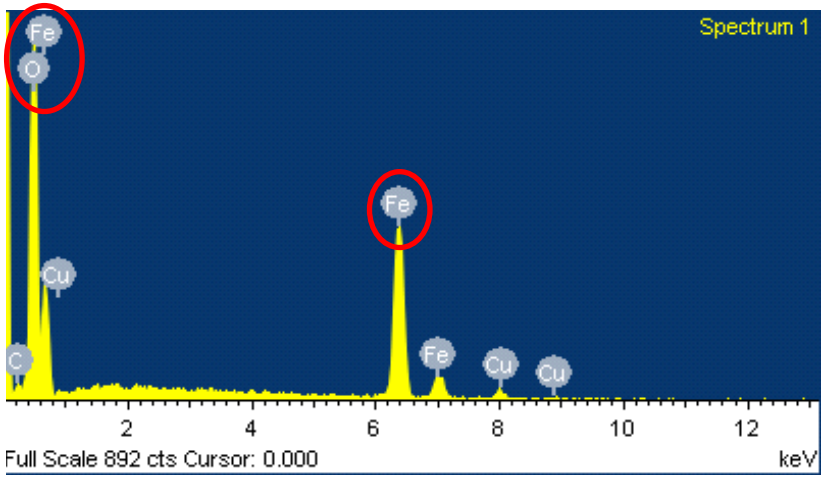

Fe_3O_4-SiO_2 NPs: TEM – FESEM - EDS

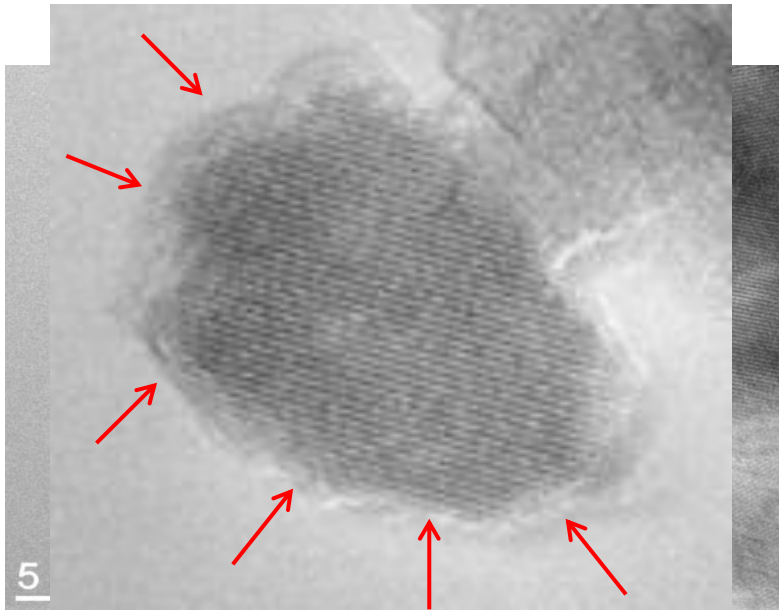

- Diffraction signals of magnetite
- Halo for the amorphous phase

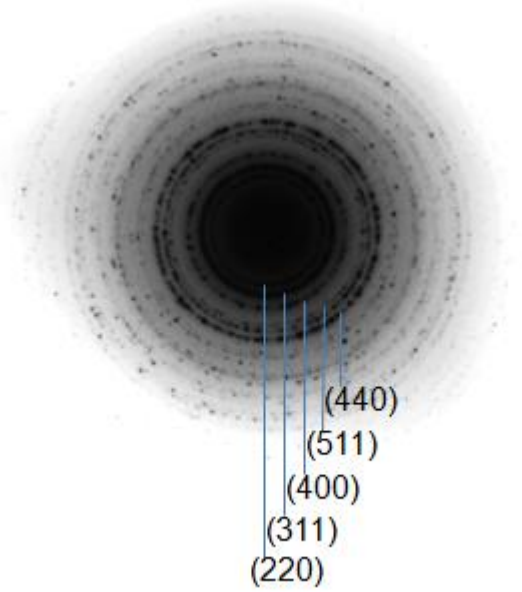

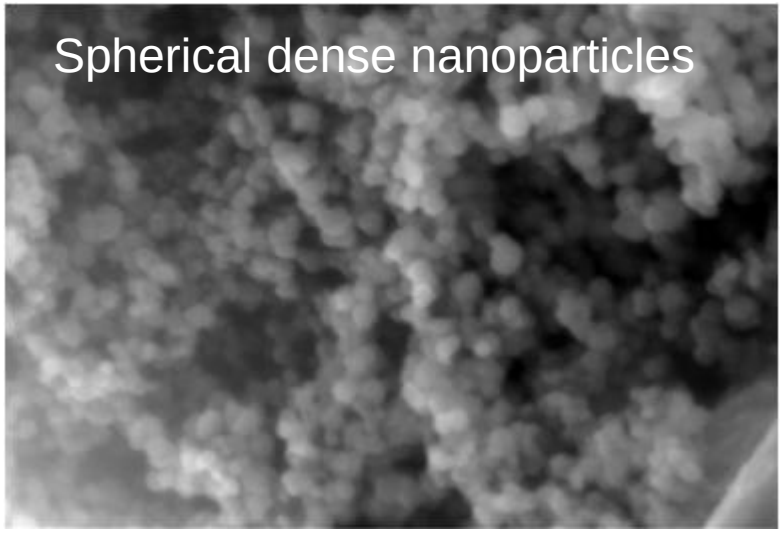

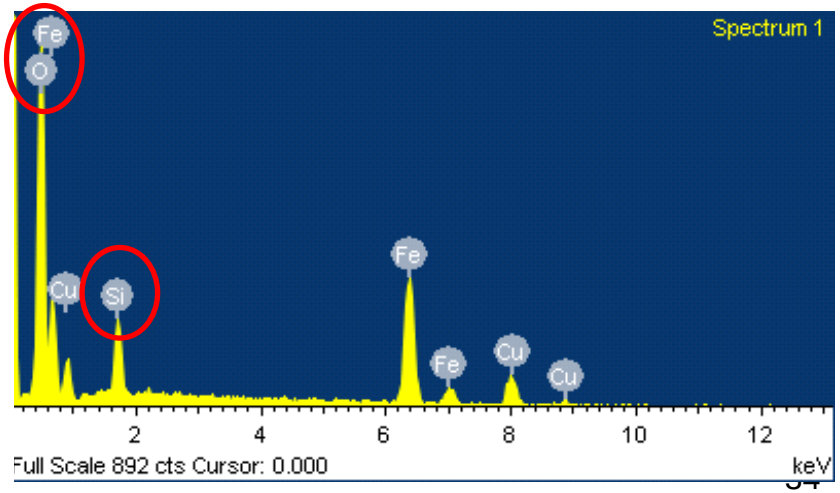

Fe_3O_4-SiO_2-Ca(3) NPs: TEM - FESEM - EDS

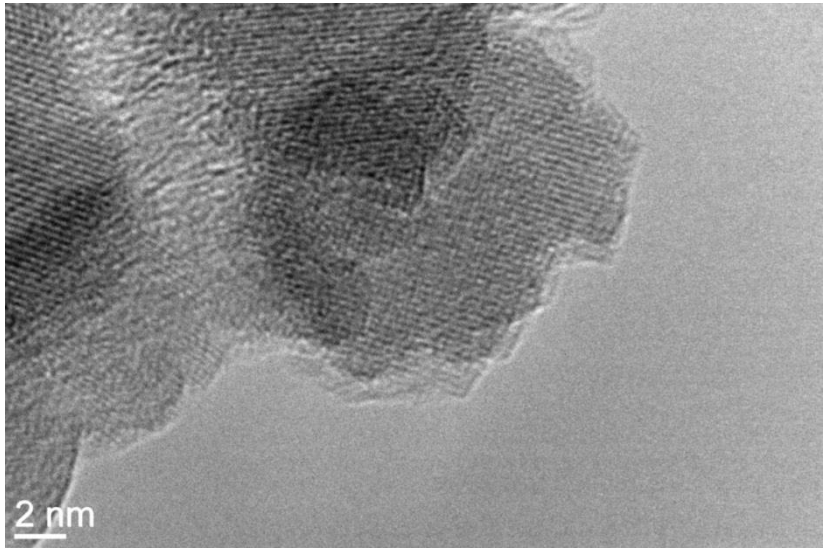

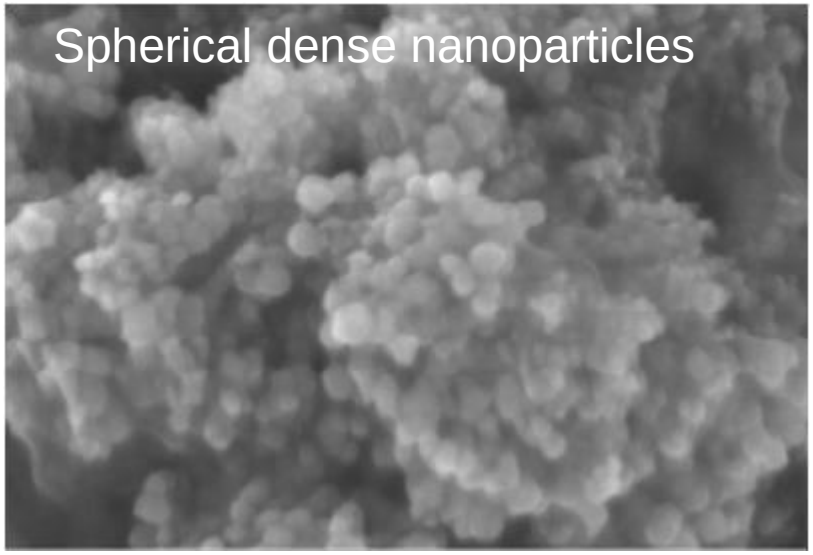

- Diffraction signals of magnetite

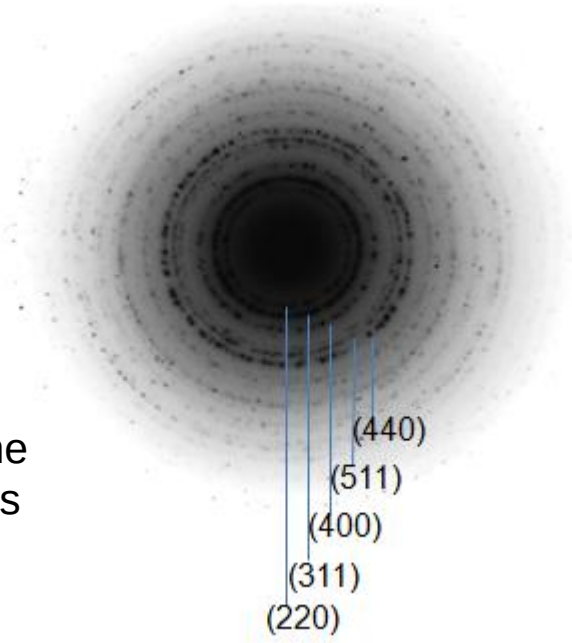

- Halo for the amorphous phase

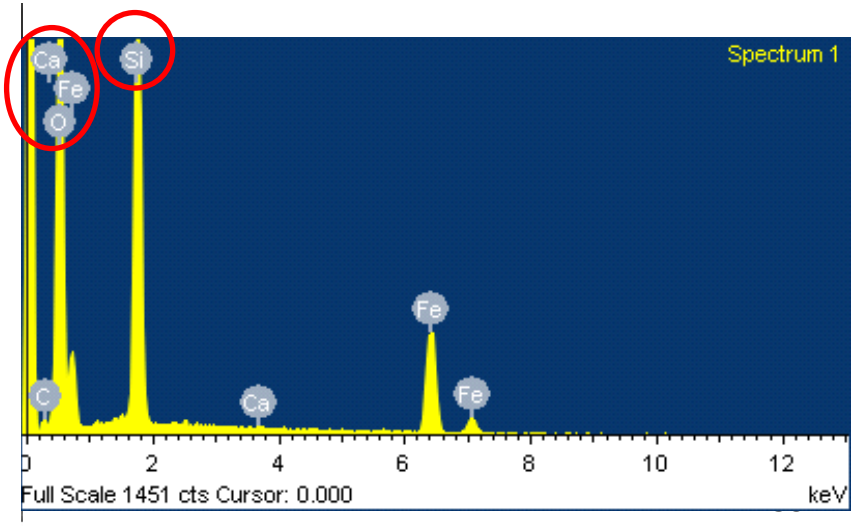

Iron oxide nanoparticles - AFM/MFM

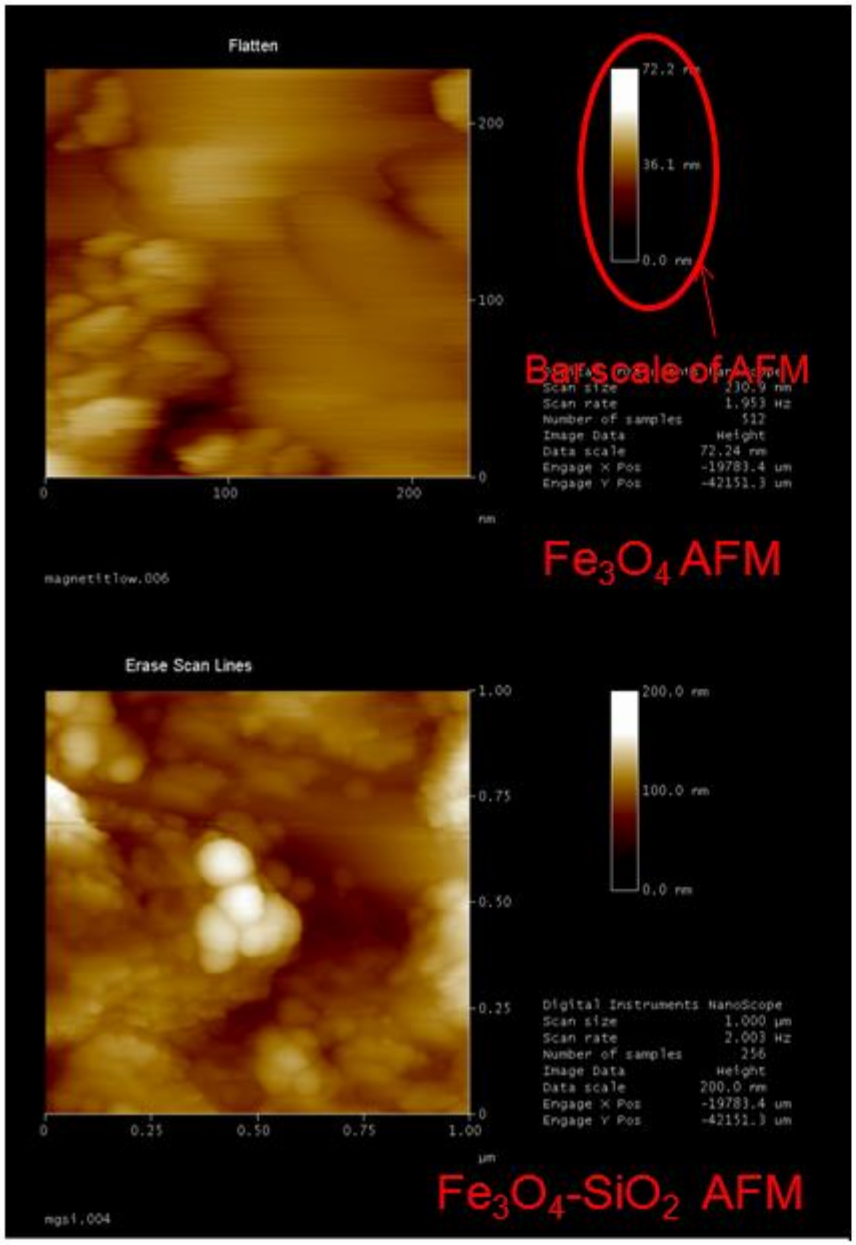

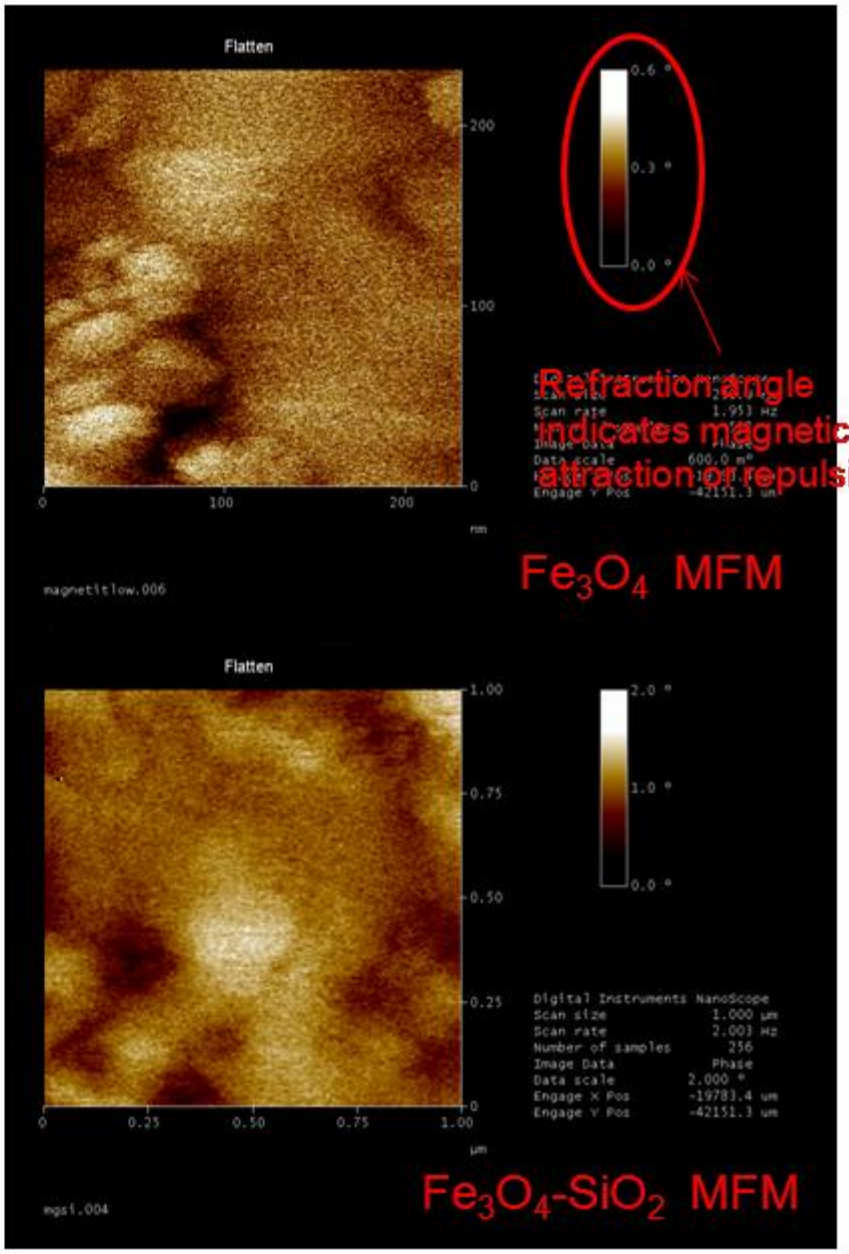

Silica-calcium core-shell iron-oxide nanoparticles - AFM/MFM

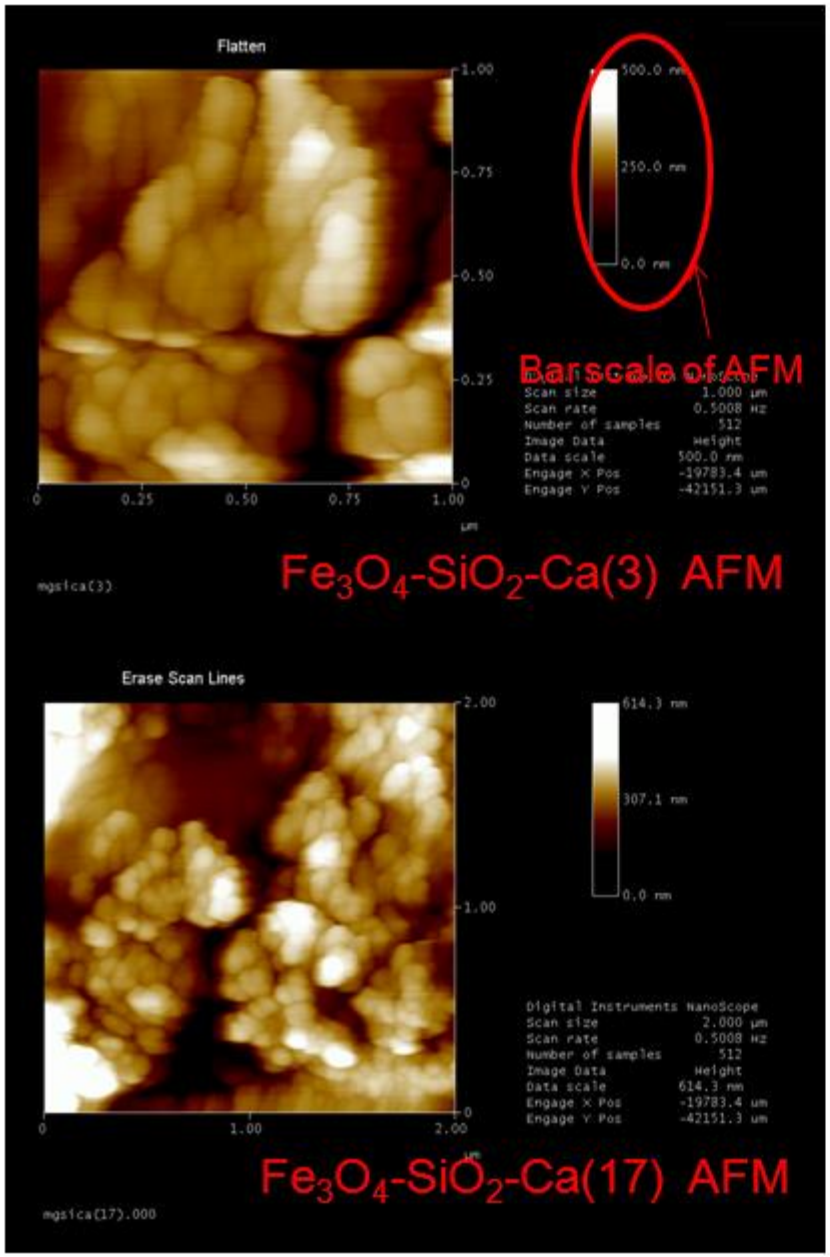

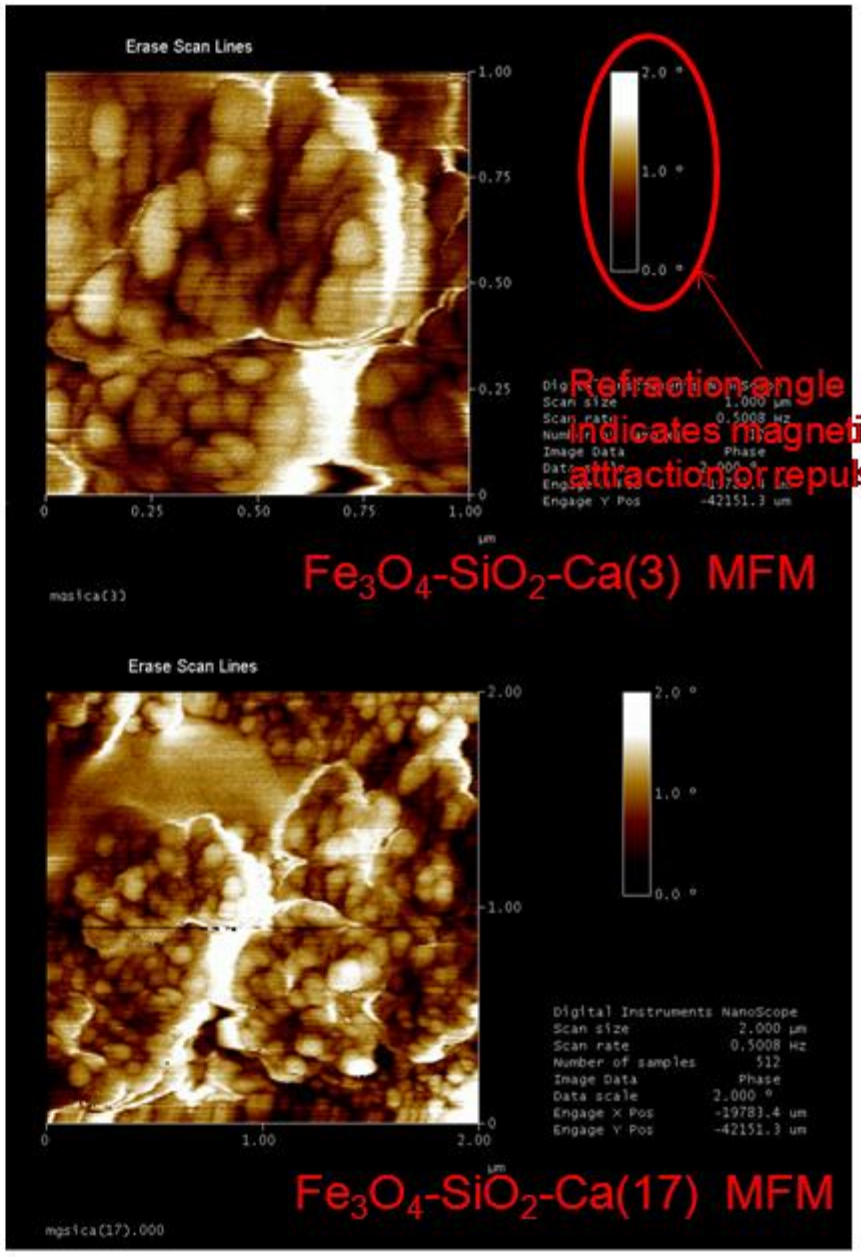

Magnetization curves of MNPs

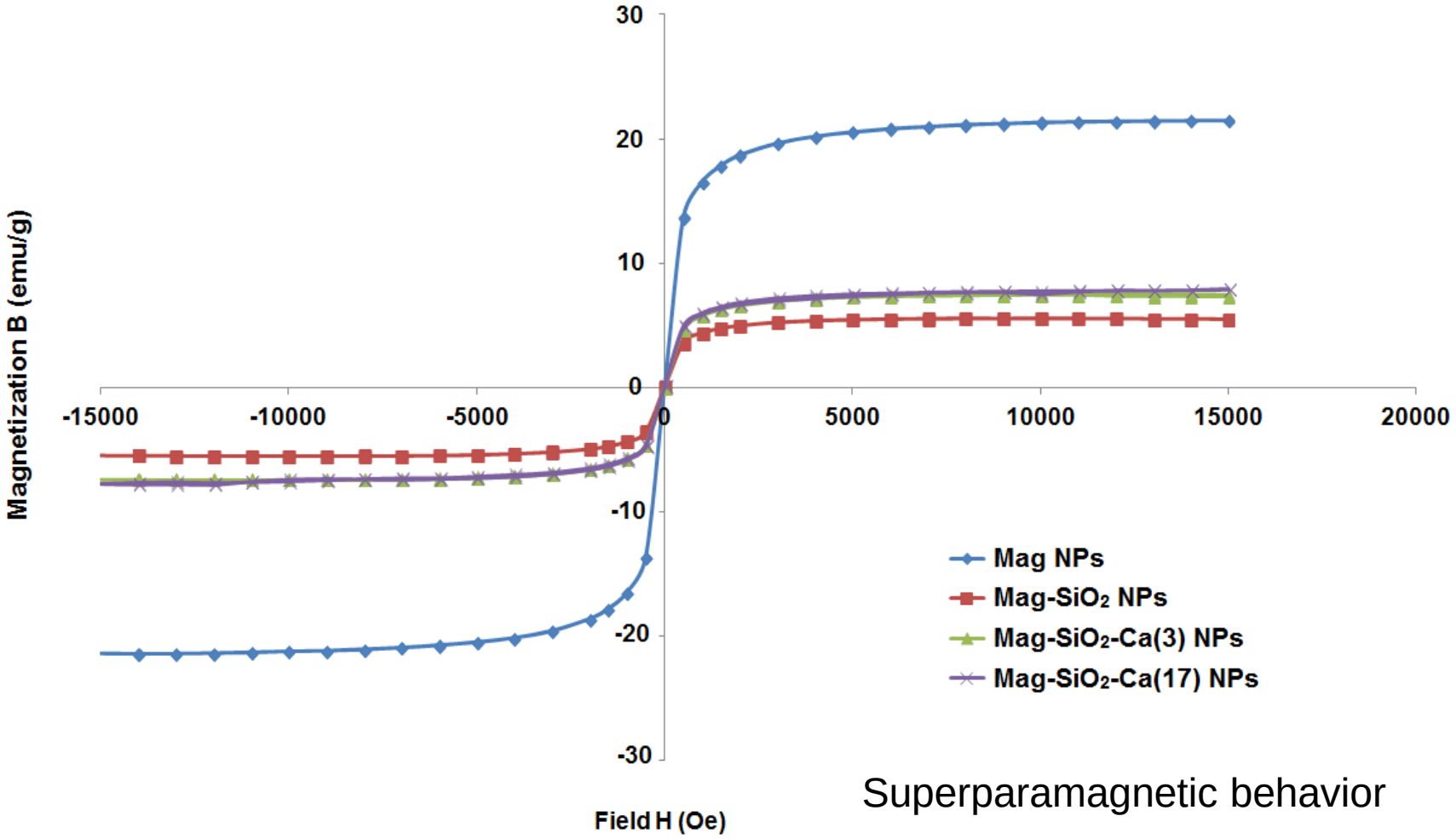

Superparamagnetic behavior

Vibrating Sample Magnetometer (VSM-Lakeshore) was used to determine the magnetic characteristics of the samples.

Magnetization curves of MNPs

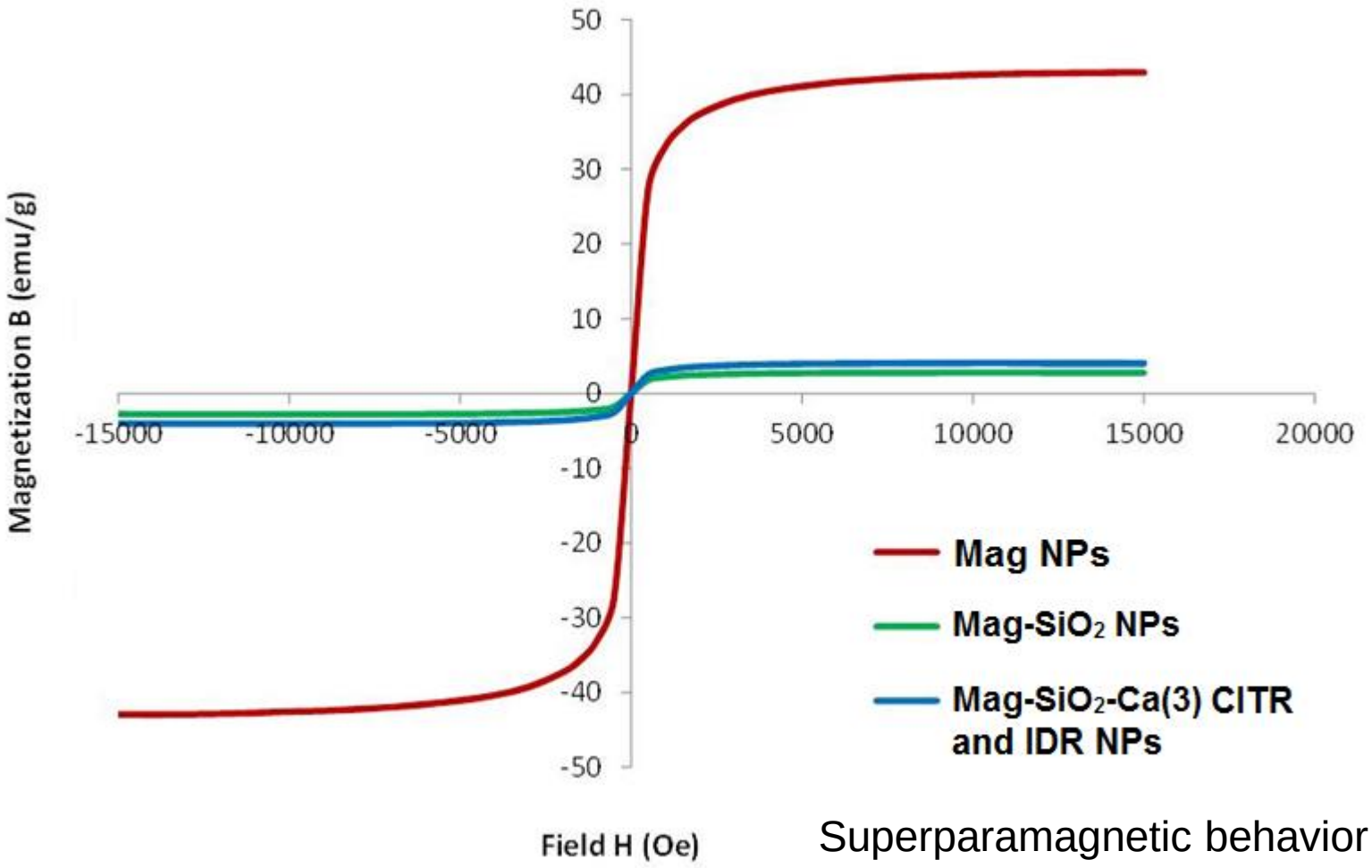

Superparamagnetic behavior

Vibrating Sample Magnetometer (VSM-Lakeshore) was used to determine the magnetic characteristics of the samples.

Definition of Zeta potential (ZP)

The significance of **Zeta potential** can be related to the stability of colloidal dispersions.

Relationship between the value of Zeta potential and colloidal stability

Zeta Potential [mV]	Stability behaviour of the colloid
da 0 a ±5	Rapid coagulation or flocculation
da ±10 a ±30	Incipient instability
da ±30 a ±40	Moderate stability
da ±40 a ±60	Good stability
> ±61	Excellent stability

Robert JH. Zeta Potential in Colloid Science: Principles and Applications. Colloid Sciences Series, Sydney. Academic Press 1989; 1-38.

Zeta potential of magnetic nanoparticles

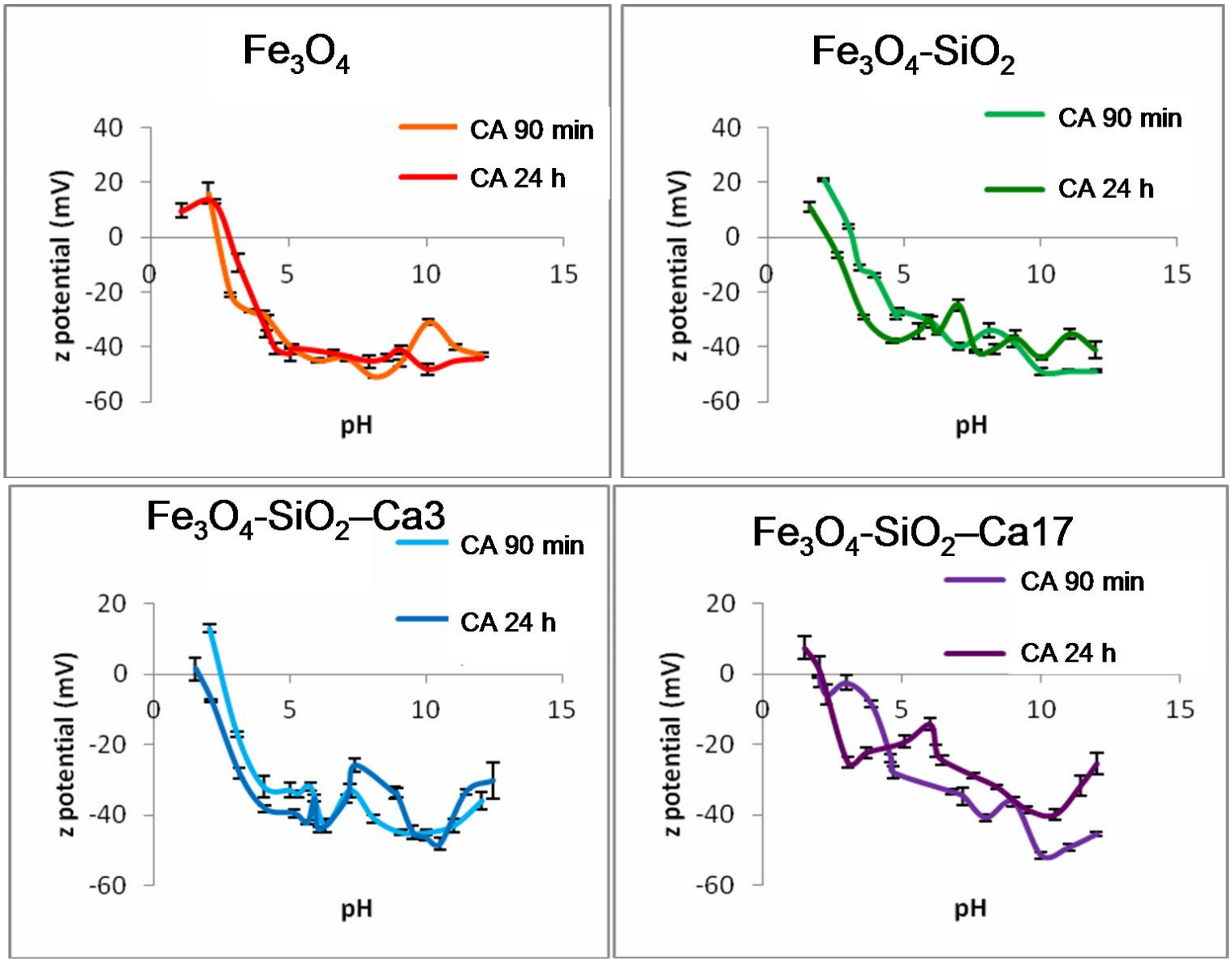

Zeta potential of magnetic nanoparticles

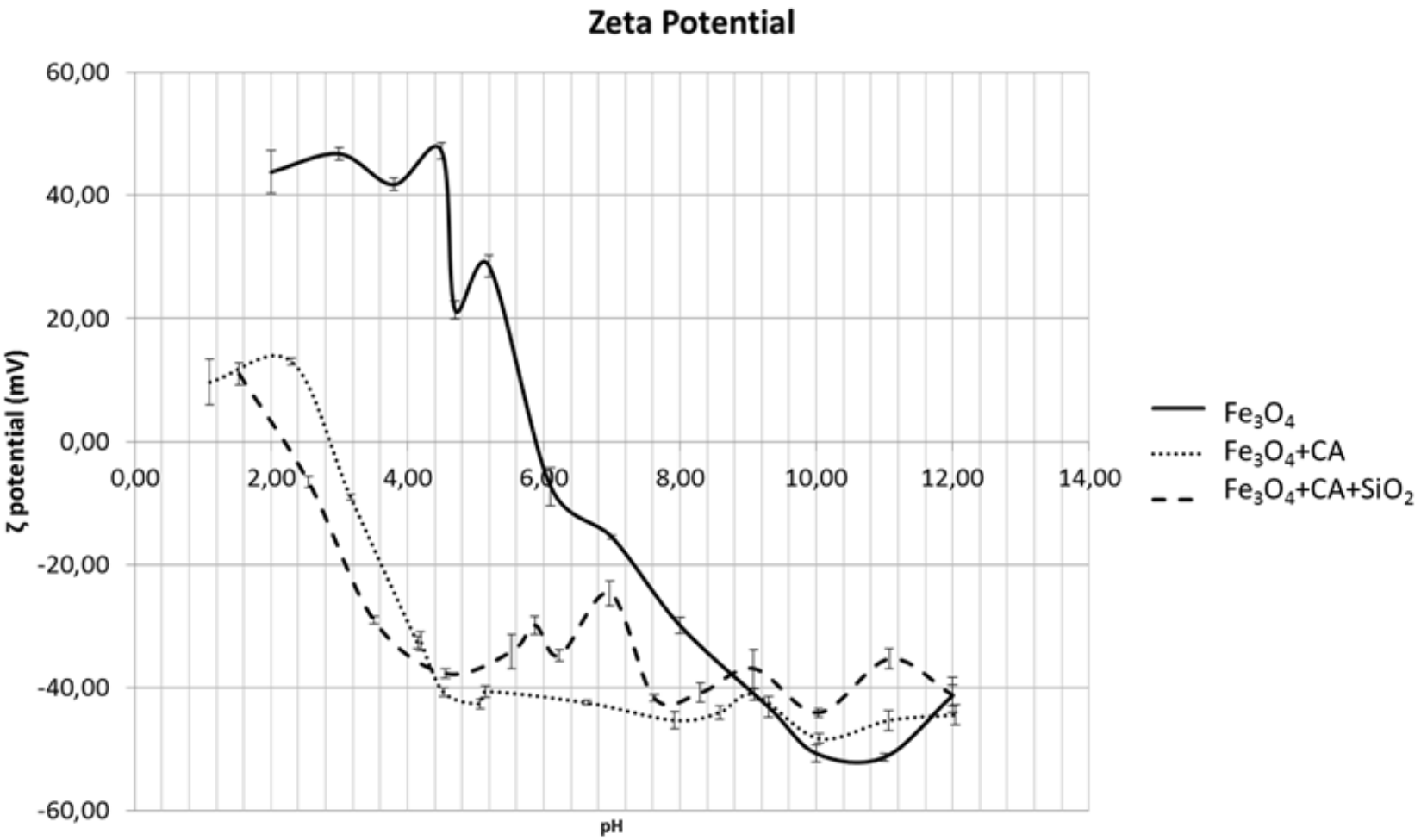

Values of Zeta potential of third synthesis of magnetic nanoparticles

Type of nanoparticle	starting pH	ZP (mV)	Stability behaviour of the colloid
Fe_3O_4 NPs	4.26	- 30.23 ± 1.49 mV	Moderate stability
Fe_3O_4-SiO_2 NPs	4.70	- 30.41 ± 0.81 mV	Moderate stability
Fe_3O_4-SiO_2-Ca(3) CITR NPs	5.63	- 43.14 ± 1.95 mV	Good stability
Fe_3O_4-SiO_2-Ca(3) IDR NPs	5.54	- 42.67 ± 1.61 mV	Good stability

Heating ability of magnetic nanoparticles in a magnetic field

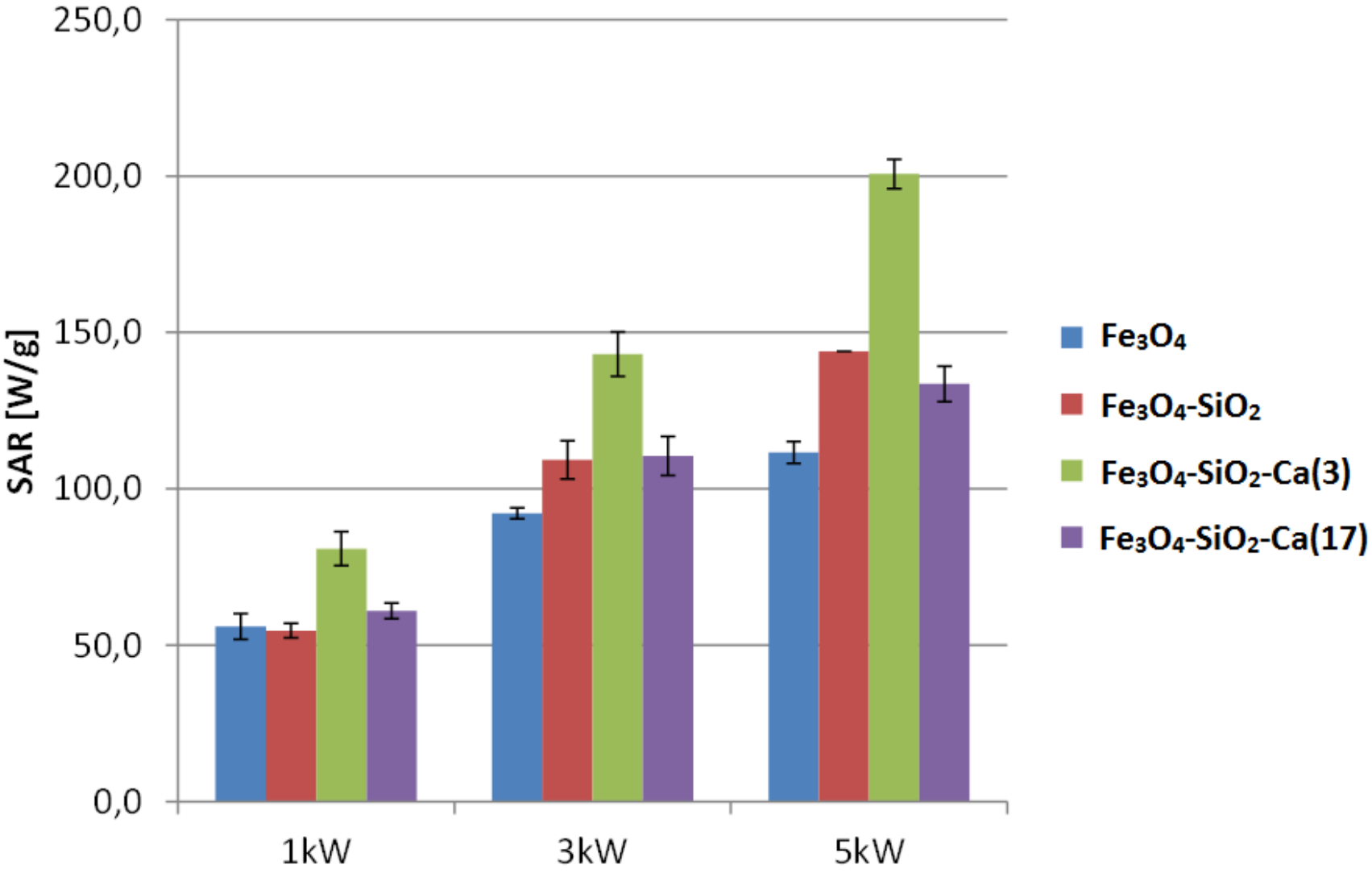

Cytocompatibility evaluation of iron-oxide nanoparticles

Experimental design

Sterilization of MNPs with UV for 30 minutes

Seeding of endothelial murine cells (MS1) in well plates in a defined number to obtain 90% of confluence

Indirect cytotoxicity evaluation

By soaking of MNPs in DMEM cell culture medium for 24 and 72 hours

Direct cytotoxicity evaluation

Addition of MNPs (24 hours after cell seeding) using the following concentrations: 2 and 20 µg/ml

Experimental times: 24, 48 and 72 hours

Viability test: MTT assay

Brigitta Szalay et al, Journal of Applied Toxicology

Not direct contact cytotoxicity evaluation of MNPs

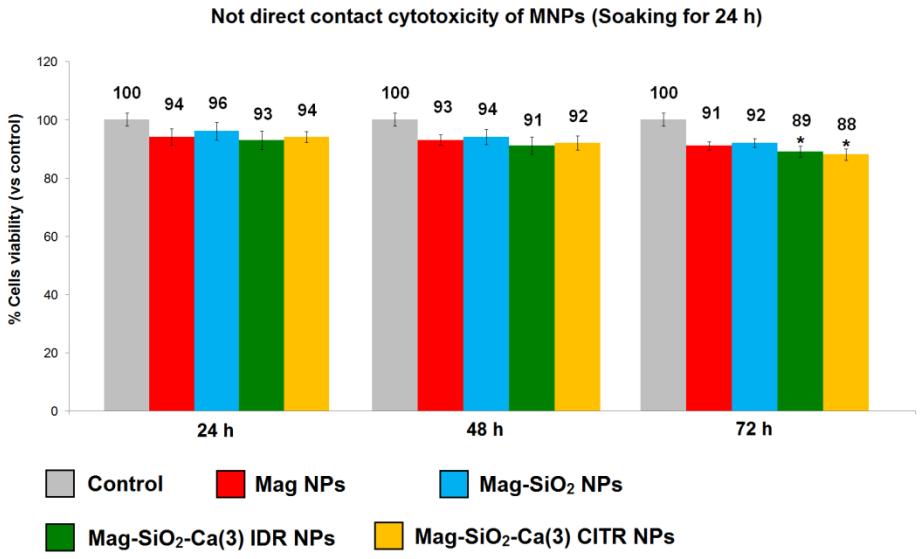

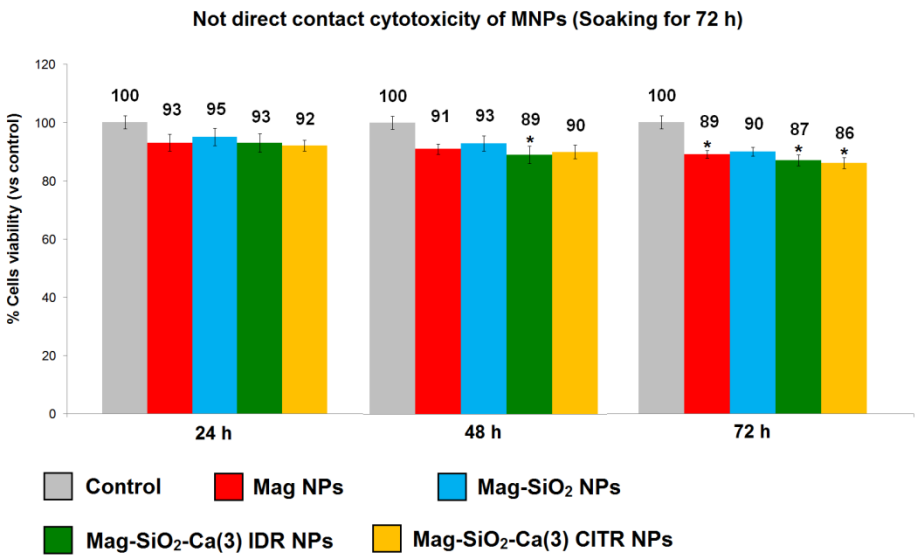

*P < 0.05 compared with control

Cytocompatibility of MNPs in static conditions (72 hours)

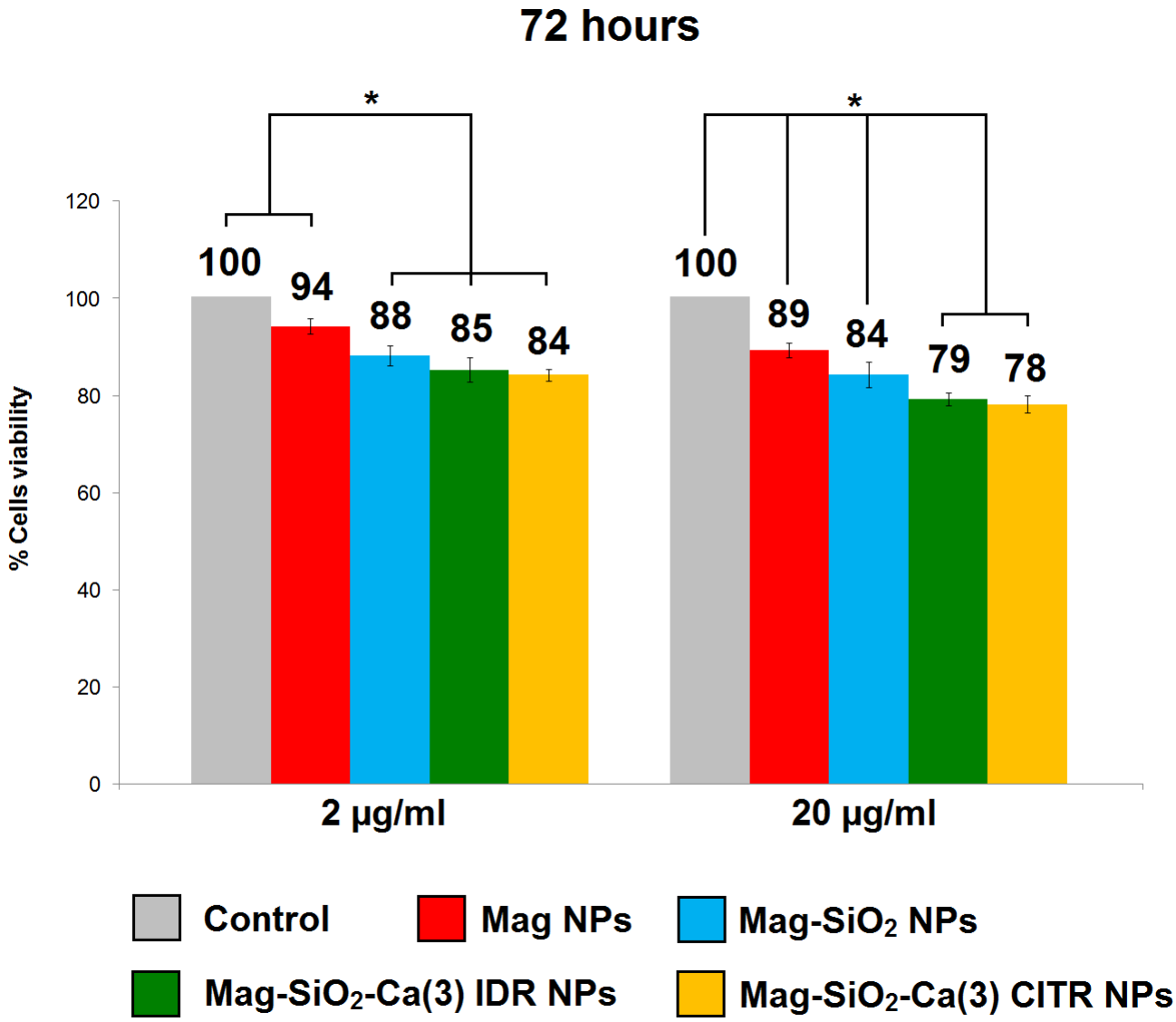

*P < 0.05 One way analysis of variance (ANOVA) followed by Scheffe's test

Cytocompatibility of MNPs in dynamic conditions

Cytocompatibility of MNPs was investigated also in dynamic conditions

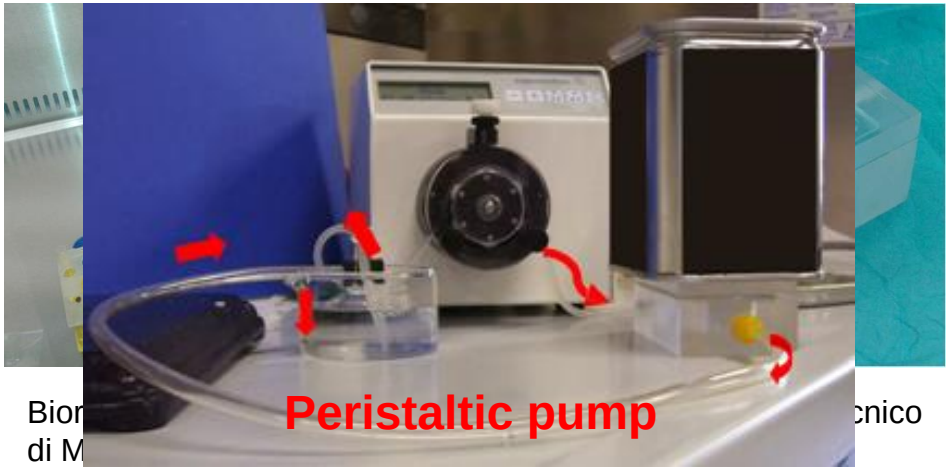

Experimental setting

- Continuous flow bioreactor with a peristaltic pump simulating cytocompatibility in dynamic conditions
- Humidified incubator at 37°C, 5% CO_2 atmosphere

MS1 cells (30.000 cells/cm^2) were seeded at confluence on a strip of electrospun polycaprolactone (PCL)

When MS1 cells were confluent → strips were inserted in the bioreactor.

MS1 cells were subjected to a continuous flow of cell culture medium (DMEM) with MNPs at the concentration of 20 µg/ml.

- **Experimental times: 2 h, 12 h and 24 h.**
- **Cell viability tests used: XTT and LDH assay.**

Ucciferri N. Nanotoxicology. 2014 Sep; 8(6):697-708.

Cytocompatibility in dynamic conditions

Cell viability was evaluated using LDH assay and XTT assay

LDH release (% of total)			
Stimulation	Fe_3O_4 NPs	Fe_3O_4-SiO_2 NPs	Control
2 h	2.77 ± 0.39%	2.59 ± 0.28%	2.24 ± 0.41%
12 h	3.19 ± 0.46%	3.04 ± 0.35%	2.48 ± 0.30%
24 h	3.56 ± 0.51%	3.98 ± 0.46%	2.74 ± 0.37%

XTT assay			
Stimulation	Fe_3O_4 NPs	Fe_3O_4-SiO_2 NPs	Control
2 h	93.8 ± 4.2%	96.9 ± 3.7%	100%
12 h	89.5 ± 2.8%*	93.1 ± 3.3%	100%
24 h	86.8 ± 3.1%*	90.9 ± 2.7%	100%

The viability ranged between 86% and 97% in XTT assay and the results for both assays were comparable.

*$P < 0.05$ compared to control

Cytocompatibility in dynamic conditions (Fe_3O_4 and Fe_3O_4 -SiO_2 NPs)

Cells were analyzed with FESEM equipped to EDS probe, in order to evaluate the presence, if any, of Fe_3O_4 and Fe_3O_4-SiO_2 nanoparticles deposits.

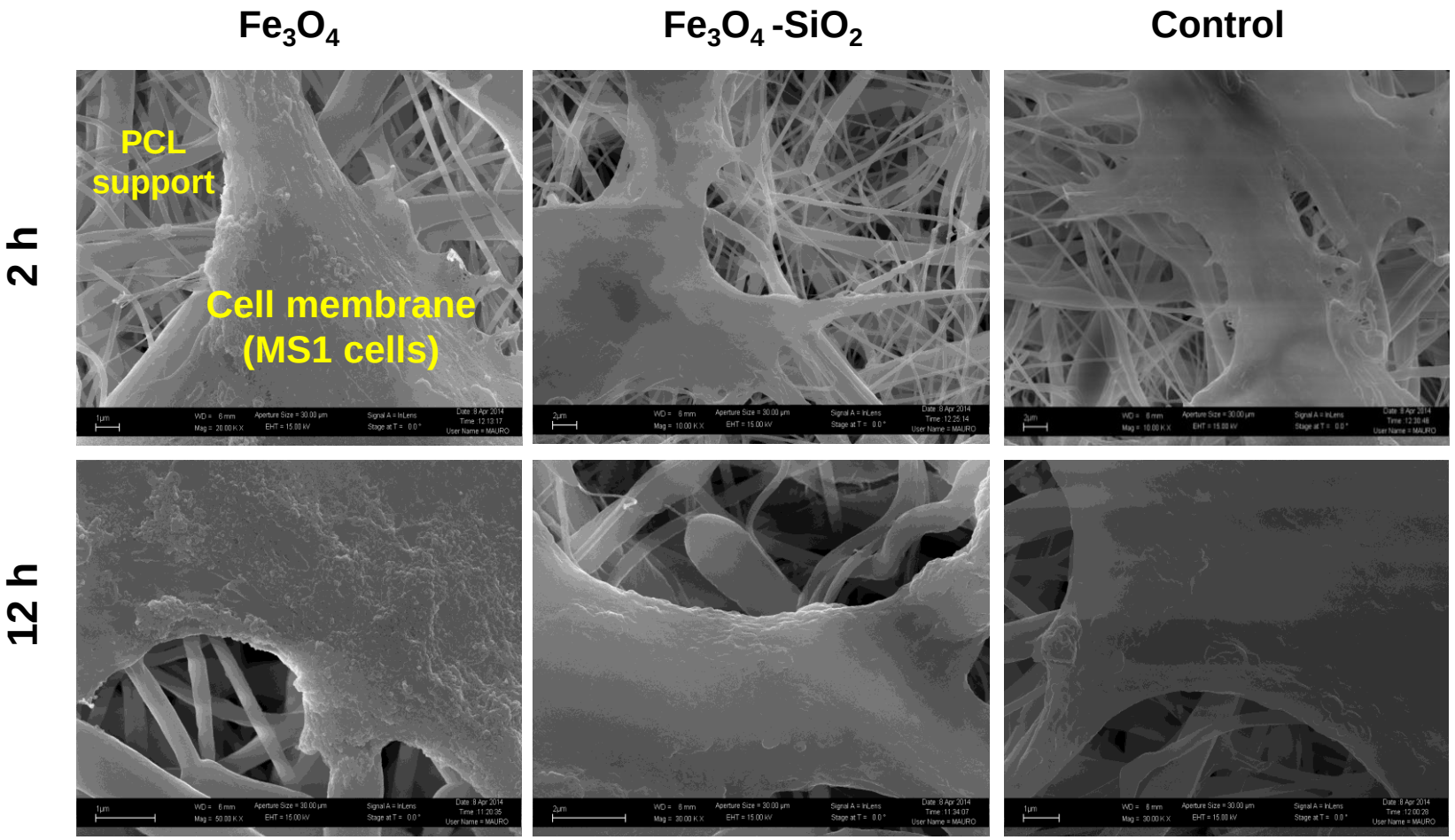

Using dynamic culture conditions, the cells morphology appeared typically elongated.

Cytocompatibility in dynamic conditions

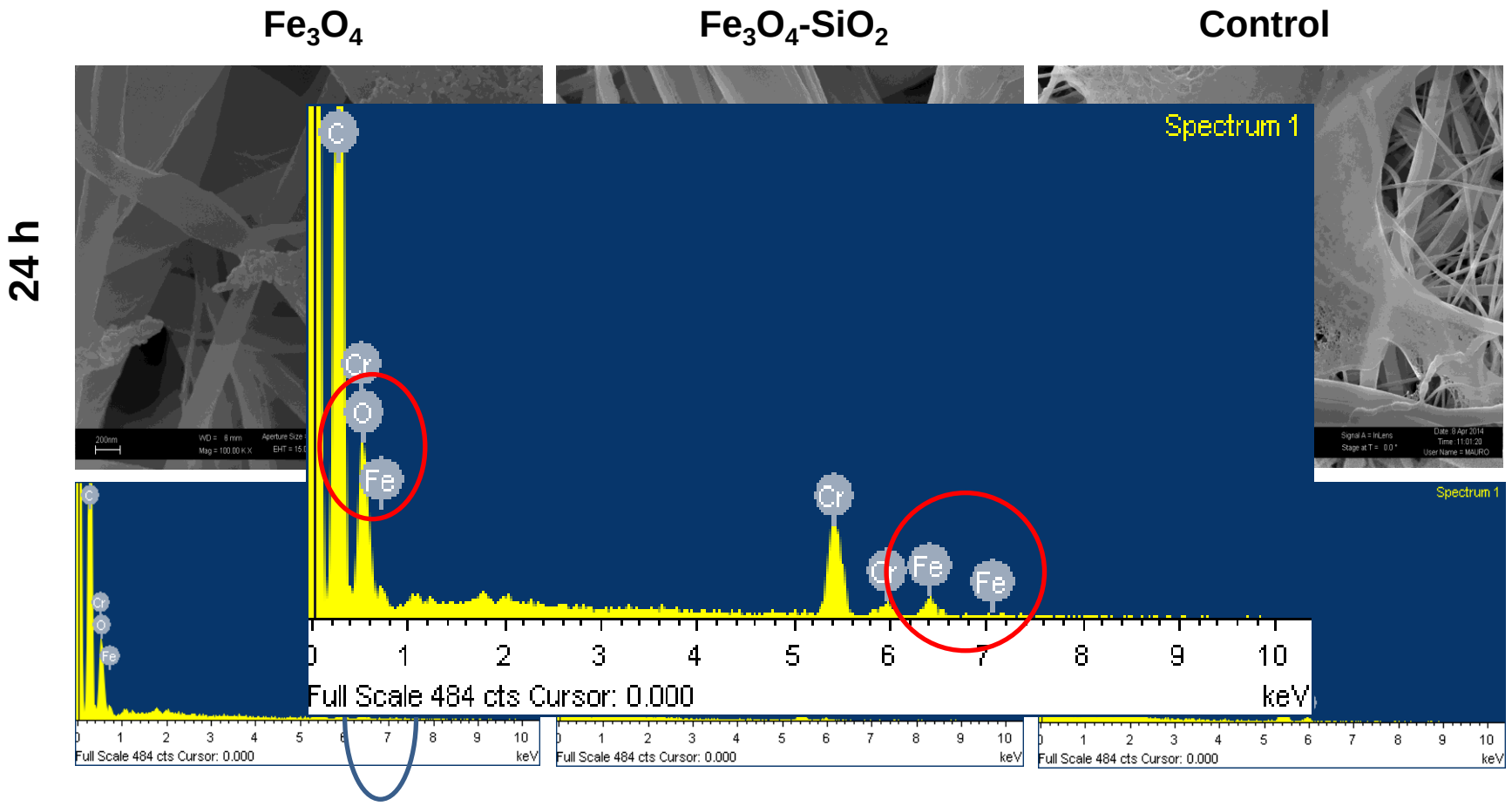

FESEM and EDS analyses showed MNPs adsorbed onto the MS1 cell membrane. MNPs deposition was not observed when Fe_3O_4-SiO_2 nanoparticles were used

ROS generation induced by MNPs

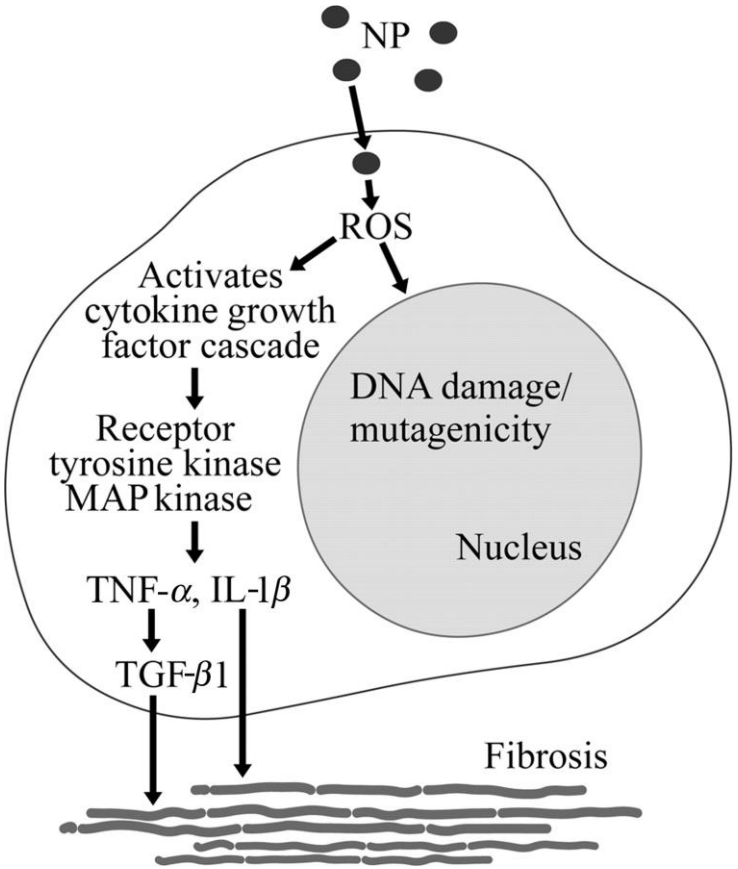

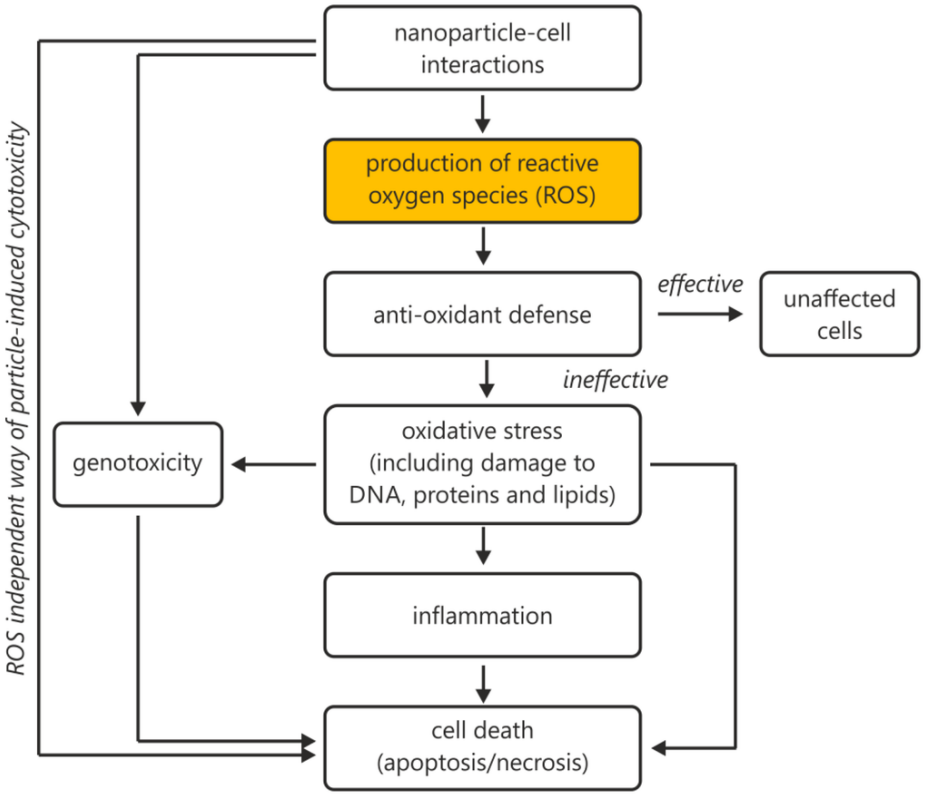

Matthias Roesslein et al., Int. J. Mol. Sci. 2013

ROS generation induced by MNPs after 24 hours (First synthesis)

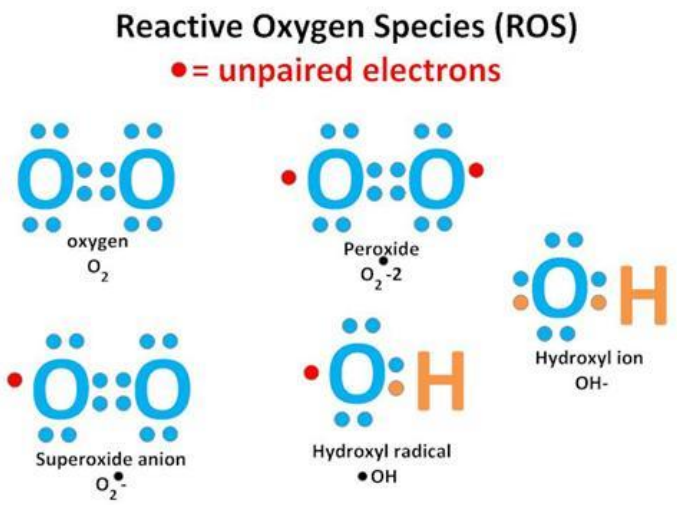

CellROX Green Reagent measures reactive oxygen species (ROS) in live cells

Protocol

1. MS1 cells were treated for 24 h with the following concentrations of MNPs: 10, 20, 40 and 80 µg/ml.
2. Add the CellROX Green Reagent at concentration of 5 µM.
3. Incubate the cells for 30 minutes at 37°C.
4. Remove medium and wash the cells with PBS.
5. Analyze the cells to FACS.

ROS production after 24 hours induced by MNPs

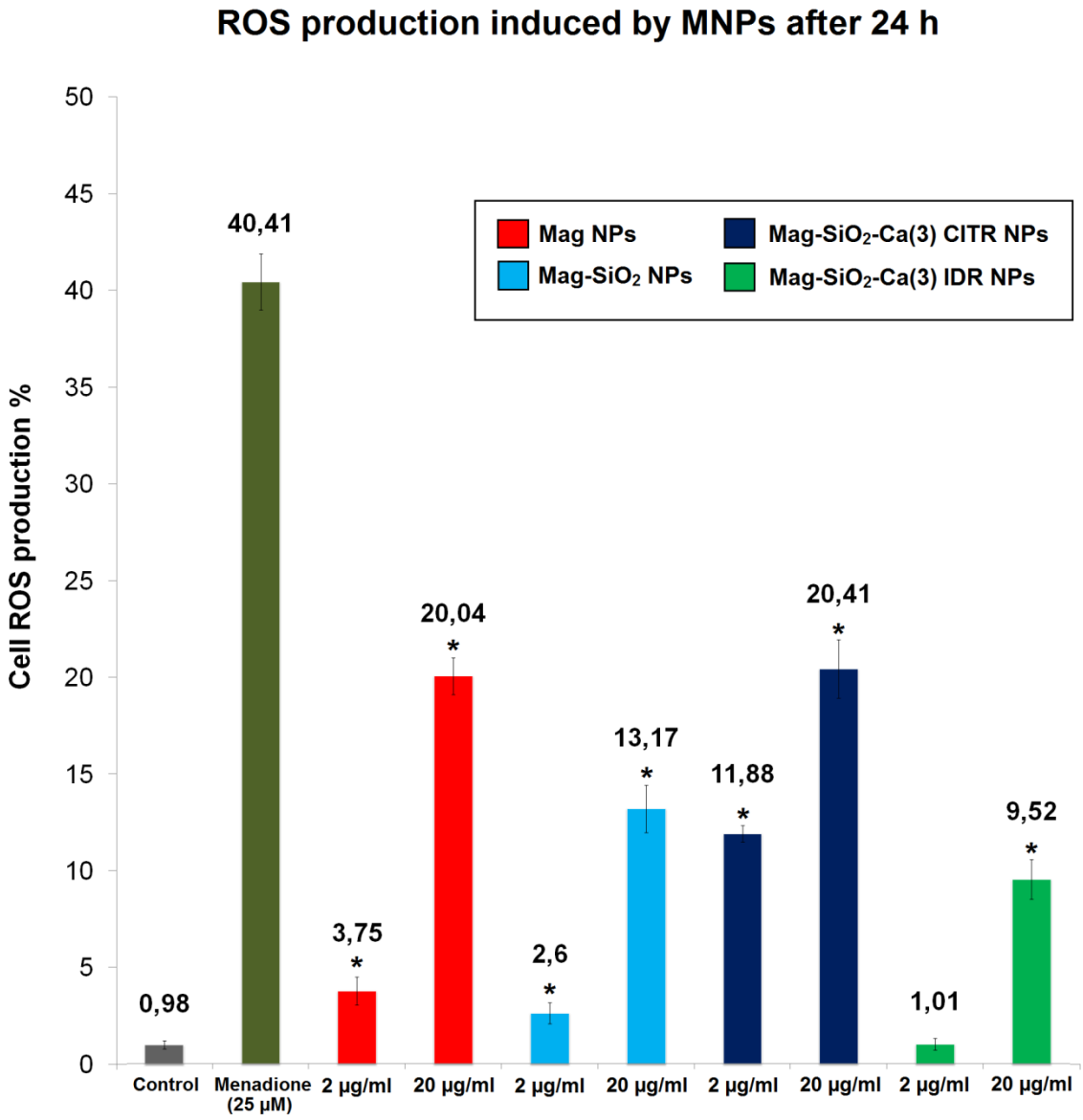

*P < 0.05 compared with control untreated and positive control (Menadione 25 µM).

Apoptosis evaluation: Annexin V/PI

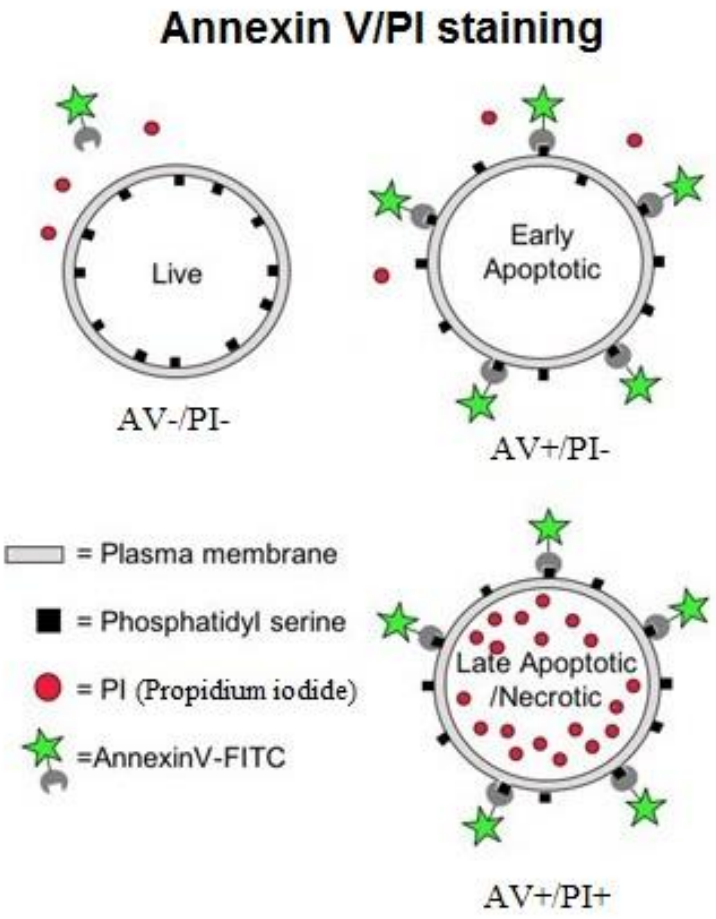

- Apoptosis evaluation of MNPs effect on MS1 cells using the following concentrations: 2 and 20 µg/ml
- Annexin V-FITC - PI (Propidium iodide) staining
- Experimental time-points: 24, 48 and 72 hours

MS1 cells were seeded

at a density of:

- $2{,}5 \times 10^5$ cells (24 hours)
- $1{,}75 \times 10^5$ cells (48 and 72 hours)
- FACS Analysis

Apoptosis evaluation after 72 hours

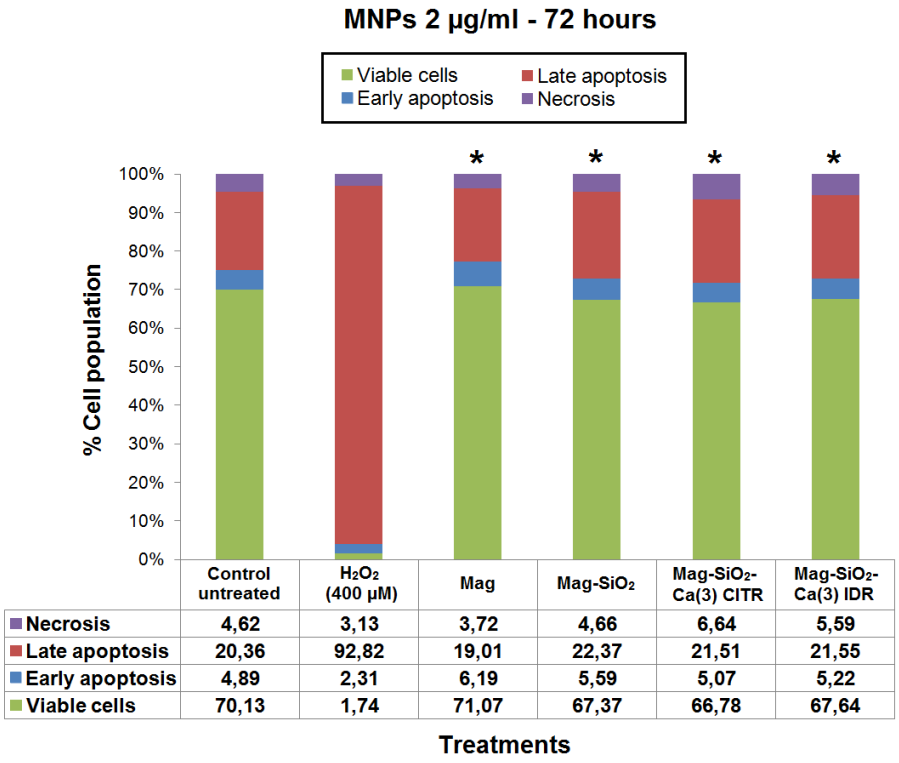

	Control untreated	H_2O_2 (400 µM)	Mag	Mag-SiO_2	Mag-SiO_2-Ca(3) CITR	Mag-SiO_2-Ca(3) IDR
Necrosis	4,62	3,13	3,72	4,66	6,64	5,59
Late apoptosis	20,36	92,82	19,01	22,37	21,51	21,55
Early apoptosis	4,89	2,31	6,19	5,59	5,07	5,22
Viable cells	70,13	1,74	71,07	67,37	66,78	67,64

Treatments

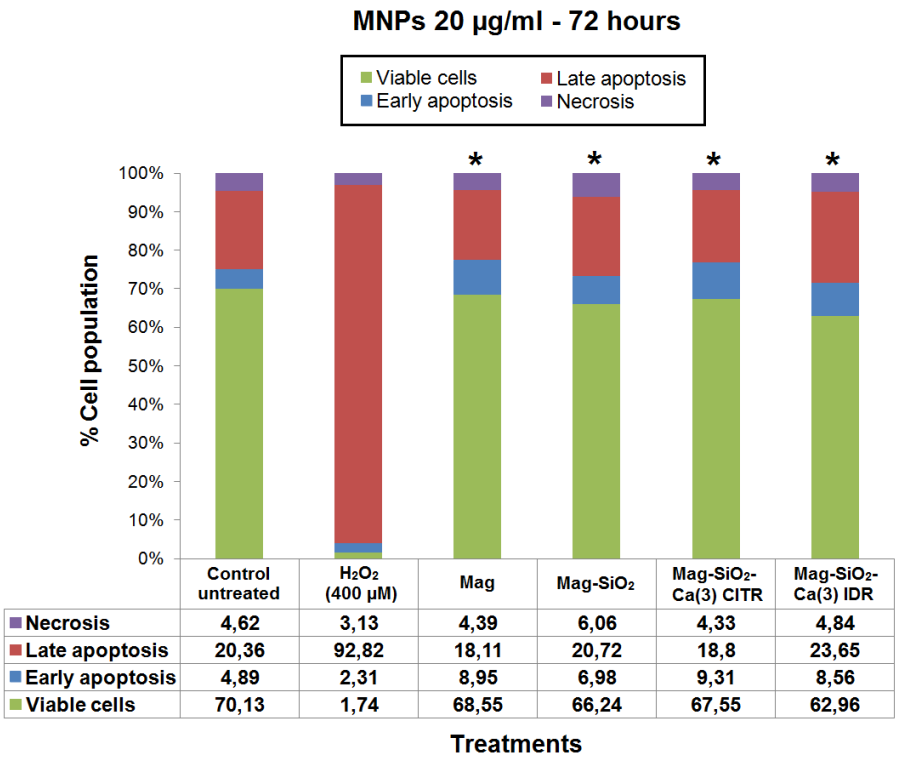

	Control untreated	H_2O_2 (400 µM)	Mag	Mag-SiO_2	Mag-SiO_2-Ca(3) CITR	Mag-SiO_2-Ca(3) IDR
Necrosis	4,62	3,13	4,39	6,06	4,33	4,84
Late apoptosis	20,36	92,82	18,11	20,72	18,8	23,65
Early apoptosis	4,89	2,31	8,95	6,98	9,31	8,56
Viable cells	70,13	1,74	68,55	66,24	67,55	62,96

Treatments

*P < 0.05 compared to control (Chi-square test)

In vivo evaluation of iron-oxide nanoparticles

Biodistribution of MNPs - 7 days (Short term evaluation)

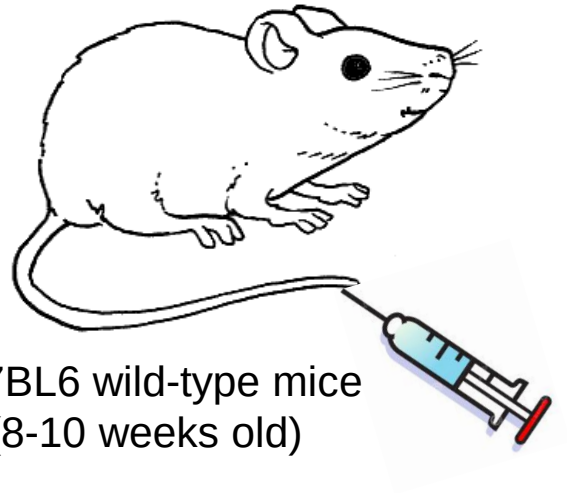

C57BL6 wild-type mice
(8-10 weeks old)

- **Fe_3O_4 and Fe_3O_4-SiO_2 nanoparticles were tested using the following concentration: 2 mg Fe/kg body weight**
- **Evaluation of hematological parameters after 3 and 7 days (May-Grunwald-Giemsa staining for counting of blood cells)**
- **Evaluation of biochemical parameters of renal and hepatic functionality after 7 days: ALT, AST, CRE, LDH**

Aspartate transaminase (AST), alanine transaminase (ALT), creatinine (CRE), lactic acid dehydrogenase (LDH)

Serum biomarkers analysis (2 mg Fe/kg - 7 days)

	Control	**Fe_3O_4 NPs**	**Fe_3O_4-SiO_2 NPs**
ALT (U/l)	39.42 ± 2.69	43.15 ± 2.72	44.26 ± 2.06*
AST (U/l)	127.35 ± 12.07	129.34 ± 7.12	134.81 ± 6.83*
CRE (µmol/l)	19.21 ± 1.25	21.91 ± 1.03	23.48 ± 1.47*
LDH (U/l)	833.75 ± 53.28	841.67 ± 57.91	843.46 ± 46.35

ALT alanine transaminase, AST aspartate transaminase, CRE creatinine, LDH lactic acid dehydrogenase

Data are presented as mean ± SD (n = 4).

*P < 0.05 compared with control

Hematological parameters (2 mg Fe/kg)

	Control	Fe_3O_4 NPs	Fe_3O_4-SiO_2 NPs
Red blood cell (10^6/µl) after 3 days	**9.83 ± 0.52**	**9.76 ± 0.93**	**9.71 ± 1.19**
Red blood cell (10^6/µl) after 7 days	**9.75 ± 0.83**	**9.69 ± 1.07**	**9.64 ± 0.71**
White blood cell (10^3/µl) after 3 days	**6.51 ± 0.73**	**6.63 ± 1.18**	**6.72 ± 1.26**
White blood cell (10^3/µl) after 7 days	**6.57 ± 1.14**	**6.73 ± 1.22**	**6.88 ± 1.61**

Prussian Blue staining (2 mg Fe/kg - Liver, Spleen)

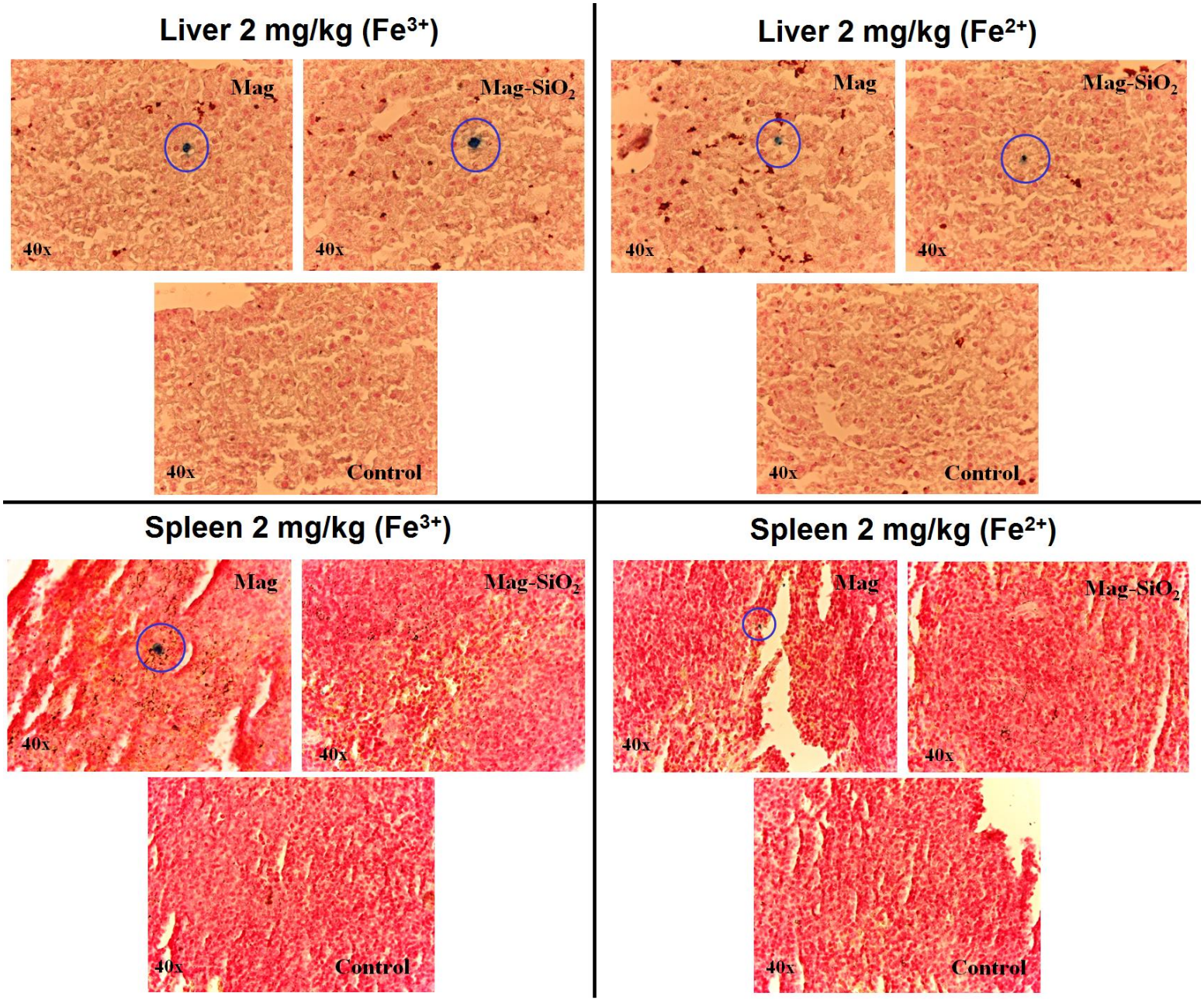

Prussian Blue staining (2 mg Fe/kg - Kidney, Brain)

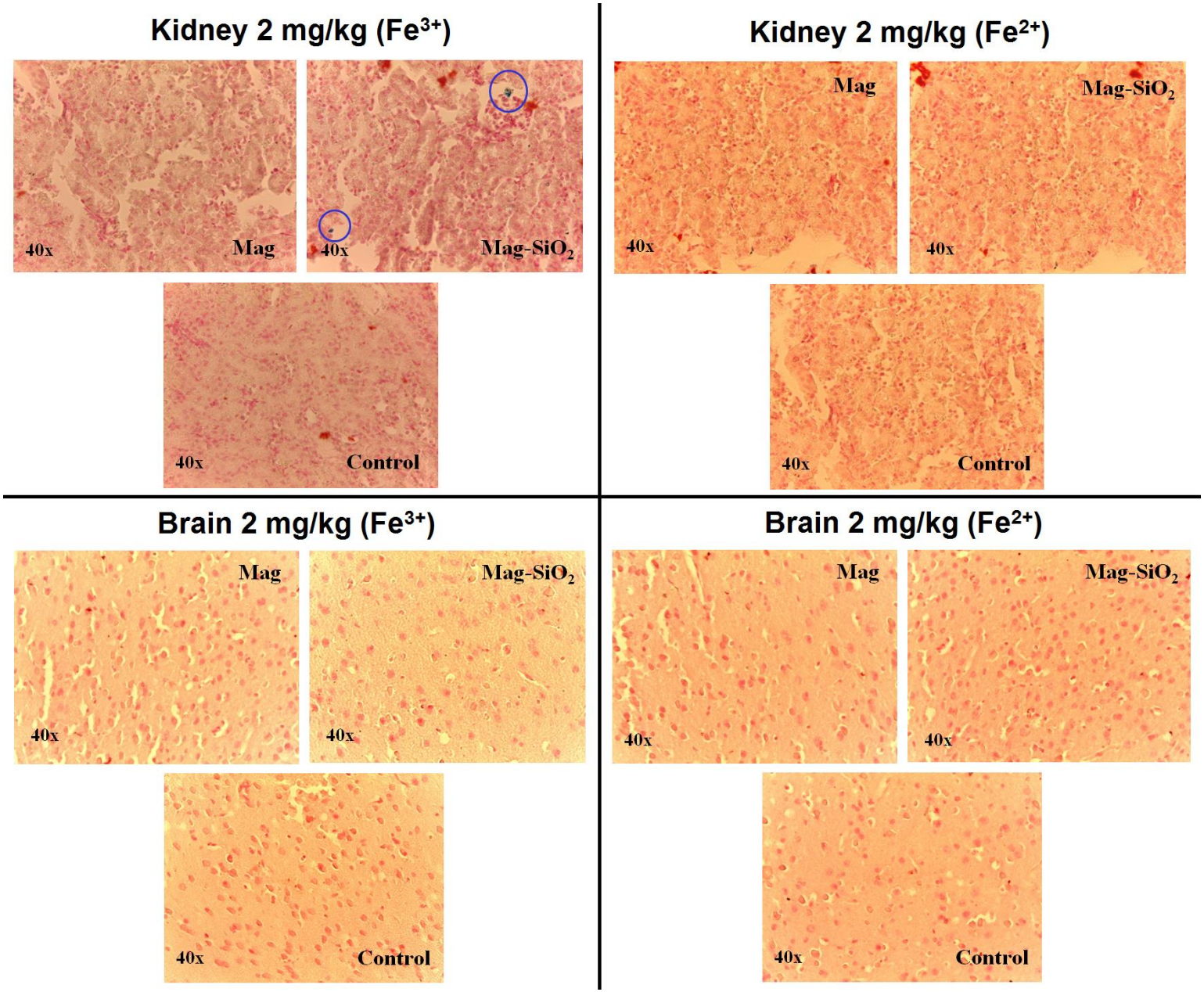

Prussian Blue staining (2 mg Fe/kg - Lung, Heart)

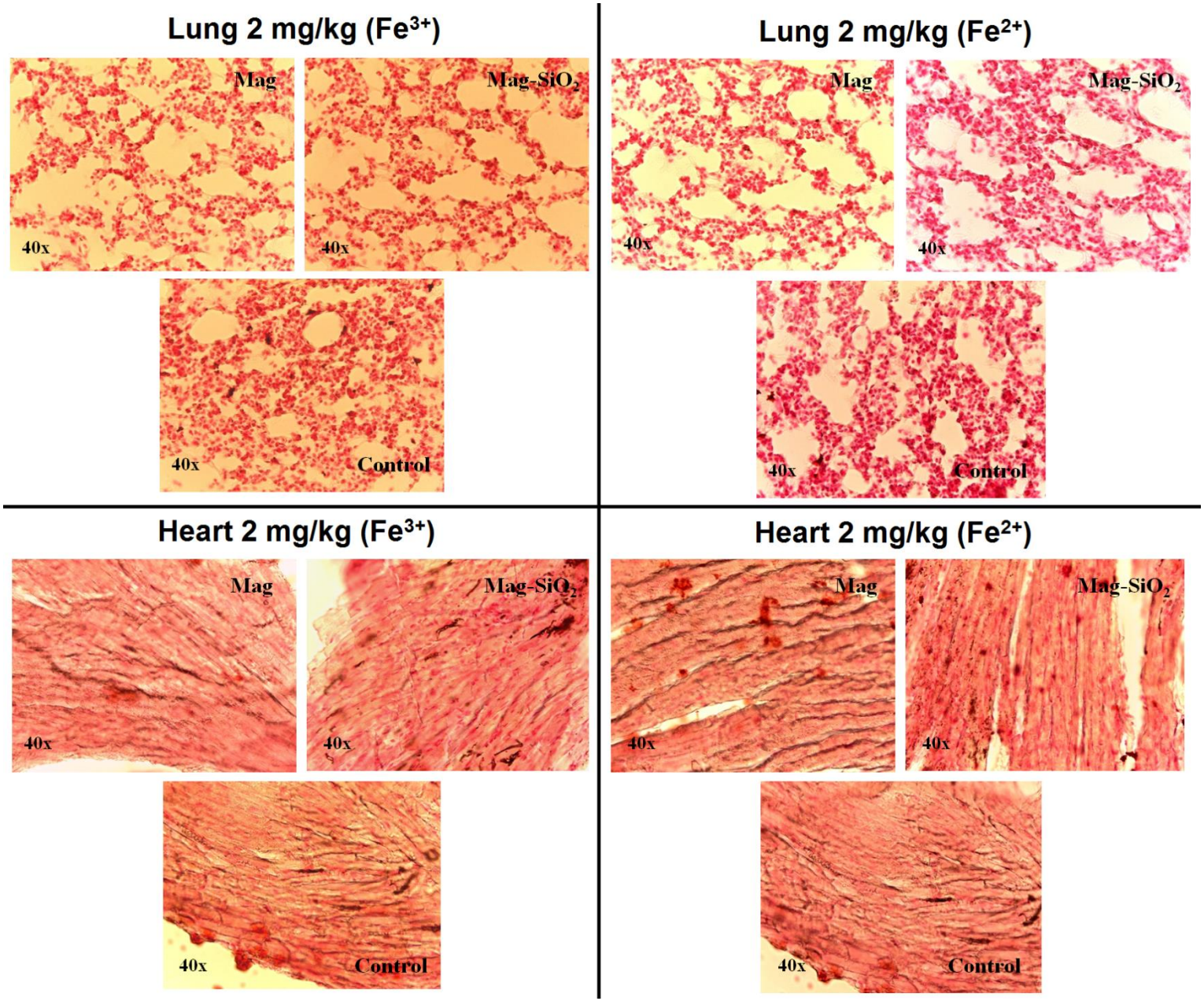

ICP-AES analysis results (2 mg Fe/kg)

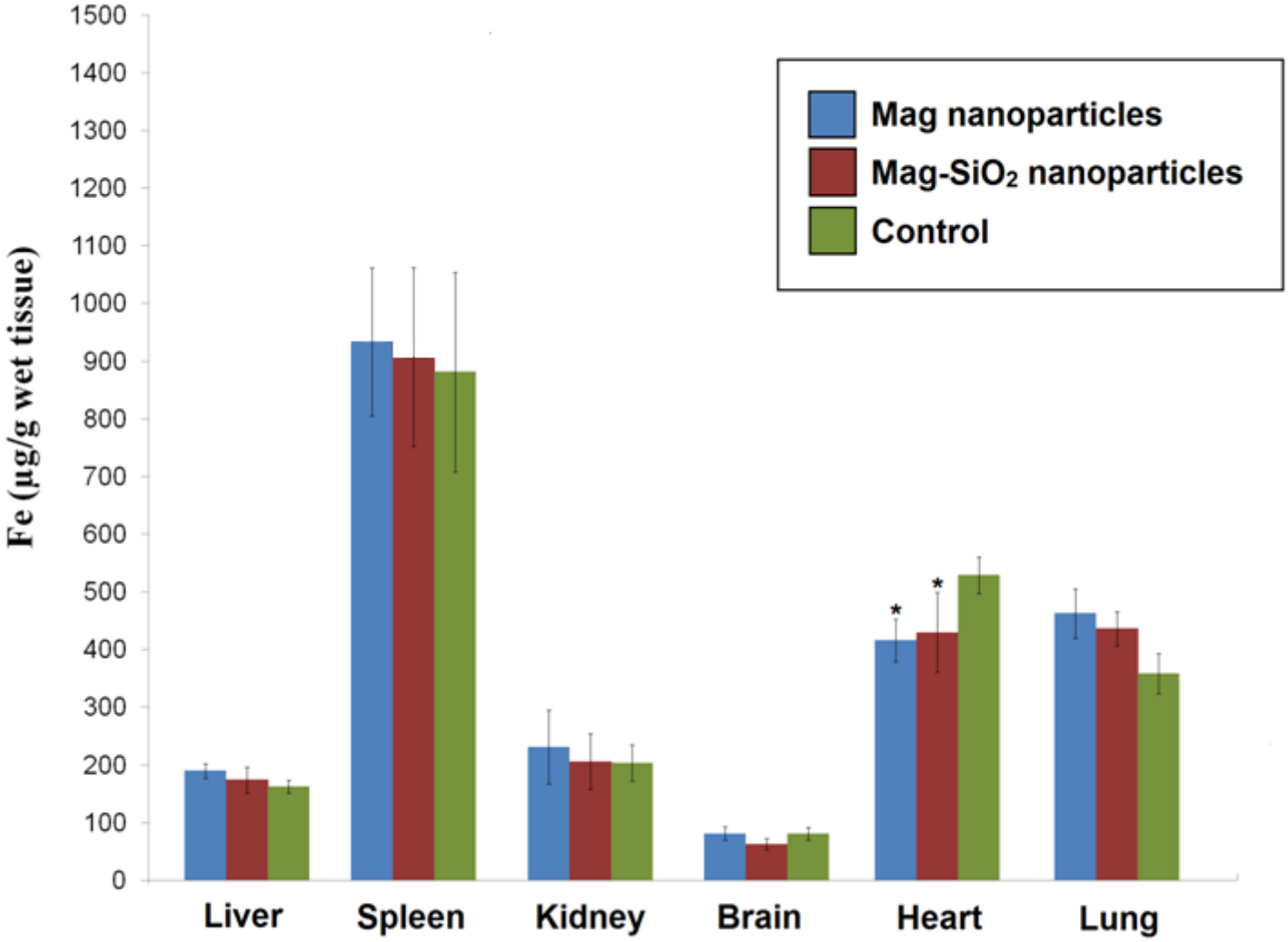

*P < 0.05 compared to control - One way analysis of variance (ANOVA) followed by Scheffe's test

Cell/MNPs interaction via Lentivirus coupling

- Retrovirus (RNA)
- Peri-capside
- Used in cell trasduction as a vector
- Different types of MNPs were assembled with lentiviral vectors with different MOI (multiplicity of infection) ratios

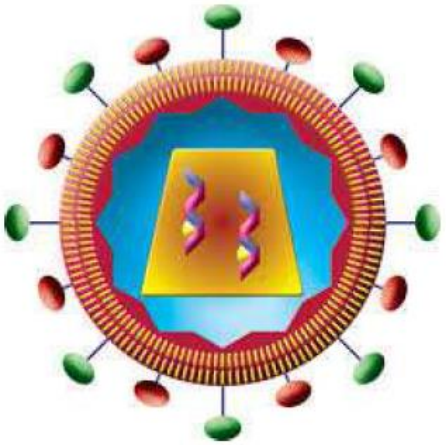

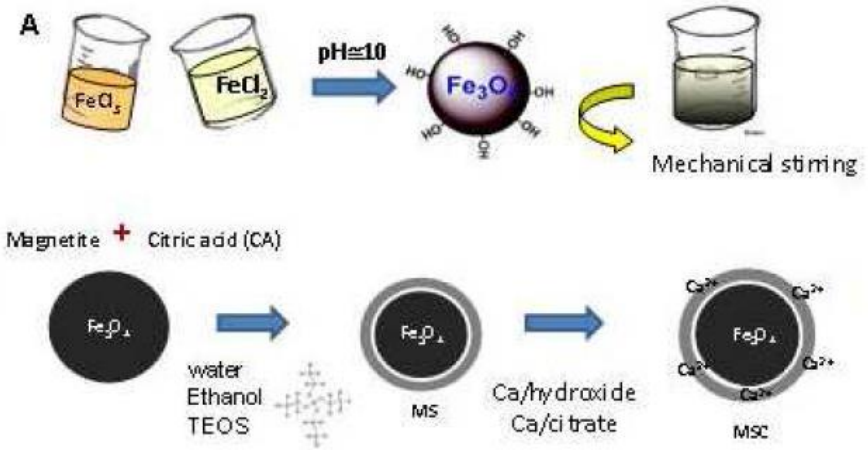

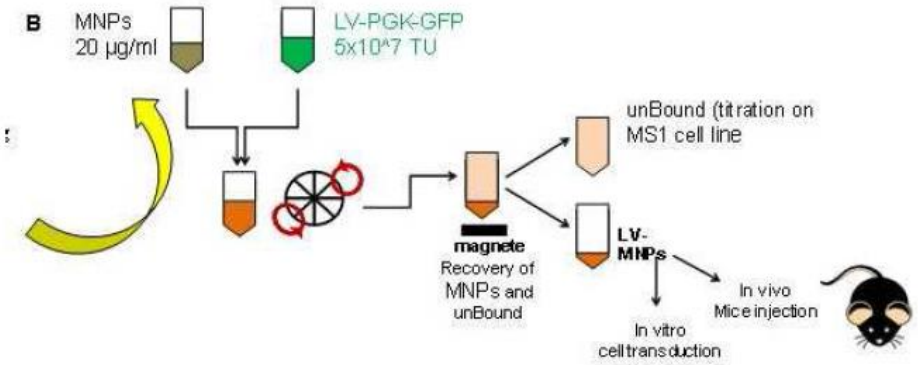

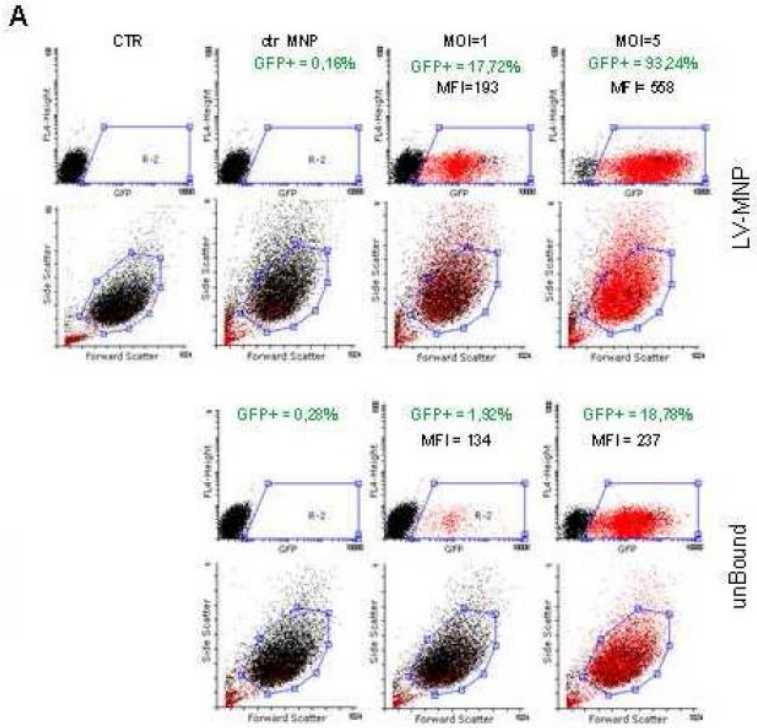
A
CTR
ctr MNP
GFP+ = 0,16%
MOI=1
GFP+ = 17,72%
MFI=193
MOI=5
GFP+ = 93,24%
MFI = 558
LV-MNP
GFP+ = 0,28%
GFP+ = 1,92%
MFI = 134
GFP+ = 18,78%
MFI = 237
unBound
Forward Scatter
Side Scatter

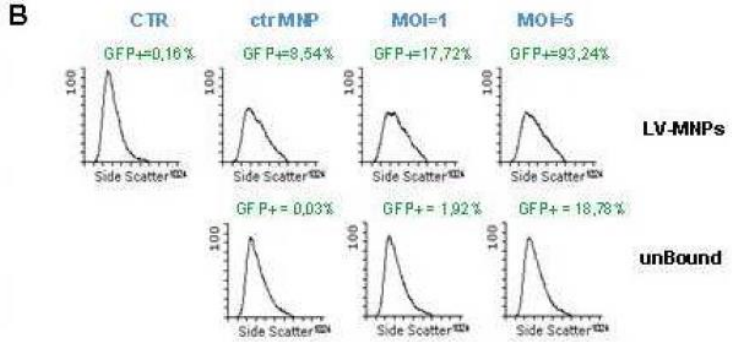
B
CTR
ctrMNP
MOI=1
MOI=5
GFP+=0,16%
GFP+=8,54%
GFP+=17,72%
GFP+=93,24%
LV-MNPs
GFP+ = 0,03%
GFP+ = 1,92%
GFP+ = 18,78%
unBound
Side Scatter

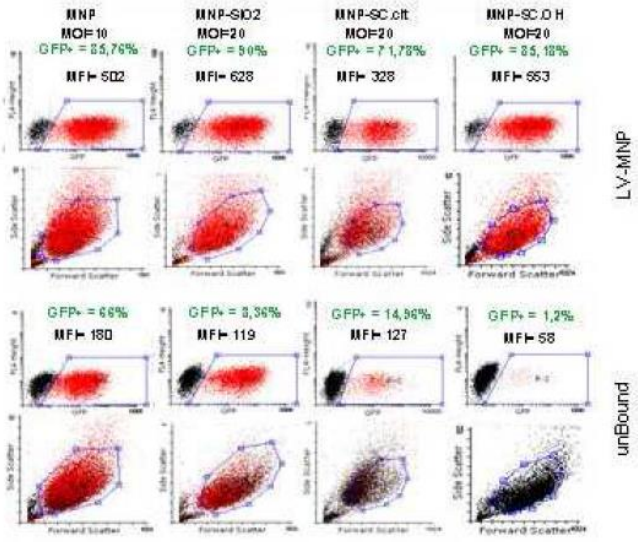
C
MNP
MOI=10
GFP+ = 85,76%
MFI= 502
MNP-SiO2
MOI=20
GFP+ = 90%
MFI= 628
MNP-SC.cit
MOI=20
GFP+ = 71,78%
MFI= 328
MNP-SC.OH
MOI=20
GFP+ = 85,12%
MFI= 553
LV-MNP
GFP+ = 66%
MFI= 180
GFP+ = 8,36%
MFI= 119
GFP+ = 14,96%
MFI= 127
GFP+ = 1,2%
MFI= 58
unBound
Forward Scatter
Side Scatter

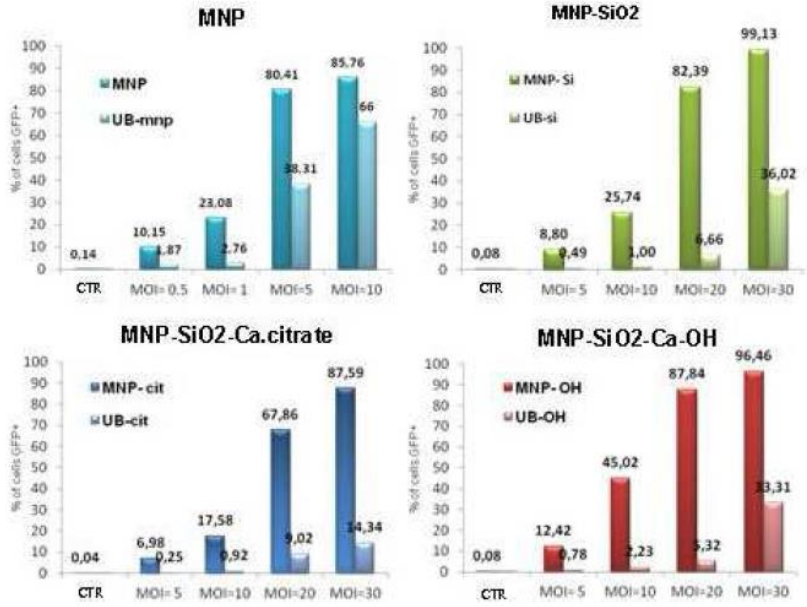
D
MNP
MNP
UB-mnp
% of cells GFP+
0,14
10,15
1,87
23,08
2,76
80,41
38,31
85,76
66
CTR
MOI= 0.5
MOI= 1
MOI=5
MOI=10
MNP-SiO2
MNP- Si
UB-si
0,08
8,80
0,49
25,74
1,00
82,39
6,66
99,13
36,02
CTR
MOI=5
MOI=10
MOI=20
MOI=30
MNP-SiO2-Ca.citrate
MNP- cit
UB-cit
0,04
6,98
0,25
17,58
0,92
67,86
9,02
87,59
14,34
CTR
MOI= 5
MOI=10
MOI=20
MOI=30
MNP-SiO2-Ca-OH
MNP- OH
UB-OH
0,08
12,42
0,78
45,02
2,23
87,84
5,32
96,46
33,31
CTR
MOI=5
MOI=10
MOI=20
MOI=30

Figure 1. GFP expression after in vivo delivery of LV-MNPs complexes. C57Bl/6 mice were tail vein injected with 2µg/g mouse of MNPs after assembly with $5x10^7$ TU of LV.PGK-GFP. **(A)** GFP expression was checked at 1 week in liver and **(B)** spleen for all the different nanoparticles. **(C)** Comparison of MNPs or MNPs-SiO2 complexes in vivo, liver (400x) and spleen (100x).
After LV-MNPs injection, GFP was mainly expressed by macrophages (F4/80+ cells; in red) in liver, while, interestingly, pattern of GFP+ cells in spleen varies according to MNPs coating. Nuclei are stained in blue.

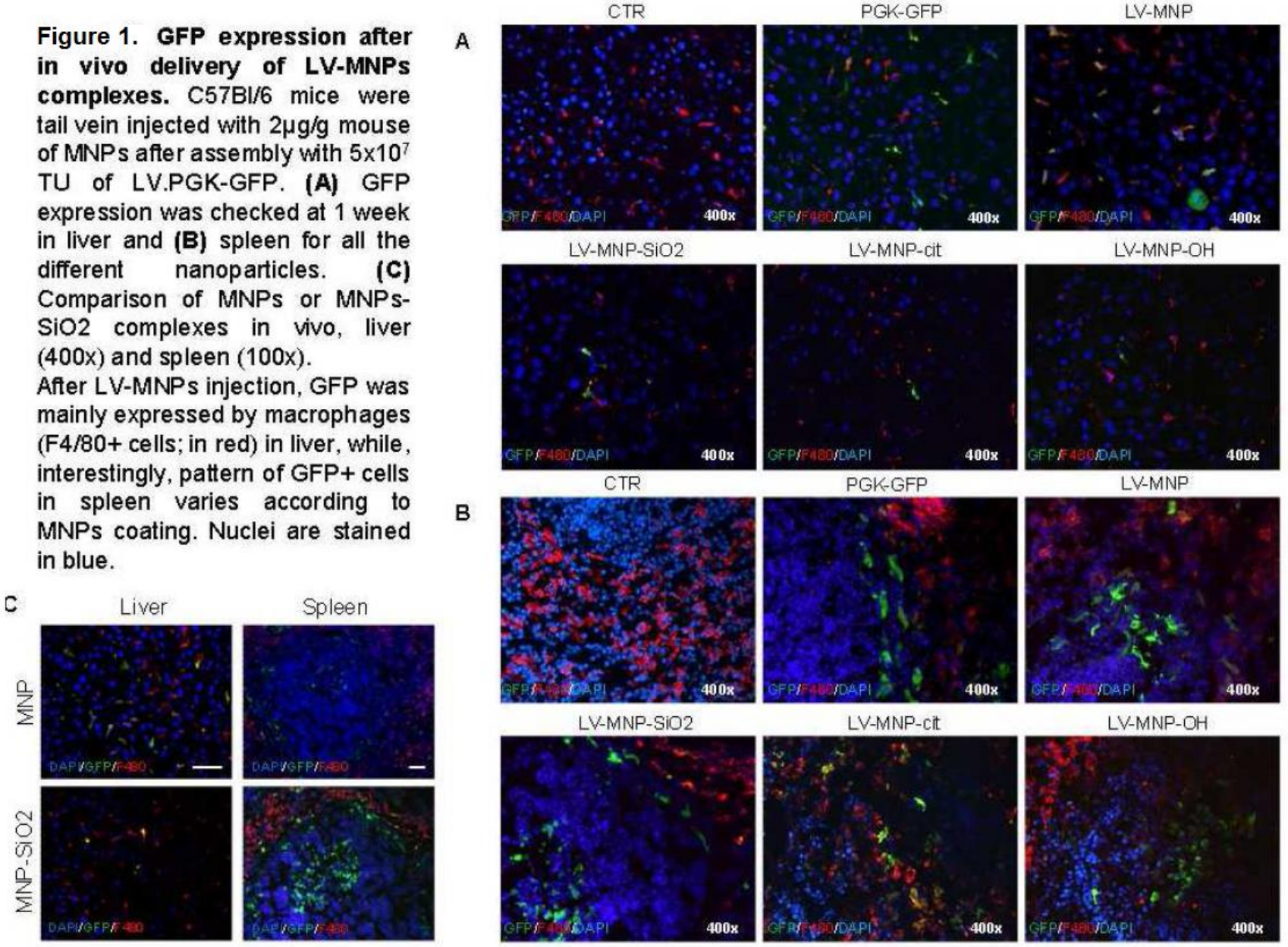

In vivo biocompatibility evaluation of nanoparticles

- The MNPs used in this study demonstrated to be biocompatible both in vitro and in vivo conditions.

- MS1 cells in contact with MNPs showed a small percentage of apoptotic and necrotic cells comparable to untreated control.

- The in vivo data confirmed a good performance of the nanoparticles using a concentration of 2 mg Fe/kg body weight for biomedical applications.

MNPs interaction via Lentivirus coupling

- Lentiviral vectors coupled with SPIONs increased gene expression in liver and spleeen. Thus it can be used for applications of cancer gene therapy.

Breast cancer

- Breast cancer is the most common invasive cancer in women worldwide. It affects about 12% of women worldwide. Breast cancer comprises 22.9% of invasive cancers in women and 16% of all female cancers. In 2012, it comprised 25.2% of cancers diagnosed in women, making it the most common female cancer.

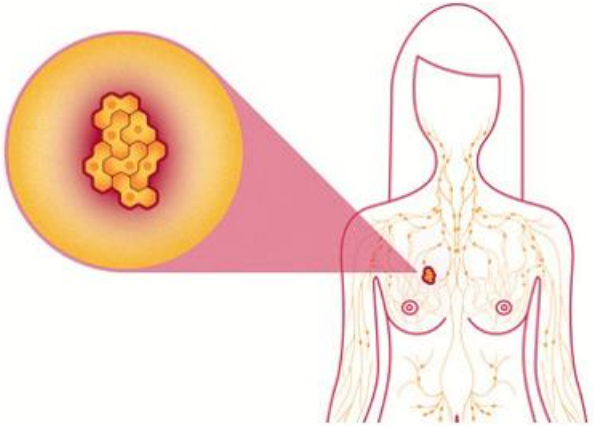

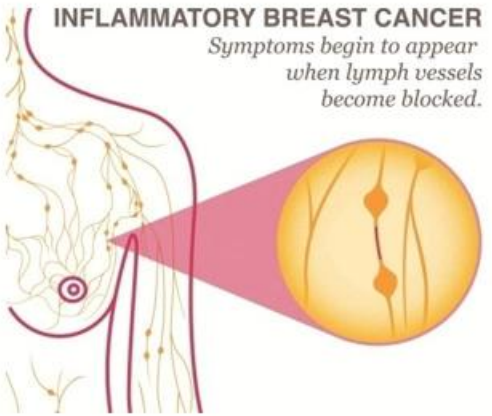

Various approaches explored to target breast cancer cells using nanomedicines

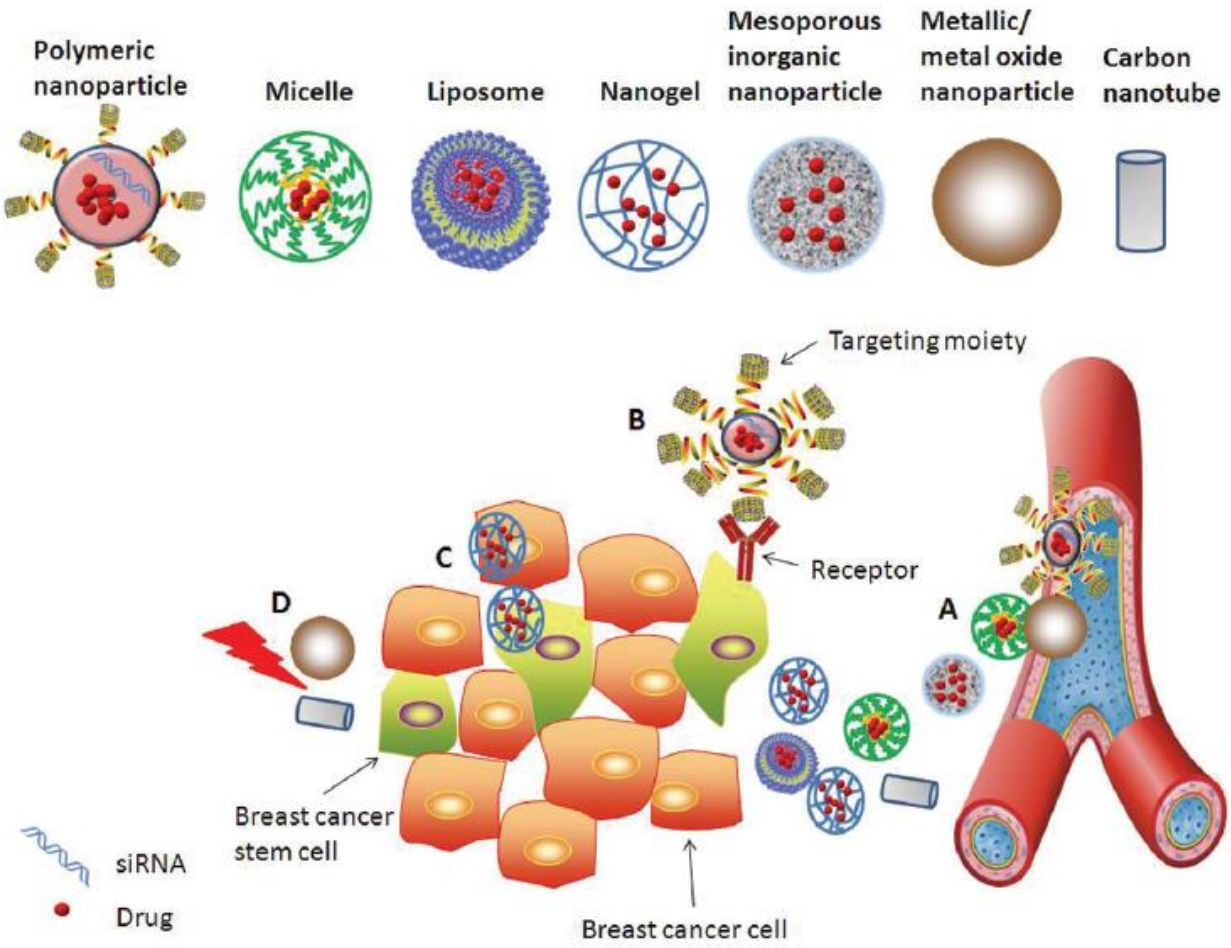

He L, Gu J et al. Front. Pharmacol. 2016; 7:313

Electrostatic conjugation of doxorubicin with CA-SPIONs

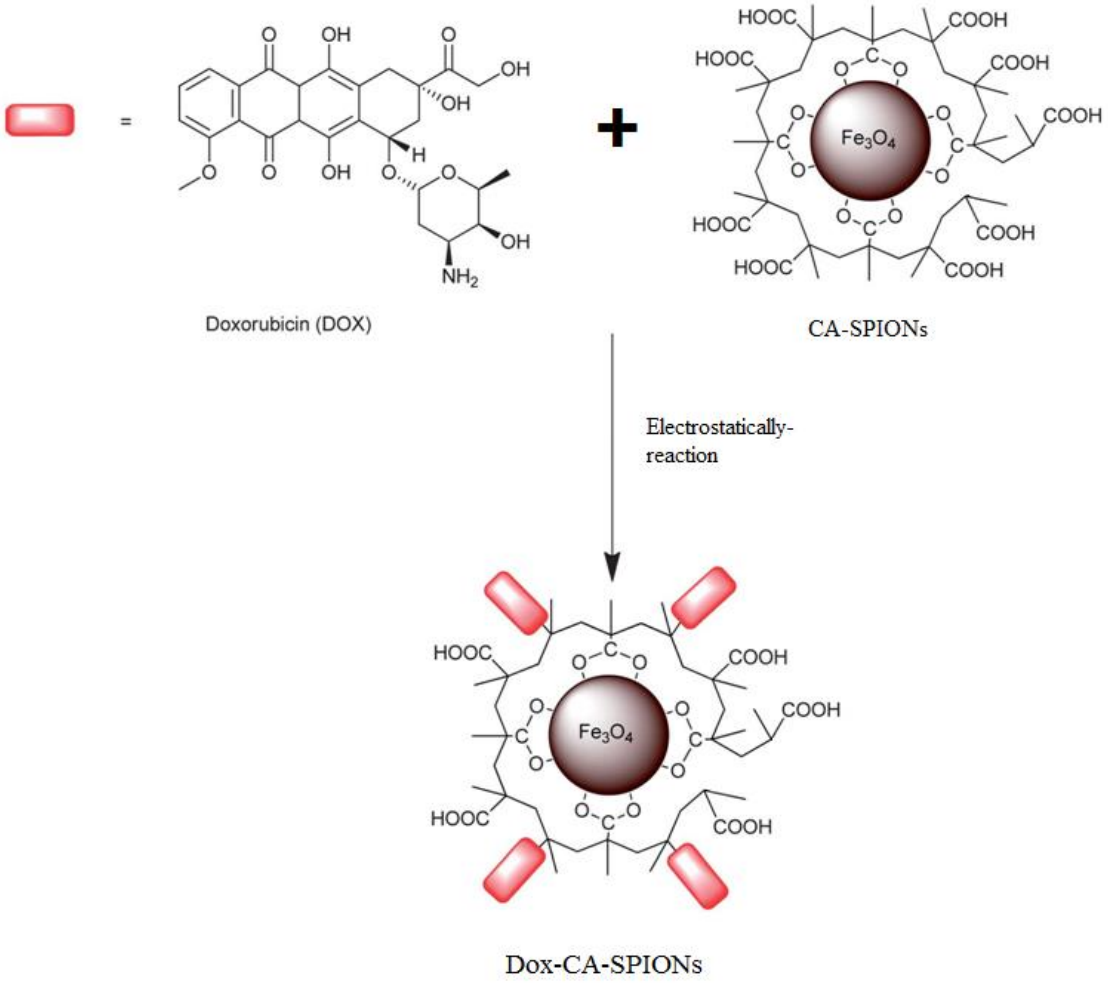

Goal of the project

- This project aims to implement an extremely **innovative multi-therapeutic strategy that combines targeted drug delivery of chemotherapeutics, the use of MNPs properties of hyperthermia to target *in vitro* breast cancer drug-resistant and not drug-resistant cell lines.**

1st objective of Scientia fellows project

The first objective of the project will be planned as follows:

MNPs conjugation with chemotherapy drugs

- Chemotherapy drugs could be conjugated to **carboxylic acid functionalized iron-oxide nanoparticles** or to other types of nanoparticles.

- Different antineoplastic agents (doxorubicin, epirubicin, cyclophosphamide and methotrexate) or monoclonal antibody Trastuzumab (Herceptin) could be used for in vitro testing efficacy of combined effect on breast cancer cell lines.

1st objective of Scientia fellows project

- **Analysis of the biological activity of the MNPs loaded with chemotherapy drugs on human mammary epithelial cells and breast cancer cells to evaluate their antitumor activity without or under hyperthermic conditions**

- The in vitro efficacy of conjugated MNPs will be tested on the following cell lines: **MCF-7** (ATCC, human breast cancer cells) and **MDA-MB-231** cells (ATCC, human breast cancer cells derived from metastatic site), **MCF-10A** (ATCC, mammary epithelial cells), as negative control.

The following *in vitro* tests could be performed:

- Evaluation of the cytotoxicity of the MNPs: **MTT test** and **Apoptosis evaluation.**
- Cell growth: cell counting in Burker chamber.
- Cell morphology will be evaluated by inverted phase contrast microscopy.
- Induction of ROS production will be evaluated by fluorimetric assay.
- Further in vitro tests

Hyperthermia selectivity treatment on breast cancer cells

Hyperthermia selectivity treatment on breast cancer cells	Single cell colture	Double cell colture	Three cell coltures
For hyperthermia treatment, cells will be put in the incubator at 46°C for 30 minutes, corresponding to a temperature dosage of 90 cumulative equivalent minutes at 43°C	**MCF-10A**	**MCF-7 + MCF10A**	**MDA-MB-231 + MCF-7 + MCF10A**
	MDA-MB-231	**MDA-MB-231 + MCF10A**	
	MCF-7		

Magnetic hyperthermia induced by iron-oxide nanoparticles loaded with doxorubicin

- MCF-7 cells and MDA-MB-231 cells (5000 cells) in 96 well-plates
- Cells to passage 15-18
- For hyperthermia treatment, cells were put in the incubator at 46°C for 30 minutes with Dox-CA-SPIONs conjugates. Cells not in contact with MNPs was considered like control.
- 50 µL aqueous dispersion of CA-SPIONs (50 µg/mL) were added to a 1 mL of Dox solution (50 µM), and mixed with shaking at room temperature for 2 minutes.
- After formation of the drug-nanoparticle conjugates, they are separated from the free drugs via magnetic separation and washing in the aqueous medium.
- Experimental time: 24, 48 and 72 hours
- MTT assay
- Cell viability was calculated as follow: (experimental o.d. / mean control o.d.)*100 – optical density (o.d.)

Magnetic hyperthermia on breast cancer cells 46°C - 30 minutes

- Triple negative breast cancer cells MDA-MB-231. It corresponds to human breast cancer cells derived from metastatic site
- MCF-7 (Human breast cancer cells ER+/PR+)
- Magnetic hyperthermia at 46°C for 30 minutes in contact with MNPs

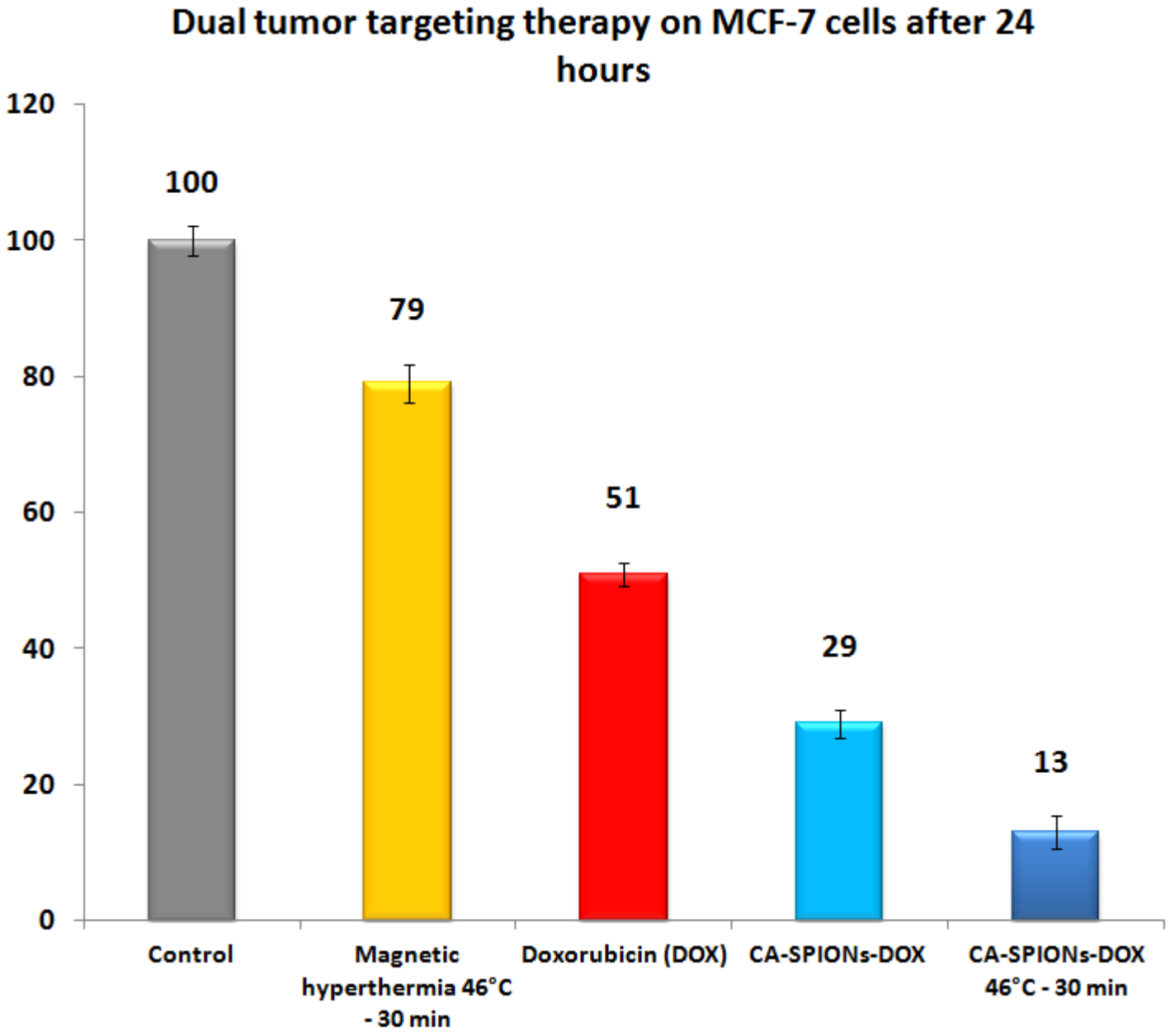
Dual tumor targeting therapy on MCF-7 cells after 24 hours
120
100
80
60
40
20
0
100
79
51
29
13
Control
Magnetic hyperthermia 46°C - 30 min
Doxorubicin (DOX)
CA-SPIONs-DOX
CA-SPIONs-DOX 46°C - 30 min

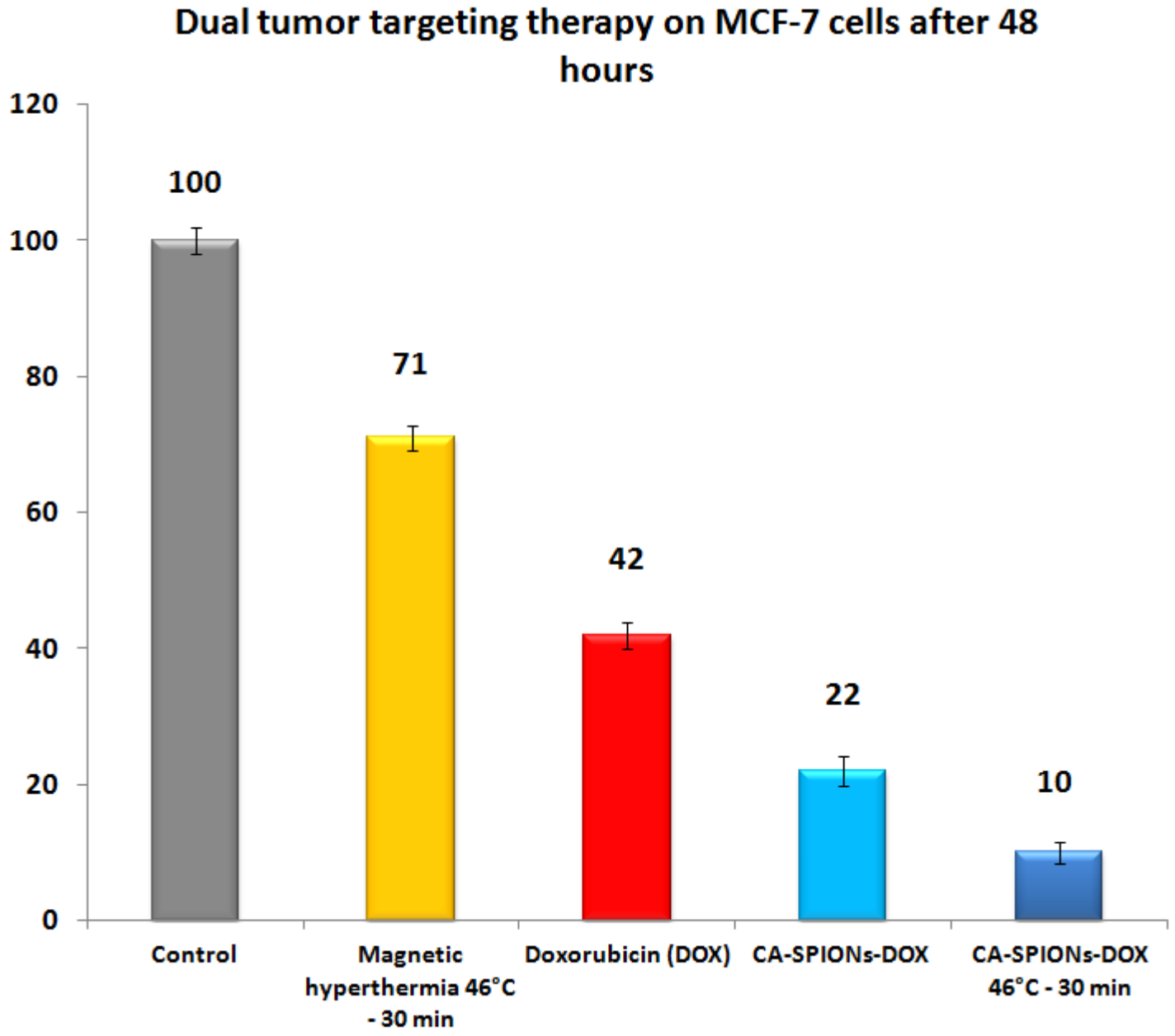
Dual tumor targeting therapy on MCF-7 cells after 48 hours
120
100
80
60
40
20
0
100
71
42
22
10
Control
Magnetic hyperthermia 46°C - 30 min
Doxorubicin (DOX)
CA-SPIONs-DOX
CA-SPIONs-DOX 46°C - 30 min

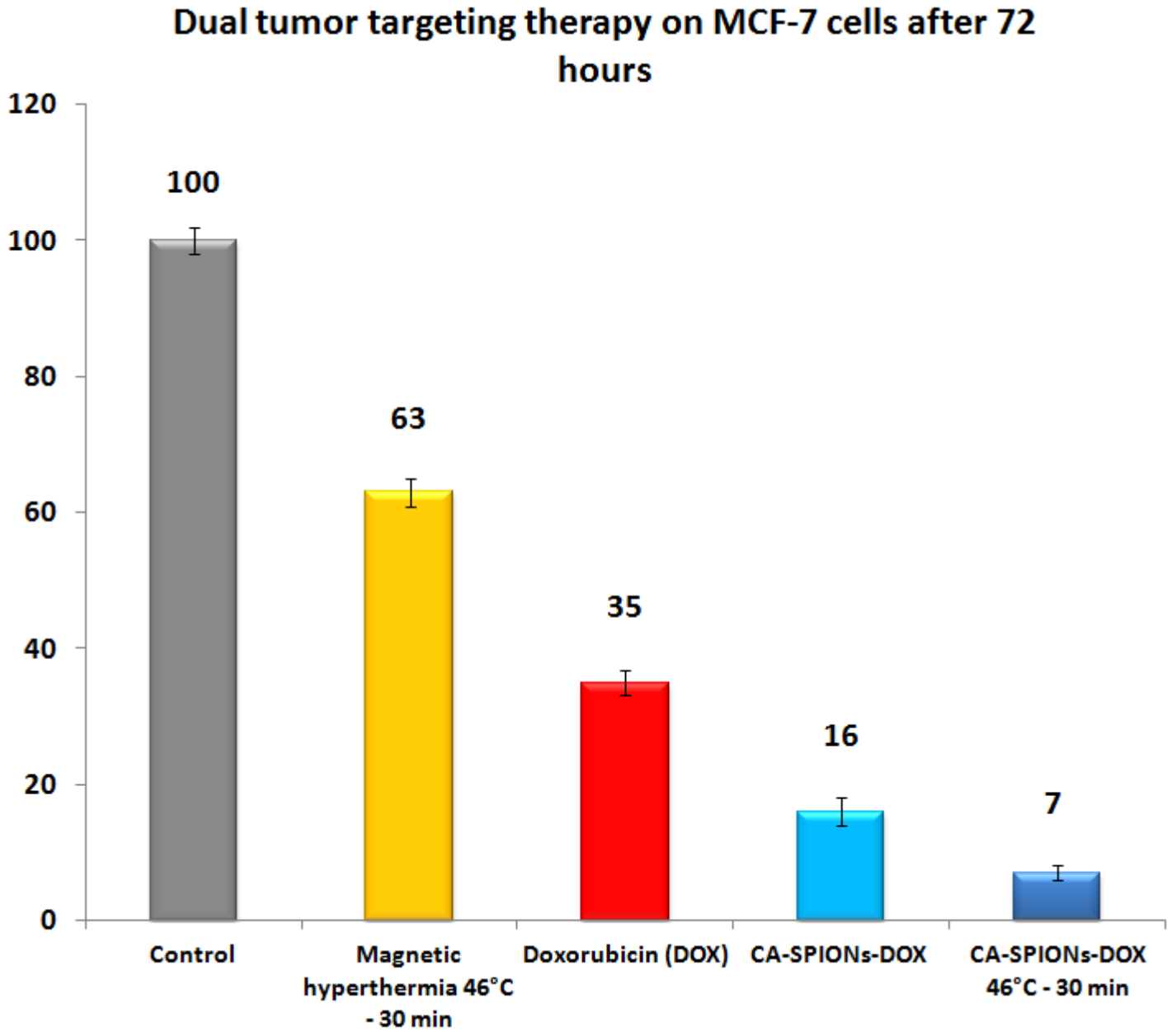
Dual tumor targeting therapy on MCF-7 cells after 72 hours
120
100
80
60
40
20
0
100
63
35
16
7
Control
Magnetic hyperthermia 46°C - 30 min
Doxorubicin (DOX)
CA-SPIONs-DOX
CA-SPIONs-DOX 46°C - 30 min

Table 1. Direct contact treatment

% Trypan Blue positive estrogen receptor-positive MCF-7 cells (mean±standard deviation)

24 h	
	% Trypan Blue positive MCF-7 cells
Control	**5.1 ± 0.5**
CA-Fe_3O_4 46°C 30 min	**78.2 ± 0.9**
Doxorubicin	**49.5 ± 1.0**
CA-Fe_3O_4-DOX	**30.2 ± 0.8**
CA-Fe_3O_4-DOX 46°C 30 min	**13.9 ± 0.7**
48 h	
	% Trypan Blue positive MCF-7 cells
Control	**6.4 ± 0.4**
CA-Fe_3O_4 46°C 30 min	**71.5 ± 0.8**
Doxorubicin	**43.7 ± 1.2**
CA-Fe_3O_4-DOX	**24.8 ± 0.9**
CA-Fe_3O_4-DOX 46°C 30 min	**11.6 ± 1.0**
72 h	
	% Trypan Blue positive MCF-7 cells
Control	**7.2 ± 0.6**
CA-Fe_3O_4 46°C 30 min	**64.5 ± 0.8**
Doxorubicin	**36.7 ± 1.2**
CA-Fe_3O_4-DOX	**17.2 ± 0.7**
CA-Fe_3O_4-DOX 46°C 30 min	**9.3 ± 0.5**

MDA-MB-231 cells

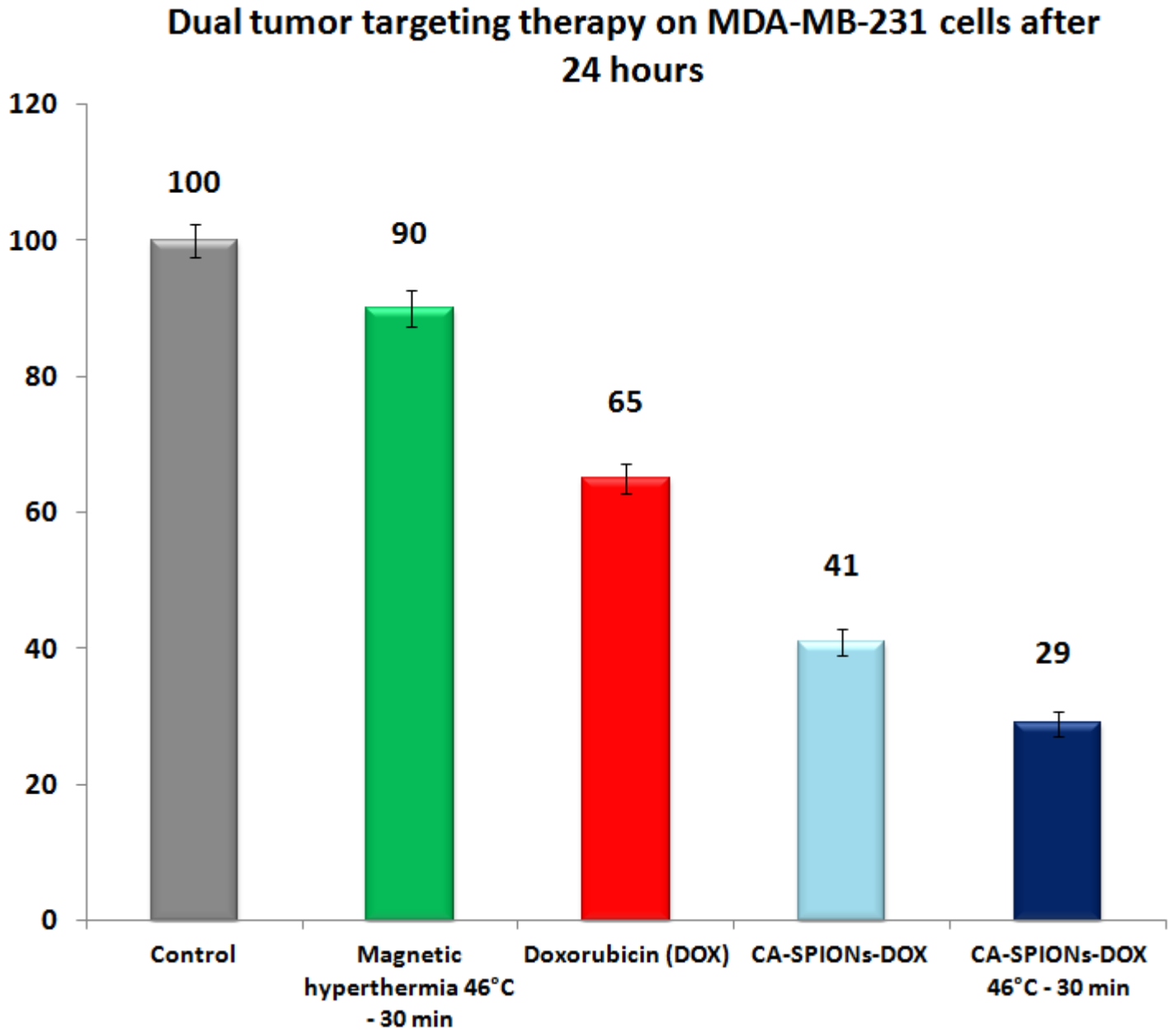
Dual tumor targeting therapy on MDA-MB-231 cells after 24 hours
120
100
80
60
40
20
0
100
90
65
41
29
Control
Magnetic hyperthermia 46°C - 30 min
Doxorubicin (DOX)
CA-SPIONs-DOX
CA-SPIONs-DOX 46°C - 30 min

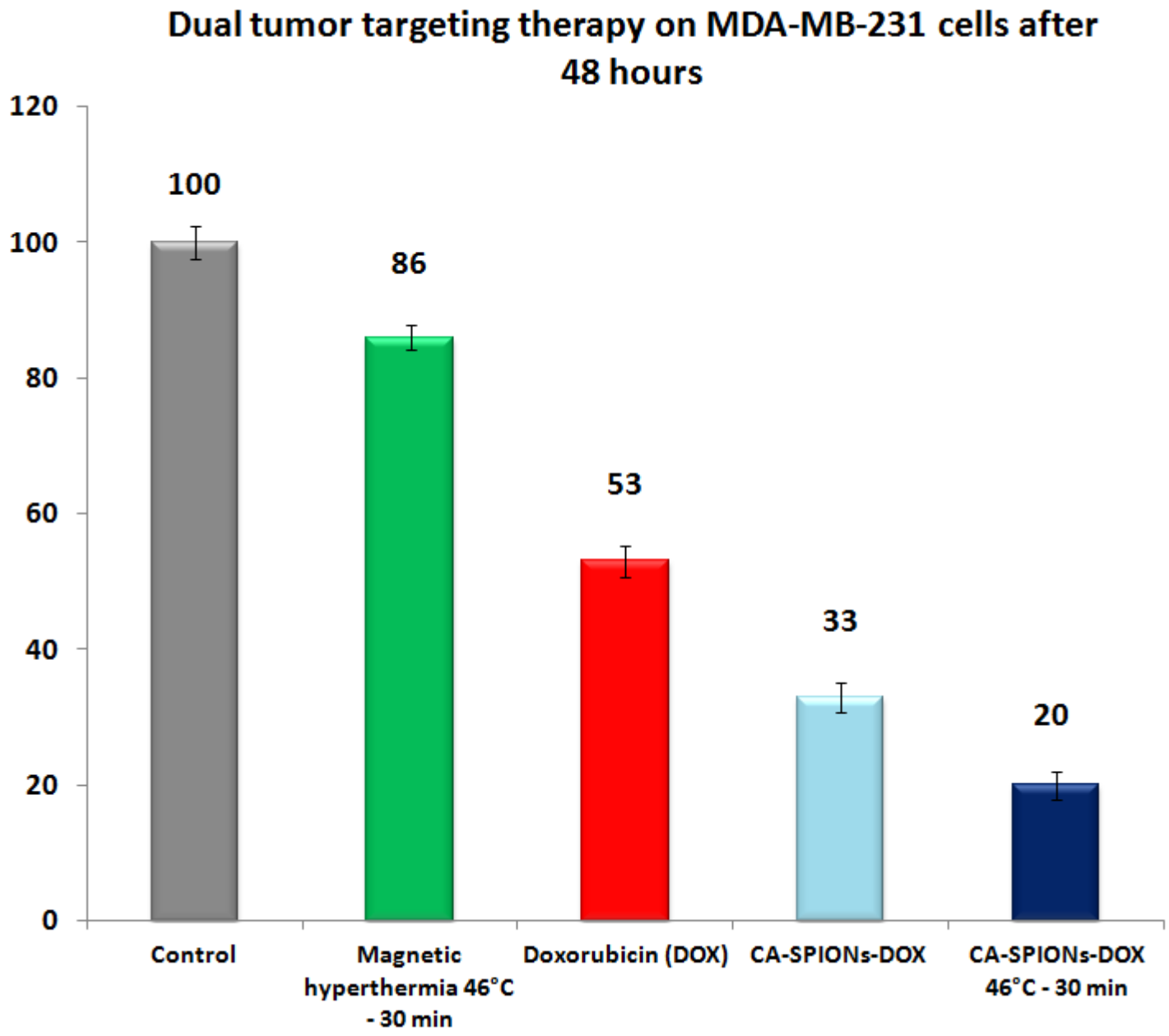
Dual tumor targeting therapy on MDA-MB-231 cells after 48 hours
120
100
80
60
40
20
0
100
86
53
33
20
Control
Magnetic hyperthermia 46°C - 30 min
Doxorubicin (DOX)
CA-SPIONs-DOX
CA-SPIONs-DOX 46°C - 30 min

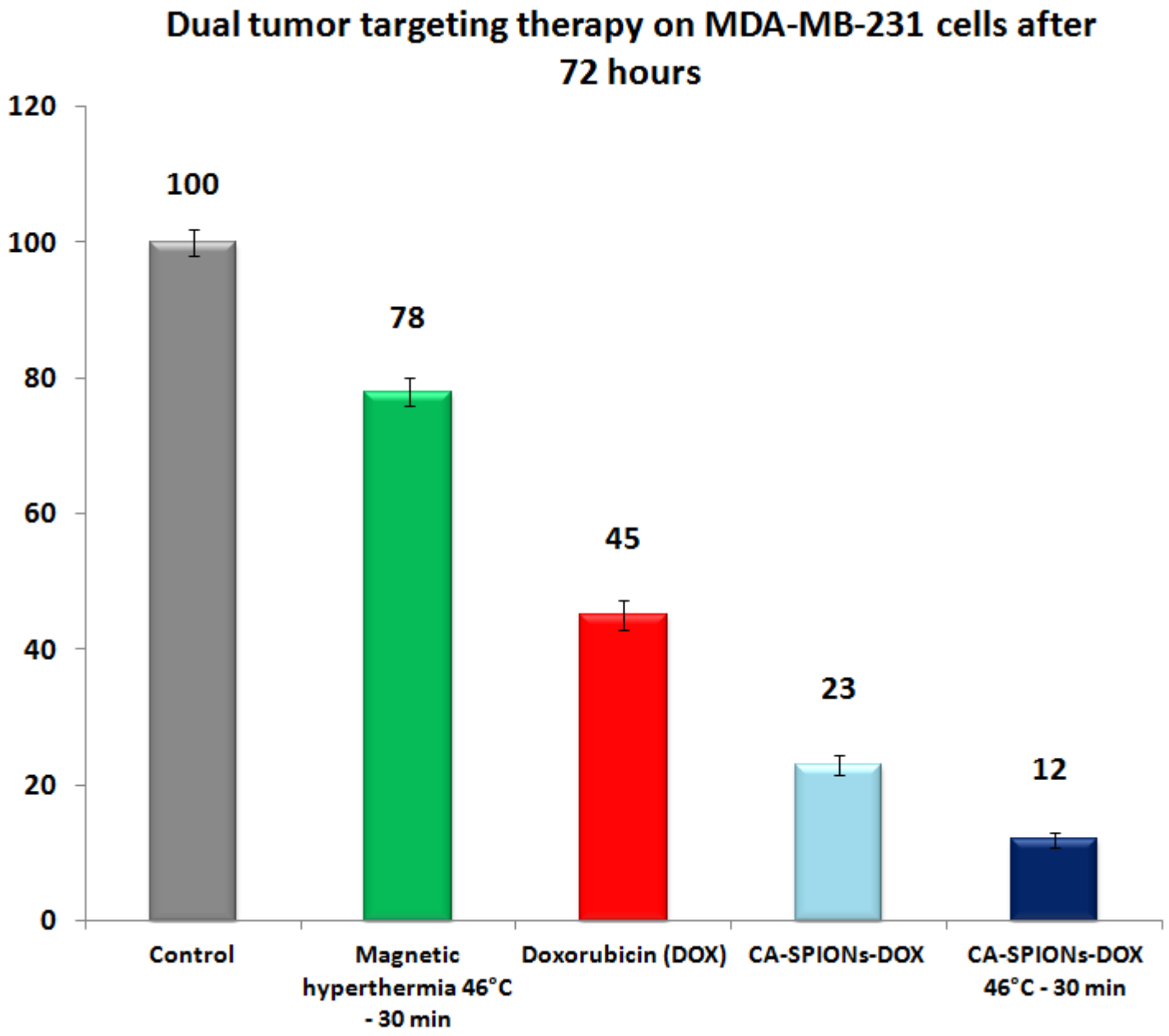
Dual tumor targeting therapy on MDA-MB-231 cells after 72 hours
120
100
80
60
40
20
0
100
78
45
23
12
Control
Magnetic hyperthermia 46°C - 30 min
Doxorubicin (DOX)
CA-SPIONs-DOX
CA-SPIONs-DOX 46°C - 30 min

Table 2. Direct contact treatment

% Trypan Blue positive triple-negative MDA-MB-231 cells

(mean±standard deviation)

24 h

	% Trypan Blue positive MDA-MB-231 cells
Control	**6.6 ± 0.7**
CA-Fe_3O_4 46°C 30 min	**90.2 ± 0.8**
Doxorubicin	**66.3 ± 1.1**
CA-Fe_3O_4-DOX	**41.5 ± 0.9**
CA-Fe_3O_4-DOX 46°C 30 min	**29.4 ± 0.7**

48 h

	% Trypan Blue positive MDA-MB-231 cells
Control	**5.9 ± 0.6**
CA-Fe_3O_4 46°C 30 min	**86.5 ± 1.3**
Doxorubicin	**52.3 ± 1.4**
CA-Fe_3O_4-DOX	**33.5 ± 0.8**
CA-Fe_3O_4-DOX 46°C 30 min	**21.7 ± 1.1**

72 h

	% Trypan Blue positive MDA-MB-231 cells
Control	**6.9 ± 0.8**
CA-Fe_3O_4 46°C 30 min	**77.2 ± 1.1**
Doxorubicin	**46.5 ± 1.3**
CA-Fe_3O_4-DOX	**23.2 ± 0.8**
CA-Fe_3O_4-DOX 46°C 30 min	**12.2 ± 0.7**

Cytocompatibility evaluation of iron-oxide nanoparticles on MCF-10A cells

- MCF-10A cells - mammary epithelial cells (5000 cells) in 96 well-plates
- Cells to passage 1-2
- 30 nm diameter Carboxylic acid functionalized iron-oxide nanoparticles CA-SPIONs: 25 and 50 µg/mL
- For hyperthermia treatment, cells were put in the incubator at 46°C for 30 minutes. Cells not in contact with MNPs was considered like control.
- Experimental time: 24, 48 and 72 hours
- MTT assay
- Cell viability was calculated as follow: (experimental o.d. / mean control o.d.)*100 – optical density (o.d.)

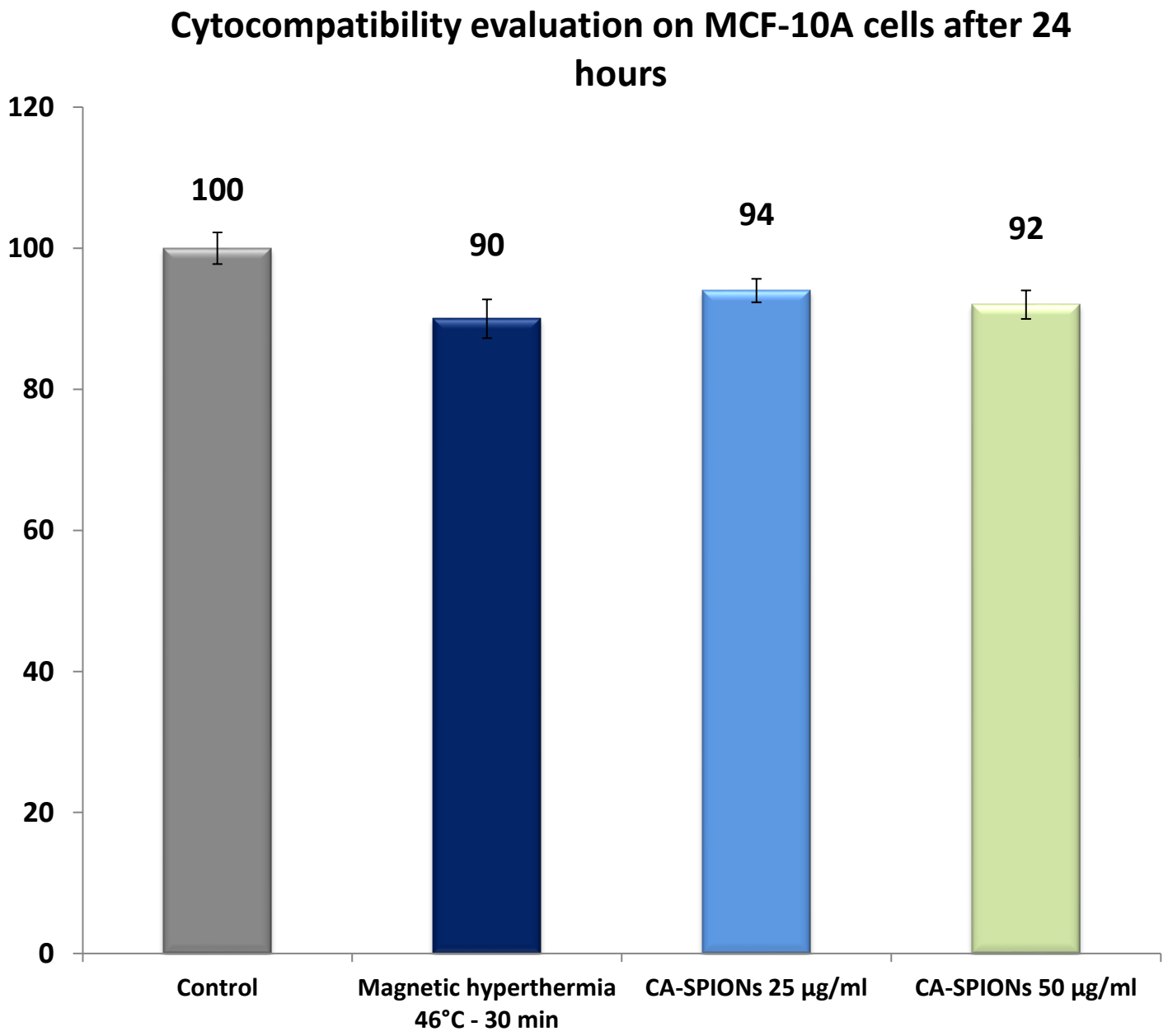
Cytocompatibility evaluation on MCF-10A cells after 24 hours
120
100
80
60
40
20
0
100
90
94
92
Control
Magnetic hyperthermia 46°C - 30 min
CA-SPIONs 25 µg/ml
CA-SPIONs 50 µg/ml

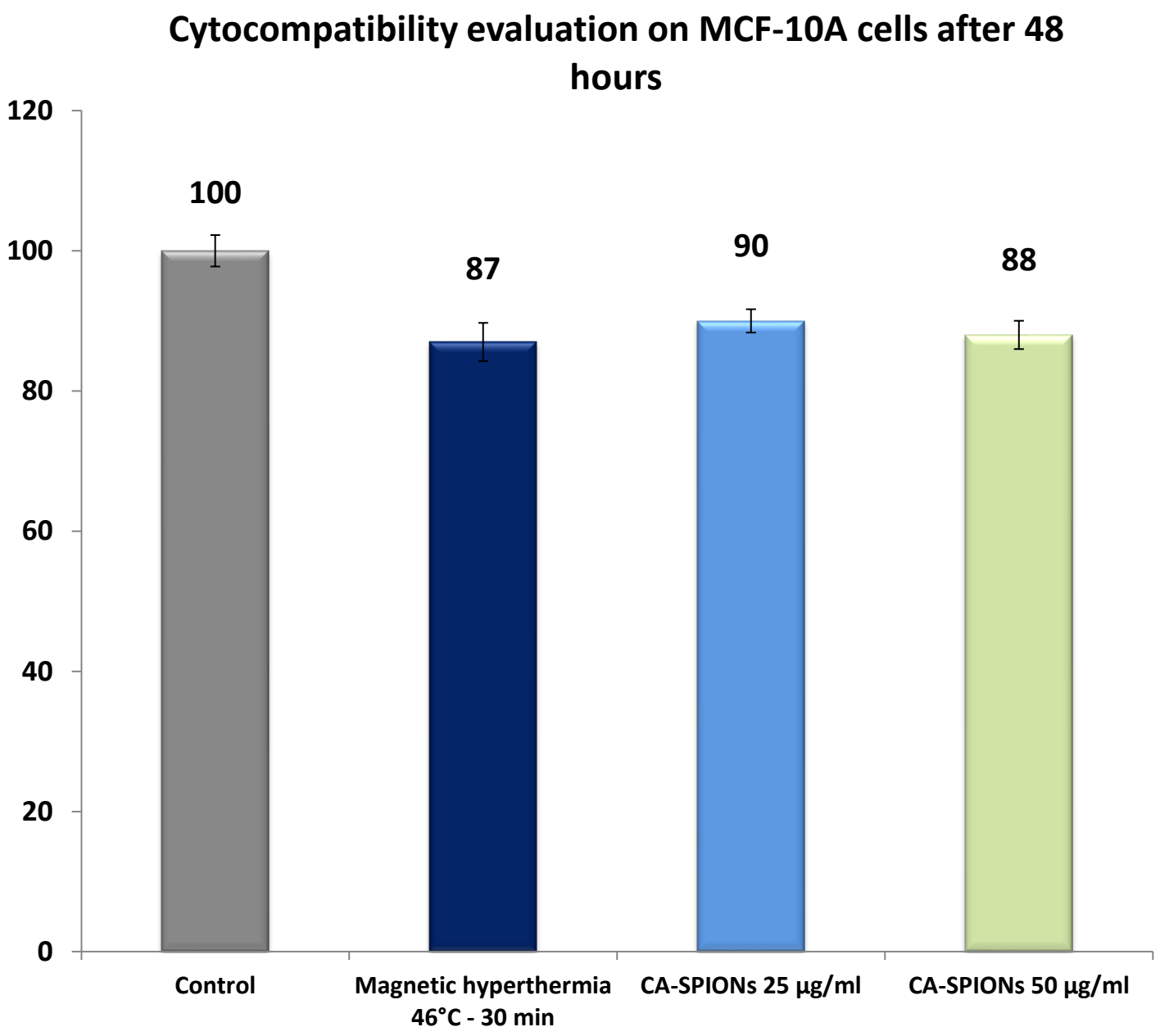
Cytocompatibility evaluation on MCF-10A cells after 48 hours
120
100
80
60
40
20
0
100
87
90
88
Control
Magnetic hyperthermia 46°C - 30 min
CA-SPIONs 25 µg/ml
CA-SPIONs 50 µg/ml

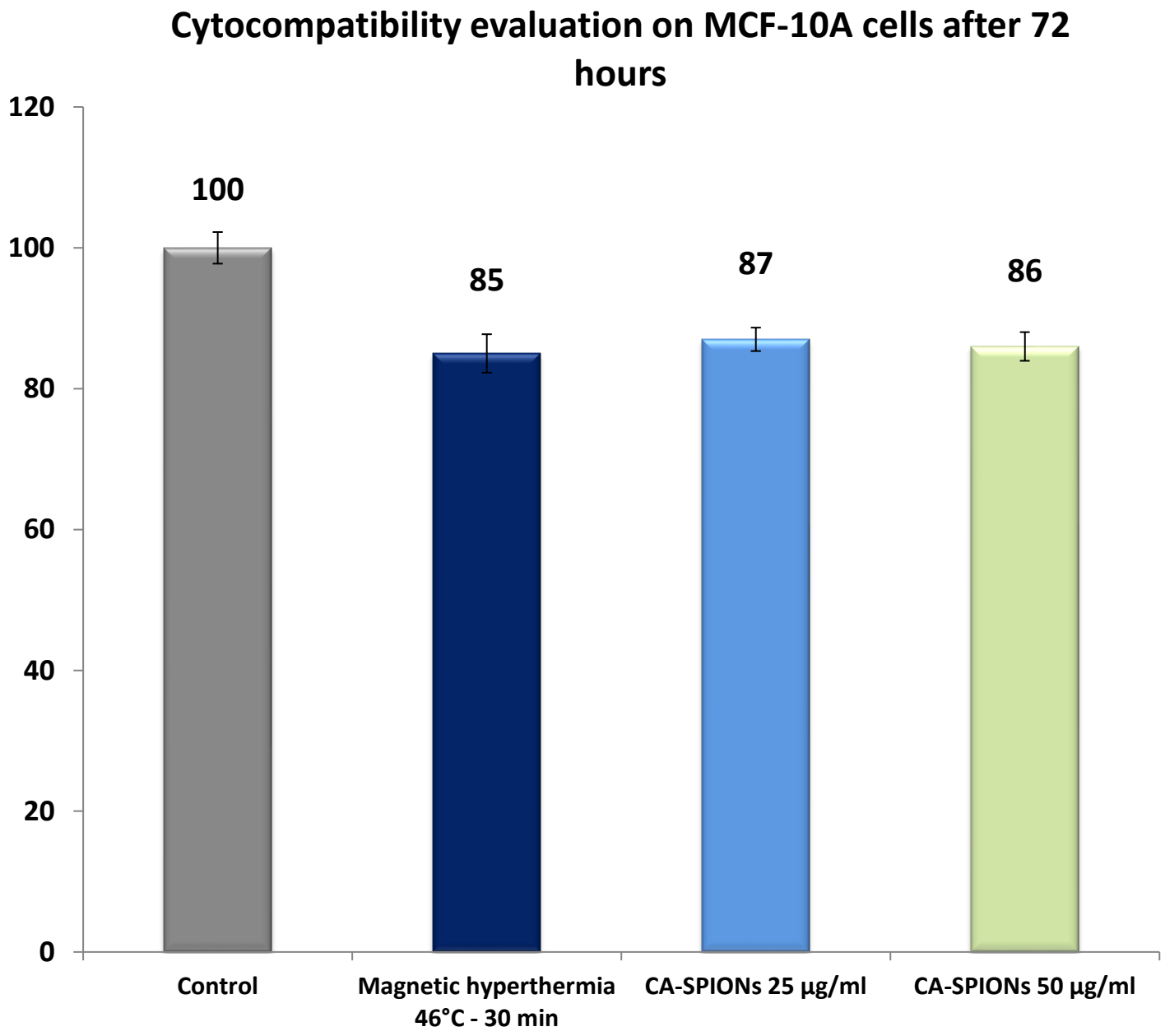
Cytocompatibility evaluation on MCF-10A cells after 72 hours
120
100
80
60
40
20
0
100
85
87
86
Control
Magnetic hyperthermia 46°C - 30 min
CA-SPIONs 25 µg/ml
CA-SPIONs 50 µg/ml

Results

- These first preliminary data seem to indicate that the magnetic hyperthermia at 46°C for 30 minutes induced by CA-SPIONs led to increasing cytotoxic effects of the nanoparticles on breast cancer cells after 24, 48 and 72 hours from treatment.

- Magnetic hyperthermia at 46°C for 30 min kill ER+/PR+ and conjugation of doxorubicin to SPIONs is able to kill MCF-7 cells and also more resistant MDA-MB-231 cells after 24, 48 and 72 hours.

- The difference in cell mortality of MCF-7 cells compared to MDA-MB-231 cells could be explained probably due to the increased susceptibility of MCF-7 cells.

- Carboxylic acid functionalized iron-oxide nanoparticles CA-SPIONs were demonstrated to be cytocompatible on mammary epithelial cells (MCF-10A cells)

Thank you for your attention!

Prof. Vessela N. Kristensen, Xavier Tekpli, Shakila Jabeen, Andliena Tahiri, Jovana Klajic, Surendra Kumar, Torben Lüders

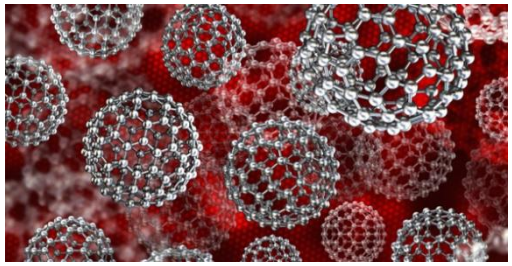

Prof. Jürgen Geisler